DEVELOPMENT OF THE TIMING SYSTEM FOR THE BUNCH-TO-BUCKET TRANSFER BETWEEN THE FAIR ACCELERATORS

Vom Fachbereich
Institut für Angewandte Physik
der Goethe-Universität, Frankfurt am Main
zur Erlangung des akademischen Grades
eines Doktor der Naturwissenschaften
genehmigte Dissertation

Von
Jiaoni Bai
geboren am 9. November 1986 in Taiyuan, Shanxi Province, China

Referent:	Prof. Dr.
Korreferent:	Prof. Dr.
Tag der Einreichung:	Date. Month Year
Tag der mündlichen Prüfung:	Date. Month Year

Darmstadt 2016

I would like to dedicate this dissertation to my dear parents, loving husband and good friends ...

Acknowledgement

First and foremost, I would like to thank my professor Prof. Dr. Oliver Kester. It is a great honour for me to be his Ph.D. student. He gave me the chance to study at Goethe Universität, Frankfurt am Main and work in GSI for this interesting Ph.D. topic. I appreciate all his contributions of time and ideas to make my Ph.D. successful. I was deeply influenced by his enthusiasm for his research and his selfless support for his students. I was thankful for his support, that I participated many international conferences, schools and workshops. This experience enriched my life and broadened my horizons.

I wish to express my sincere gratitude to Dr. David Ondreka and Dr. Dietrich Beck for their supervision, valuable guidance and helpful suggestions throughout my Ph.D. study. I have been greatly lucky to have so good supervisors, who cared much about my work and who answered my doubts patiently. They were like a lighthouse in the ocean, which guides me in the right direction. They are not only my scientific supervisors, but also my mentors. They encouraged and motivated me during tough time of my Ph.D. Hence, I will keep a positive attitude and keep moving forward when I face with challenges, difficulties and temporary setbacks in the future.

I would like to acknowledge all colleagues in the timing group, CSCO department, GSI, Mathias Kreider, Stefan Rauch, Marcus Zweig, Alexander Hahn and former employee Dr. Wesley Terpstra, who provided me much technical support. I would like to extend my appreciation to department leader Dr. Ralph Bär, who gave much support for my Ph.D. topic. Thanks for their friendship and collaboration. I am especially grateful for the group member Cesar Prados, by whom I learned not only technical knowledge, but also how to work efficiently and how to become a good engineer. I would also like to thank Matthias Thieme, who provided me the devices for the test setup and Marko Stanislav Mandakovic for the discussion about the MPS. I would like to extend gratitude to Dr. Udo Krause and Peter Kainberger for the information about the GSI control system.

I am also thankful for the good cooperation with Thibault Ferrand, who studies at Technische Universität Darmstadt and works in PBRF department, GSI. Thanks for his valuable contribution of the development of the LLRF system for the B2B transfer system for FAIR. I would like to extend my sincerest thanks and appreciation to PBRF department leader Prof. Dr. Ing. Harald Klingbeil for his support. In addition, a special thanks is also extended to Dr. Dieter Lens and Stefan Schäfer for their technical support. Thanks for Dr. Bernhard Zipfel to give me support about BuTiS.

I wish to express my sincere gratitude to SBES department leader Dr. Markus Steck for his technical support of ESR and CRYRING, Dr. Udo Blell in PBHV department for the technical support of kicker and Dr. Michael Block in SHE-P department for the supply of two SRS function generators.

I must express my gratitude to GSI and also HGS-HiRe, who provided the scholarship which allowed me to undertake this research.

Lastly, I would like to thank my family for all their love and encouragement. My parents always support me to pursuing my dreams. Most of all, my loving husband Zigao Li is so appreciated, who always encourages me to realize my dreams. Thank you.

Jiaoni Bai
Darmstadt, September 2016

Abstract

This dissertation contributes to the conceptual development, the systematic investigation and the timing system realization of the FAIR bunch-to-bucket transfer system.

The FAIR B2B transfer system plays an important role for the FAIR project, which will achieve various complex bunch-to-bucket transfer for FAIR accelerators in the future. It focuses first of all on the transfer from the SIS18 to the SIS100, but it will be firstly tested for the transfer from the SIS18 to the ESR and from the ESR to the CRYRING. The system is developed based on the FAIR existing infrastructures, the Low Level Radio Frequency system (LLRF) and the FAIR control system. It coordinates with the Machine Protection System (MPS), which protects SIS100/SIS300 from fatal errors and considerable damage and indicates beam status for Beam Instrumentation (BI).

The B2B transfer system obtains the radio frequency (rf) phase difference between two synchrotrons by means of a campus wide distributed reference signal with picosecond precision, which is provided by the Bunchphase Timing System (BuTiS). The part of the B2B electronic locates in the the source synchrotron supply room and serves as a kind of the "B2B transfer master". The most important tasks of B2B transfer master are:

- The data collection (e.g. the rf phase collection).
- The data processing (e.g. the calculation of the synchronization window, the phase shift for the phase match between two rf systems, the phase correction for the bucket label, the B2B transfer status check and etc.).
- The data redistribution (e.g. the synchronization window).

The synchronization window is a coarse time frame for the transfer (coarse synchronization) and the bucket label signal is used to indicate a specified bucket to be injected within the window, which is called the "fine synchronization". This system is applied to all FAIR B2B transfer use cases and all transfers have to achieve the bunch-to-bucket injection center mismatch within the tolerate limits.

This dissertation presents the basic idea of the FAIR B2B transfer system, the basic procedure of the FAIR B2B transfer and the realization of each function.

Because the system focuses first of all on the transfer from the SIS18 to the SIS100, the beam dynamic of the B2B transfer from the SIS18 to the SIS100 is simulated for two synchronization methods, the phase shift and the frequency beating method. In addition, the SIS18 extraction and SIS100 injection kickers are analyzed for different triggering strategies. This dissertation also explains the timing constraints of the system, the calculation of the synchronization window and presents the usage of the WR network for the B2B transfer system.

A test setup of the timing system of the FAIR B2B transfer system is presented and the test result is analyzed in this dissertation.

Kurzfassung

Contents

List of Figures

List of Tables

Glossary

accuracy of the start of the synchronization window	Time closeness of agreement between the observed and the best estimate start of the synchronization window, which is the sum of the precision and trueness
batch	A train of bunches circulating along a synchrotron to be transferred to buckets
best estimate of alignment	Fine time for the alignment of two RF Reference Signals
bucket label signal	Time indication of a dedicated bucket passing on the virtual rf cavity of the target synchrotron, when it is correct phase aligned with the rf system of the source synchrotron for the bunch-to-bucket injection.
bucket pattern	Rules for the buckets to be filled
bucket area factor	Ratio of bucket size of a running bucket to a stationary bucket
bucket size	Area in longitudinal phase space plane enclosed by the bucket
bucket height	Maximum momentum deviation of the rf bucket
bunch	Collection of particles captured within one rf bucket
bunch gap	Area without any bunches in a batch
Cavity DDS	Cavity DDS provides rf signal for cavities

circumference ratio	Ratio of the circumference for synchrotrons of different size
coarse synchronization	Bunches are transferred into buckets with the bunch-to-bucket center mismatch smaller than the upper bound
error propagation	Uncertainties in the original measurements “propagate“ through calculations to cause uncertainties in the calculated final answers
extraction kicker	Diverts a circulating beam to leave a synchrotron
fine synchronization	Bunches are transferred into correct buckets
frame transfer jitter	The time deviation between the transfer latencies of two consecutive frames
frame transfer latency	The time interval between the frame reception and sending
frame loss rate	The ratio of the number of the lost Ethernet frames to the number of the theoretic received frames of a tested port
Group DDS	DDS module that generates an Reference RF Signal for a group of cavities
harmonic number	Integer ratio between the rf frequency and the revolution frequency
injection kicker	Merges one beam into a circulating beam in a synchrotron
kicker fall time	A period of time of kicker magnet to reduce to zero magnetic field
kicker flat-top	A period of time of kicker magnet with a stable magnetic field
kicker rise time	A period of time for kicker magnet to reach a stable magnetic field

longitudinal emittance	Area occupied by a bunch in the longitudinal phase space plane
machine cycle	One complete operation cycle of a machine, i.e. injection, ramp up, flattop, ejection and ramp down
precision of the start of the synchronization window	Time closeness of agreement between the actual start of the synchronization window of different timing notes
probable range of alignment	Range within which the fine alignment lies because of the propagation of the uncertainty
Reference RF Signal	DDS module that generates an Reference RF Signal for a group of cavities
revolution frequency ratio	Ratio of the revolution frequencies for synchrotrons of different size
running rf bucket	Rf system provides a region in the longitudinal phase space, within which all particles oscillate around the synchronous particle and stay together with energy gain/loss per turn
stationary rf bucket	Rf system provides a region in the longitudinal phase space, within which all particles oscillate around the synchronous particle and stay together without energy gain/loss per turn (short: bucket)
Synchronization Reference Signal	Shared synchronous reference signal at each supply room (same frequency and in phase)
synchronization frequencies	An integral multiple of the derived rf frequency, which is the division of the revolution frequency. It is used for the phase alignment of two rf systems
synchronous particle	A particle who always sees a constant rf phase at the rf cavity

synchrotron motion	Oscillation of asynchronous particles around the synchronous particle
timing frame	A specific Ethernet frame with 110 byte frame length, which contains one timing message
trueness of the start of the synchronization window	Time closeness of agreement between the average actual start of the synchronization window of different timing notes and the best estimate start of the synchronization window
tune	Number of particle trajectory oscillations during one revolution in the ring (transverse and longitudinal)
uncertainty	A non-negative parameter characterizing the dispersion of the values attributed to a measured quantity
virtual rf cavity	A virtual position around the ring, to which the Reference RF Signal corresponds

Abbreviations

AGS	Alternating Gradient Synchrotron at BNL
API	Application Programming Interface
B2B	Bunch-to-bucket
BNL	Brookhaven National Laboratory
BuTiS	Bunchphase Timing System
CCS	Central Control System
CERN	Conseil Européen pour la Recherche Nucléaire
CM	Clock Master
CPU	Central Processing Unit
CR	Collector Ring at GSI
CSCO	Common Systems Control Systems
CSRe	Cooler Storage Ring experimental ring at IMP
CSRm	Cooler Storage Ring main ring at IMP
DDS	Direct Digital Synthesizer
DM	Data Master
DSP	Digital Signal Processor
ESR	Experimental Storage Ring at GSI
FAIR	Facility for Antiproton and Ion Research at GSI
FEC	Front End Controller

Fermilab	Fermi National Accelerator Laboratory
FESA	Front-End software Architecture
FPGA	Field Programmable Gate Array
FRS	Fragment Seperator
GCD	Greatest Common Divisor
GMT	General Machine Timing
GSI	GSI Helmholtzzentrum *für* Schwerionenforschung
GUI	Graphical User Interface
HESR	High Energy Storage Ring at GSI
HIRFL	Heavy Ion Research Facility at IMP
IMP	Institute of Modern Physics
J-PARC	Japan Proton Accelerator Complex
LEIR	Low Energy Ion Ring at CERN
LHC	Large Hadron Collider at CERN
LLRF	Low-level RF
LSA	LHC Software Architecture
MM	Management Master
MPS	Machine Protection System
MR	Main Ring at J-PARC
NESR	New Experimental Storage Ring at GSI
PAM	Phase Advance Measurement module
Pbar	Proton bar
PBHV	Primary Beam High Voltage
PBRF	Primary Beam Radio Frequency

PC	Personal Computer
PS	Proton Synchrotron at CERN
PSB	Proton Synchrotron Booster at CERN
RCS	Rapid Cycle Synchrotron at J-PARC
RESR	Recycled Experimental Storage Ring at GSI
rf	Radio Frequency
RHIC	Relativistic Heavy Ion Collide at BNL
RIB	Rare Isotope Beams
SBES	Experimentierspeicherring ESR
SCU	Scalable Control Unit
SFC	Sector Focusing Cyclotron at IMP
SHE-P	SHE-Physik
SIS100	SchwerIonen Synchrotron (100 Tm magnetic rigidity) at GSI
SIS18	SchwerIonen Synchrotron (18 Tm magnetic rigidity) at GSI
SIS300	SchwerIonen Synchrotron (300 Tm magnetic rigidity) at GSI
SM	Settings Management
SPS	Super Proton Synchrotron at CERN
SSC	Separated Sector Cyclotron at IMP
TM	Timing Master
TOF	Time-Of-Flight
TTL	Transistor–Transistor Logic
UNILAC	Universal Linear Accelerator at GSI

VLAN	Virtual LAN
WR	White Rabbit

Abbreviations related to FAIR B2B transfer system

B2B transfer master	Responsible for the data collection of two synchrotrons, the data calculation, the data redistribution and the B2B transfer status check
B2B target SCU	Collects the predicted phase of the target synchrotron and transfers it to the source synchrotron
B2B source SCU	Works as the B2B transfer master
PAP	Phase Advance Prediction module
PCM	Phase Correction Module
PSM	Phase Shift Module
SR	Signal Reproduction module
Trigger SCU	Production of the trigger signal for kicker electronics

Parameters related to synchrotron and beam

p	Particle momentum
R	Orbit radius
β	Relative speed to the speed of light
c	Speed of the light
γ	Relativistic factor, which measures the total particle energy, E, in units of the particle rest energy, E_0
E	Total particle energy
E_0	Particle rest energy
α_p	Momentum compaction factor
η	Phase-slip factor
q	Charge of a particle
α_b	Bucket area factor
ω_{syn}	Angular synchrotron frequency
B	Magnetic field
ρ	Bending radius of a particle immersed in a magnetic field B
h^X	Harmonic number of a specific synchrotron
ε	Adiabaticity parameter
ω_{syn_0}	Angular synchrotron frequency with no frequency modulation

$Q_{x/y}$	Horizontal/vertical tune
$Q^{‘}_{x/y}$	Horizontal/vertical chromaticity
$\Delta Q_{x/y}$	Horizontal/vertical tune shift
$Q^{‘}_{x}$	Horizontal chromaticity
$Q^{‘}_{y}$	Vertical chromaticity
ΔQ_{x}	Horizontal tune shift
ΔQ_{y}	Vertical tune shift
ϕ_s	Synchronous phase
f_{rf}	Rf frequency
h	Harmonic number
f_{rev}	Revolution frequency
V	Longitudinal accelerating voltage at rf cavity
V_0	Amplitude of the rf voltage
m_0	Rest mass
C^X	Circumference of the extraction/injection orbit of a specific synchrotron
f^X_{rev}	or $f^X_{h=1}$. Revolution frequency of a specific synchrotron
f^X_{rf}	or $f^X_{h=cavity\_harmonic}$. Cavity rf frequency of a specific synchrotron
T^X_{rev}	Period of the revolution period of machine X
T^X_{rf}	Period of the cavity rf frequency of machine X

Parameters related to FAIR B2B transfer system

f_{syn}^{X}	Synchronization frequency
$\Delta\varphi$	Phase step growth because of the frequency beating
T_{sync_win}	Length of the synchronization window
t_{bucket}	Time delay for a specific bucket pattern
t_{TOF}	Time-of-Flight between two synchrotrons
t_{v_ext}	Time corresponding to the distance between the virtual rf cavity and the extraction position of the source synchrotron
t_{v_inj}	Time corresponding to the distance between the virtual rf cavity and the injection position of the target synchrotron
t_{ext}	Extraction kicker delay
t_{inj}	Injection kicker delay
t_{diff_sync}	Time difference between rf systems of two synchrotrons after the synchronization
$\Delta\varphi^{X}$	Measured phase advance between the Reference RF Signal and the Synchronization Reference Signal of the synchrotron X by PAM module
ψ^{X}	Extrapolated phase advance between the Reference RF Signal and the Synchronization Reference Signal of the synchrotron X by PAP module

t_{ψ^X}	Timestamp corresponding to the extrapolated phase advance ψ^X
$f_{normalized}$	Normalized rf frequency modulation profile, preloaded from SM
f_{actual}	Actual rf freqnecy modulation profile, calculated by PSM
ψ_0^X	Initial phase advance in a linear relationship between the phase advance and time
t_{v_emg}	Time corresponding to the distance between the virtual rf cavity and the emergency extraction position of SIS100
t_{emg}	Extraction kicker delay of SIS100 for the emergency kick
t_{best}	Best estimate of alignment of zero crossing points of Reference RF Signals of source and target synchrotrons
δt_{best}	Uncertainty of the best estimate of alignment of zero crossing points of Reference RF Signals of source and target synchrotrons
$\psi_{h=1}^{SIS100}$	Predicted SIS100 h=1 rf phase at t_ψ
$\psi_{h=1/5}^{SIS18}$	Predicted SIS18 h=1/5 rf phase at t_ψ
t_ψ	Time of the predicted phase
$\phi_{h=2}^{SIS18}$	Phase at the h=2 cavity rf frequency of SIS18 at t_ψ
$\phi_{h=10}^{SIS100}$	Phase at the h=10 cavity rf frequency of SIS100 at t_ψ
δt_ψ	Uncertainty of the predicted phase advance at time domain
$\delta\psi_{h=1}^{SIS100}$	Uncertainty of the predicted SIS100 rf phase at h=1
$\delta\psi_{h=1/5}^{SIS18}$	Uncertainty of the predicted SIS18 rf phase at h=1/5

$\delta\phi_{h=10}^{SIS100}$	Uncertainty of rf phase at the h=10 cavity rf frequency of SIS100
$\delta\phi_{h=2}^{SIS18}$	Uncertainty of rf phase at the h=2 cavity rf frequency of SIS18
$T_{phase\_shift}^{upper\_bound}$	Upper bound time of the phase shift process
$\delta T_{phase\_shift}^{upper\_bound}$	Uncertainty of the upper bound time of the phase shift process
$\Delta\phi_{adjustment}$	Phase adjustment of the frequency beating method, calculated by B2B source SCU
Δf	Beating frequency
$\psi_{s\_alignment}$	Rf phase of the cavity driving frequency at the start of the probable rang of alignment
$\Delta t_{win\_correct}$	Time correction for the start of the probable range of alignment [t_{best}-δt_{best},t_{best}+δt_{best}] to the best estimate of the start of the synchronization window
G	Bunch gap
L	Distance from the leftmost to the rightmost SIS18 extraction/SIS100 injection kicker unit
D	Sum distance of d and the 2nd crate
d	Distance between two extraction kicker crates of SIS18
t_{B2B}	Start time of the B2B transfer
Δt	Beating time for the synchronization
f_{syn}^{REF}	Frequency of the Synchronization Reference Signal
$\Delta\phi$	Required phase shift for the phase shift method. Bunch-to-bucket injection center mismatch for the frequency beating method
Δf_{rf}	Rf frequency modulation for the phase shift method

T	Period of rf frequency modulation for the phase shift method
Y	Greatest common divisor
k^X	Slope of the phase advance between the Synchronization Reference Signal and a dedicated Reference RF Signal of the synchrotron X

Chapter 1

Introduction

Beam of high energy particles is useful for both fundamental and applied research in the sciences, and also in many technical and industrial fields unrelated to fundamental research. It has been estimated that there are approximately 30000 accelerators worldwide. Only about 1% of them are research machines with energies above 1 GeV [**?**]. As we all known, particles are accelerated by the electric field. The radio frequency (rf) system is devoted to generate the electric field at rf cavities around the ring. Particles are accelerated when they pass through rf cavities. Every rf cavity has a limited frequency range, so particles at rest could not be accelerated to several tens of GeV energy in one ring accelerator. Hence, the acceleration must be divided into several energy stages: the first energy stage is achieved usually by a small ring, which is called "booster" and the second stage by a large ring, which is usually called "main ring". The energy of a beam is related to the 'magnetic rigidity' of the dipole magnet, which is the multiplication of the magnetic field and the bending radius of a particle immersed in the magnetic field. At the time of the beam transfer, the magnetic rigidity of the booster must be equal to that of the main ring. Since the bending radius of the main ring is generally larger than that of the booster, the magnetic field in the main ring starts the further acceleration at a lower level. This allows a continuous increasing of the particle energy until the limits of the dipole magnets of the main ring. The usage of the booster and the main ring works faster to reach the required beam energy, because the booster can be filled and accelerated, when the main ring accelerates particles. The faster acceleration has the advantage to reduce the interaction time between the accelerated particles and the residual-gas atoms in the vacuum chamber, achieving a better beam quality [**?**]. Furthermore, the particle beam transfer among different rings is also used for the production of high intensity beam, e.g. the beam is transferred to a storage ring for the beam accumulation and the beam compression. Hence, the transfer of beam between rings is of great importance for high energy, high intensity and high quality beam.

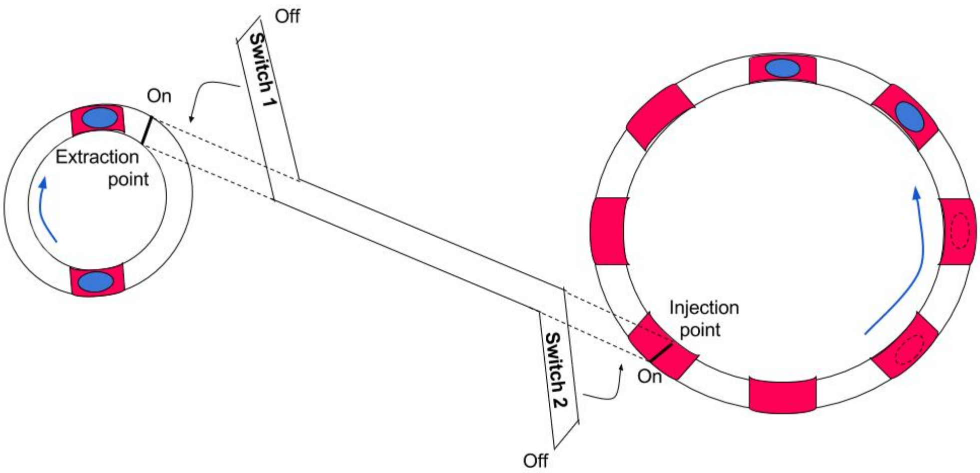

Figure 1.1: Illustration of a bunch-to-bucket transfer.
Red rectangles represent buckets and blue dots bunches.

The beam transfer is not arbitrary. A bunch of particles running in a ring should be transferred into the correct position of another ring. Fig. 1.1 illustrates the transfer of a bunch of particles between two rings. The example in Fig. 1.1 is with the circumference ratio between the right and left rings of four. Bunches of particles are transferred from the left ring to the right one. The blue ellipse represents a bunch of particles and the red rectangle represents the allowable area for particles to be injected. The red rectangles are equally spaced around the ring and determined by the rf frequency. The white space between two red rectangles is forbidden for particles. The allowable area (red rectangle) for particles is termed as a "bucket" and a bunch of particles (blue ellipse) as a "bunch". The definition of a bunch and a bucket from the accelerator physics perspective, please see Chap. 2. There are two buckets at the left ring and every bucket keeps a bunch. There are eight buckets in the right ring and two of them are filled with bunches. The left ring is connected to a track by a switch, which is called a "switch 1". When the switch 1 is off, bunches circulate around the ring. When it is on, bunches will be guided from the ring to the track at a specific position around the ring, which is called the "extraction point" (represented as a black short bar on the left ring). The track is connected to the right ring by another switch, called a "switch 2". When the switch 2 is on, bunches will be guided from the track to the right ring at a specific position around the ring, which is called the "injection point" (represented as a black short bar on the right ring). Generally both switches are off. The bunch-to-bucket (B2B) transfer is defined as that bunches of the left ring are transferred to the correct buckets at the right ring. For the B2B transfer, bunches at the left ring and buckets at the right ring must have not only a constant but same velocity. Because the circumference of the right ring is four times longer than that of the left ring, bunches run four cycles of the left ring when buckets run one cycle of the right ring. The distance between two bunches of the left ring is equal to the distance between two continuous buckets of the right ring. Besides, the relative position between bunches and buckets must match. Bunches of the left ring are guided to the track and transferred to the right ring. They are guided exactly to two empty buckets of the right ring. Every time when a bunch of the left ring passes by the extraction point, a bucket of the right ring will pass by the injection point after a specific time delay, which equals to the time-of-flight of a bunch on the track. What's more, the time for the track switch-on is of great importance, determining which buckets to be filled. In Fig. 1.1, two empty buckets closely following the filled buckets of the right ring need to be filled (represented as the dotted ellipse). The switch 2 must be switched on when the first empty bucket following two filled buckets passes the injection point and the switch 1 must be switched on a specific time earlier, when a bunch passes by the extraction point.

The ring is called a "source ring", from which the beam is extracted. The ring is called a "target ring", into which the beam is injected. From the above illustration, several preconditions are compulsory for the B2B transfer. The first precondition is that bunches of the source ring and buckets of the target ring have a constant speed, namely the revolution frequency of two rf systems of the source and target rings must be constant. Beam feedback loops on the rf system are usually implemented in order keep the stability of the beam. The constant revolution frequency requires that the beam feedback loop must be switched off before the B2B transfer. The second precondition is that bunches and buckets are with a same speed, which requires that the revolution frequency ratio between two rings is equal to the reciprocal of the circumference ratio. When the circumference ratio between two rings is an integer, the phase difference between two revolution frequencies is constant. It means that bunches always pass the extraction position a constant time earlier/later before/after buckets pass the injection position. But the constant phase difference is not correct for the transfer. In order to get the correct phase difference, an azimuthal positioning of bunches in the source ring or buckets in the target ring must be adjusted. This is called "phase shift method". After the phase shift, the phase difference of two revolution frequencies is correct and the correct phase difference keeps infinite theoretically. Because beam feedback loops are switched off, the beam is stable only for a period of time. So the beam must be transferred as soon as possible. When the circumference ratio is not an integer, the phase difference between two revolution frequencies varies periodically. Within one period, there must be one time point when the phase difference between two rf systems is correct. Before and after this time point, there exists the mismatch between bunches and buckets. The earlier and later than this time point within a period, the larger the mismatch. This is called "frequency beating method". For both the phase shift and frequency beating methods, the transfer can only happen when the mismatch is smaller than a tolerate limit, introducing a time frame. The time frame is called the "synchronization window", which achieves the "coarse synchronization".

Bunches are switched from one path to another path by kicker magnets (short: kicker). The extraction kicker kicks bunches out of the source ring to the track and the injection kicker kicks them from the track into buckets of the target ring. They are located at the extraction position and injection position in Fig. 1.1. When the phase difference between two rf systems is correct, the extraction kicker could kick bunches of the source ring at the exact time-of-flight to the track before empty buckets pass the injection kicker. With the synchronization window, the extraction and injection kickers must be fired at the correct time in order to transfer bunches into correct empty buckets. The process of the kicker firing at the correct time is termed as the "fine synchronization".

1.1 Usage of the bunch-to-bucket transfer worldwide

Nowadays, there are several accelerator institutes in the world, who operate the B2B transfer among rings for specific purposes. CERN, the European Organization for Nuclear Research, is one of the world's largest and most respected center for scientific research. The Large Hadron Collider (LHC) beam injection chain achieves the proton beam with the energy of 7 TeV. After accelerated by a linear accelerator, bunches are injected into buckets of the Proton Synchrotron Booster (PSB) and further into the Proton Synchrotron (PS), the Super Proton Synchrotron (SPS) and LHC [?]. For the LHC heavy ion beam injection chain with the achievement of the energy of 2.76 TeV/u, bunches are first of all injected into the Low Energy Ion Ring (LEIR) and the following transfer from PSB to LHC is same as the proton beam chain [?]. For Japan Proton Accelerator Complex (J-PARC), bunches are transferred from the Rapid Cycle Synchrotron (RCS) to buckets of the Main Ring (MR) [?]. The Booster of Brookhaven National Laboratory (BNL) transfers bunches to buckets of the Alternating Gradient Synchrotron (AGS) and bunches of AGS are transferred further into the Relativistic Heavy Ion Collider (RHIC) [?]. Fermi National Accelerator Laboratory (Fermilab)'s accelerator complex provides high energy proton beams for a broad range of experiments. Proton beams are injected into the Recycler from the Fermi National Accelerator Laboratory (Fermilab) Booster. Then the proton beam enters the Main Injector from the Recycler. The beam is accelerated to the energy of 120 GeV. Some of the proton beam from the Booster will be used to produce a beam of special particles for Muon Delivery Ring. The Muon Delivery Ring delivers the beam into a muon storage ring for further study [?]. Institute of Modern Physics of the Chinese Academy of Sciences (IMP) operates the Heavy Ion Research Facility (HIRFL) in Lanzhou. Two existing cyclotrons, the Sector Focusing Cyclotron (SFC) and the Separated Sector Cyclotron (SSC), are used as an injector system for the Cooler Storage Ring main ring (CSRm) for the accumulation, cooling and acceleration. Then the beam is extracted from CSRm to produce radioactive ion beams or highly-charged heavy ions, which can be transferred to the Cooler Storage Ring experimental ring (CSRe) for many experiments [? ?].

FAIR, Facility for Antiproton and Ion Research, is a new international accelerator facility under construction at GSI Helmholtz center for Heavy Ion Research GmbH (short: GSI)[1] [? ?]. It is aiming at providing high-energy beams of ions from antiproton to uranium with high intensities. The new FAIR accelerator complex with storage rings consists of the SIS100[2], the SIS300[3], the Collector Ring (CR), the Recycled Experimental Storage Ring (RESR), the New Experimental Storage Ring (NESR) and the Hign Energy Storage Ring (HESR) [? ?]. FAIR has so many rings, so the B2B transfer among FAIR ring accelerators is of great importance to accelerate beams to higher energy with high intensity and achieve beams for various experiments. Based on the existing GSI UNILAC and SIS18 serving as injectors, high intensity ion beams over the whole range of stable isotopes will be

[1]Planckstrasse 1, 64291 Darmstadt, www.gsi.de
[2]SIS18 stands for SchwerIonen Synchrotron (100 Tm magnetic rigidity).
[3]SIS300 stands for SchwerIonen Synchrotron (300 Tm magnetic rigidity).

accelerated in the new heavy ion machine SIS100/SIS300 to higher energy. The beam from the SIS100 will be transferred to the CR via the proton bar (Pbar) [4] or the Superconducting Fragment Separator (Super-FRS) [5]. The CR has the purpose of stochastic cooling of both secondary rare isotope and antiproton beams and of measuring nuclear masses [? ?]. The CR transfers the beam to the HESR and further to the RESR for the accumulation. The HESR serves experiments with high energy antiproton and rare isotope beams [?]. The proton and heavy ion beam could also be transported from the SIS18 to the existing GSI Experimental Storage Ring (ESR) and further to the first FAIR-storage ring CRYRING@ESR (short: CRYRING) for the atomic and nuclear physics experiment [? ?]. The proton and heavy ion could also be transferred from SIS18 to ESR via the Fragment Separator (FRS)[6].

For many FAIR accelerator pairs, the circumference ratio between the large and small rings is an integer, e.g. the SIS100 and the SIS18, so the phase difference between two revolution frequencies of rings is constant. The frequency is in the MHz range. In this scenario, the phase shift method must be used for the match of the phase difference between two rf systems. When the circumference ratio between FAIR accelerator pairs is not an integer, e.g. the SIS18 and the ESR [7], the phase difference between two revolution frequencies shifts automatically. The frequency of the phase difference variability is in the kHz range. The synchronization window for the FAIR B2B transfer is in the us range. The beams of ion species, from hydrogen to uranium as well as antiprotons, should be transferred among all rings. And every transfer must be achieved within the upper bound 10 ms and the B2B injection mismatch in the range between -1° and $+1^\circ$. Both the phase shift and the frequency beating method should be applicable in the upcoming FAIR facilities. The B2B transfer system is designed to work in a parallel operation, e.g. the transfer from SIS18 to SIS100 and the transfer from ESR to CRYRING can be performed at the same time. It is cable to transfer the beam between two rings via a FRS or a Super FRS. The B2B transfer system must coordinate with the SIS100 emergency dump for all unacceptable failure or situation.

1.2 Objectives, Contribution and Structure of the Dissertation

This dissertation contributes to the development of the FAIR B2B transfer system from the timing perspective. It concentrates on the introduction of the concept of the FAIR B2B transfer system and its application for FAIR accelerators. In addition, it explains the systematic investigation for the FAIR B2B transfer system in details.

The dissertation is structured as follows and as depicted in Fig. 1.2.

[4] Pbar is used to produce antiprotons in inelastic collisions of high energy protons with nucleons of a target nucleus.

[5] Super-FRS is used to produce rare isotopes of all elements up to uranium at relativistic energies and spatially separate them within a few hundred nanoseconds.

[6] An ion-optical device used to focus and separate products from the collision of relativistic ion beams with thin targets.

[7] ESR has an injection/extraction orbit, which is 15 cm longer than the design orbit. The orbit of ESR in this dissertation means the injection/extraction orbit.

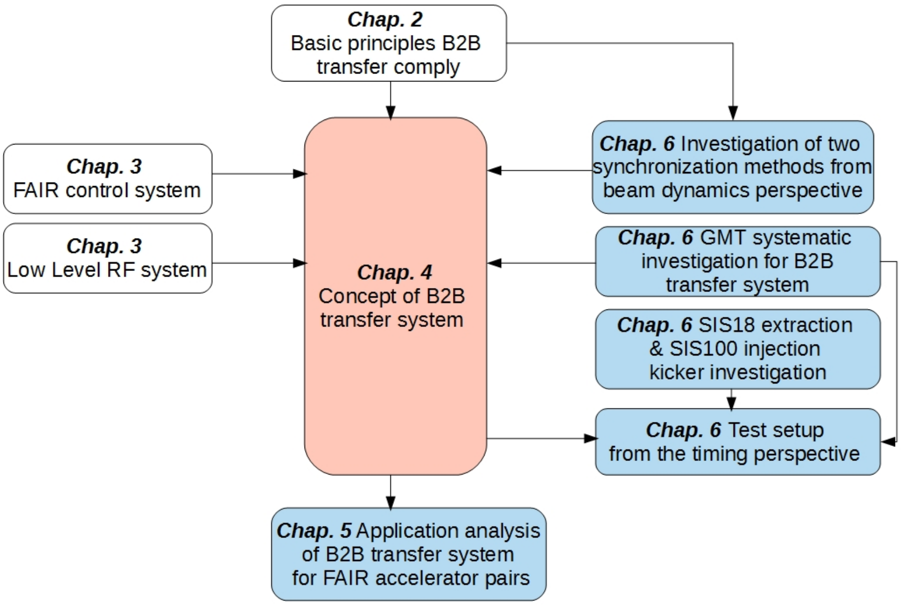

Figure 1.2: The structure of the dissertation.
Contributions are marked blue and red is team work, existing systems or theory are not colored.

In Chap.2, the theoretical background for the B2B transfer are reviewed. First of all, the energy, phase and voltage match between the source and target synchrotrons are introduced. Secondly, two rf synchronization methods are discussed from the perspective of beam dynamics in order for the phase alignment. At the end of this chapter, the synchronization of the extraction and injection kicker magnets are discussed.

Chap.3 is concerned with the existing FAIR technical basis for the development of the FAIR B2B transfer system and the uniqueness of the system. The B2B transfer system is realized based on the FAIR control system and low-level rf system, so these two systems are introduced. In addition, the comparison between the FAIR B2B transfer system and the current B2B transfer with the GSI control system is discussed before the chapter ends.

In Chap.4, a brief overview on the basic idea of the B2B transfer system is presented. After that the basic procedure of the FAIR B2B transfer is introduced and the realization of each step of the procedure is explained. In addition, the FAIR B2B transfer system is explained from the data flow perspective.

The application of the FAIR B2B transfer system for FAIR accelerator pairs are outlined in Chap.5. The applications are classified into three categories according to the feature of the circumference ratio. For many pairs with an integral circumference ratio, e.g. the SIS18 and the SIS100, the ESR and the CRYRING, there is a constant phase difference between two rf system. Although the phase shift can be used for the phase match, the frequency beating method is preferred via the detune of one rf system. Because the phase shift must be executed slowly enough to guarantee the beam quality, which needs much longer time than the frequency beating method. The ratio of the circumference between many pair of machines in FAIR is close to an integer or far away from an integer, e.g. the SIS18 and the ESR, the SIS100 and the CR, the CR and the HESR. the phase match is achieved by the frequency beating. For each category, the corresponding FAIR applications are presented.

Chap.6 presents the systematic investigation for the B2B transfer system, mainly focusing on the timing aspect. The calculation of the synchronization window is explained and the transfer of the B2B messages via the WR network is tested. In addition, for the B2B transfer from the SIS18 to the SIS100, two synchronization methods are analyzed from the perspective of the beam dynamics. The SIS18 extraction and the SIS100 injection kicker are systematically investigated. Finally, the test setup is presented and the result is analyzed.

Chapter 2

Theoretical background

In Chap. 1, the bunch and bucket are introduced with simplified definition. In this chapter, the bunch and bucket are first of all defined from the accelerator physics perspective in Sec. 2.1. Transferring bunches from a synchrotron into specific buckets of another synchrotron has several underlying basic principles. The energy of the beam is same before and after the B2B transfer, so the energy of the source synchrotron must match that of the target synchrotron. The voltage match of two rf systems is needed to ensure that buckets capture bunches efficiently. Principally speaking, every synchrotron has its independent rf system. The phase difference between bunches and buckets must be precisely controlled before the transfer. The energy and voltage match will be done by machine physicists, which are out of the scope of this dissertation, so only the phase match is explained in detail in Sec. 2.2. Two methods for the phase alignment between two rf systems are discussed in Sec. 2.3. For the correct bucket injection, the bunch extraction must happen exactly the time-of-flight before the required bucket of the target synchrotron passes the injection kicker. The synchronization of extraction and injection kicker magnets are presented in Sec. 2.4.

2.1 Bunch and bucket

For a ring accelerator, particles gain energy from electric field in longitudinal direction and are deflected by magnetic field to a particle orbit. A rf cavity operating at a resonance condition is used to provide a longitudinal accelerating voltage[1] V in the vacuum chamber.

$$V = V_0 \sin(\phi_s + 2\pi f_{rf} t) \tag{2.1}$$

where V_0 is the amplitude of the rf voltage, ϕ_s is a phase factor, and f_{rf} is the rf frequency. In order to accelerate particles with an accelerating voltage at the rf cavity, the cavity rf frequency must always be an integer multiple of the revolution frequency of particles.

$$f_{rf} = h f_{rev} \tag{2.2}$$

where the integer multiple h is called “harmonic number“.

A particle who always sees rf phase ϕ_s at the rf cavity with the revolution frequency f_{rev} and the momentum p is called a “synchronous particle“. For circular

[1]Rf voltage with a single harmonic operation is considered in this dissertation.

accelerators, the revolution frequency is decided by the machine circumference and the particle velocity.

$$f_{rev} = \frac{\beta c}{2\pi R} \tag{2.3}$$

where R is the radius of the machine, β the relative velocity to the speed of light and c the speed of light. The differential of eq. 2.3 is

$$\frac{\Delta f_{rev}}{f_{rev}} = \frac{\Delta\beta}{\beta} - \frac{\Delta R}{R} \tag{2.4}$$

Because of the relation $\Delta f_{rf}/f_{rf} = \Delta f_{rev}/f_{rev}$, so eq. 2.4 can be written as

$$\frac{\Delta f_{rf}}{f_{rf}} = \frac{\Delta\beta}{\beta} - \frac{\Delta R}{R} \tag{2.5}$$

The momentum of the synchronous particle p is related to the particle energy and its velocity.

$$p = \gamma\beta m_0 c \tag{2.6}$$

where m_0 is the rest mass and $\gamma = (1-\beta^2)^{-\frac{1}{2}}$. γ is the relativistic factor, which measures the total particle energy, $E= pc/\beta$, in units of the particle rest energy, $E_0= m_0c^2$.

The fractional change in β is related to the fractional change in p.

$$\frac{\Delta p}{p} = \gamma^2\frac{\Delta\beta}{\beta} \tag{2.7}$$

Substituting $\Delta\beta/\beta$ into eq. 2.5, we get

$$\frac{\Delta f_{rf}}{f_{rf}} = \frac{1}{\gamma^2}\frac{\Delta p}{p} - \frac{\Delta R}{R} \tag{2.8}$$

For the constant magnetic field, a particle will have a different orbit, if it is slightly shifted in momentum. The "momentum compaction factor" $\alpha_p{}^2$ is defined as:

$$\frac{\Delta R}{R} = \alpha_p\frac{\Delta p}{p} \tag{2.9}$$

Substituting eq. 2.9 into eq. 2.8, we finally obtain the required relation between the frequency offset and the momentum error.

$$\frac{\Delta f_{rf}}{f_{rf}} = (\frac{1}{\gamma^2} - \alpha_p)\frac{\Delta p}{p} \tag{2.10}$$

The phase-slip factor η is defined as

$$\eta = \frac{1}{\gamma^2} - \alpha_p \tag{2.11}$$

which gives the relationship between the revolution frequency and the momentum for a given accelerator. When particles are at low energy ($\eta > 0$), they run faster and arrive earlier at the rf cavity. When they are at high energy close to the speed of light ($\eta < 0$), they can not run faster, but rather obtain more mass and are pushed to a dispersive orbit, resulting a late arrival at the rf cavity [**?**].

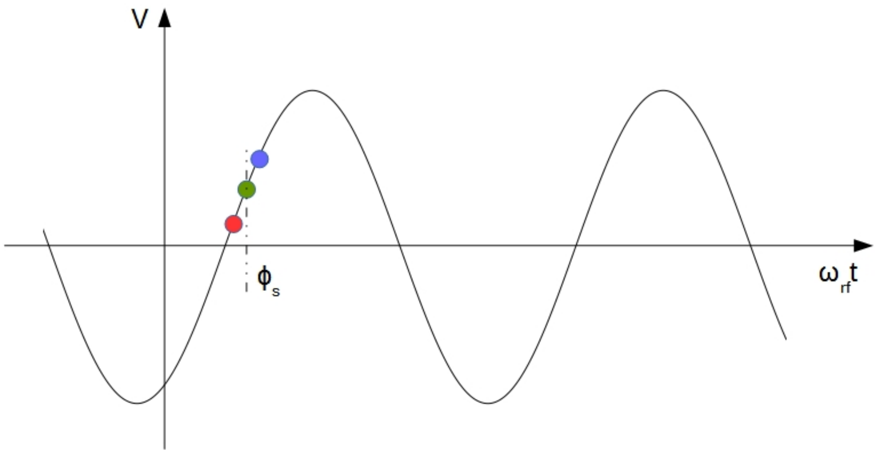

Figure 2.1: The longitudinal focusing of particles by a rf voltage ($\eta > 0$). The red spot represents a particle with a hihger energy, the blue spot a particle with a lower energy and the green dot the synchronous particle.

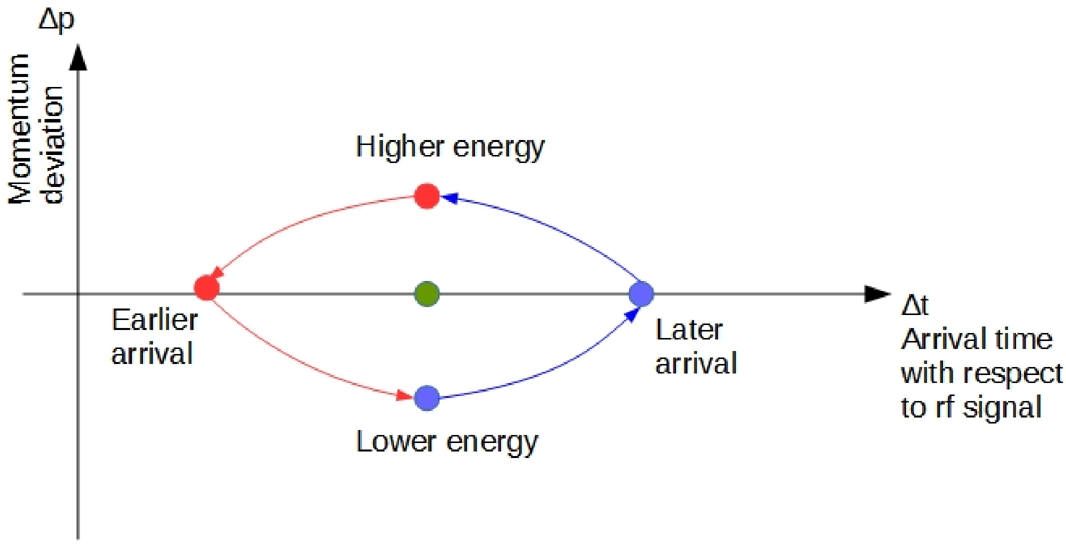

Figure 2.2: The longitudinal motion of asynchronous particles in the longitudinal phase space plane ($\eta > 0$).
The red spot represents a particle with a higher energy, the blue spot a particle with a lower energy and the green dot the synchronous particle. The red arrow shows the trend of a particle with a higher energy and the blue arrow the trend of a particle with a lower energy.

A bunch of particles consists of particles with slightly different momentum as the synchronous particle, which are called “asynchronous particles“. When $\eta > 0$, the longitudinal focusing of particles is explained in Fig. 2.1.

The synchronous particle is indicated by the green spot in Fig. 2.1. It will gain the energy of $qV_0 \sin\phi_s$ per passage through a rf cavity, where q is the charge

[2]FAIR complex is with $\alpha_p > 0$.

of a particle. When $\eta > 0$, a particle with a smaller energy (blue spot) than the synchronous particle will run slower and have a longer revolution period, arriving the same rf cavity later and seeing a higher accelerating voltage. This particle has a decreasing revolution period to the revolution period of the synchronous particle. During the decreasing process, the lack of energy is compensated step-by-step approaching to the energy of the synchronous particle. Oppositely for a particle with a higher energy. As it is faster than the synchronous particle and has a shorter revolution period, it will arrive at the rf cavity earlier, seeing a smaller accelerating voltage. This particle has an increasing revolution period to the revolution period of the synchronous particle. During the increasing process, the excess energy will be reduced step-by-step approaching to the synchronous particle. Asynchronous particles will oscillate longitudinally around the synchronous particle. This longitudinal motion is plotted in the longitudinal phase space plane, See Fig. 2.2.

All particles oscillate around the synchronous particle and stay together, forming a "bunch". The "bunch gap" is the area without any bunches. The area occupied by a bunch in the longitudinal phase space plane is called the "longitudinal emittance". First of all, we consider the synchronous particle with the synchronous phase 0°. In this scenario, particles with a small energy deviation follow an elliptical path inside the bunch. For a given rf system with a specific rf voltage and harmonic number, there exists a maximum energy deviation. For particles with energy deviations larger than the maximum energy deviation, they can not be trapped around the synchronous particle. The trajectory of a particle with the maximum energy deviation in longitudinal phase space plane defines a region with a specific size and form. This region is called the "rf bucket" or "stationary rf bucket", see Fig. 2.3. The maximum momentum deviation of the rf bucket is called the "bucket height". These buckets will exist as soon as the rf system is on and the number of circulating buckets is determined by the harmonic number and the bucket area and height are proportional to the rf voltage [**?**]. The order of buckets to be filled is called the "bucket pattern".

So far we give the definition of the bucket, when the synchronous particle sees no accelerating rf voltage. When the synchronous particle is accelerated, seeing the synchronous phase ϕ_s per passage through an rf cavity, it will gain the energy of $qV_0 \sin \phi_s$. Particles oscillate around the synchronous particle at ϕ_s with an elliptical orbit. The particle at $\pi - \phi_s$ traces a closed fish-shaped orbit, which defines a "running rf bucket", see Fig. 2.4. Particles at bigger phase than $\pi - \phi_s$ can not be captured by the bucket.

The "bucket size" is defined as the area of the longitudinal phase space plane enclosed by the bucket [**?**]. For a same rf voltage, the bucket size of a running bucket is always smaller than that of a stationary bucket. The ratio of the bucket size of a running bucket to that of a stationary bucket is called the "bucket area factor", α_b. The bucket area factor could be calculated by [**?**].

$$\alpha_b(\phi_s) \approx (1 - sin(\phi_s))(1 + sin(\phi_s)) \tag{2.12}$$

The oscillation of asynchronous particles is called the "synchrotron motion". The

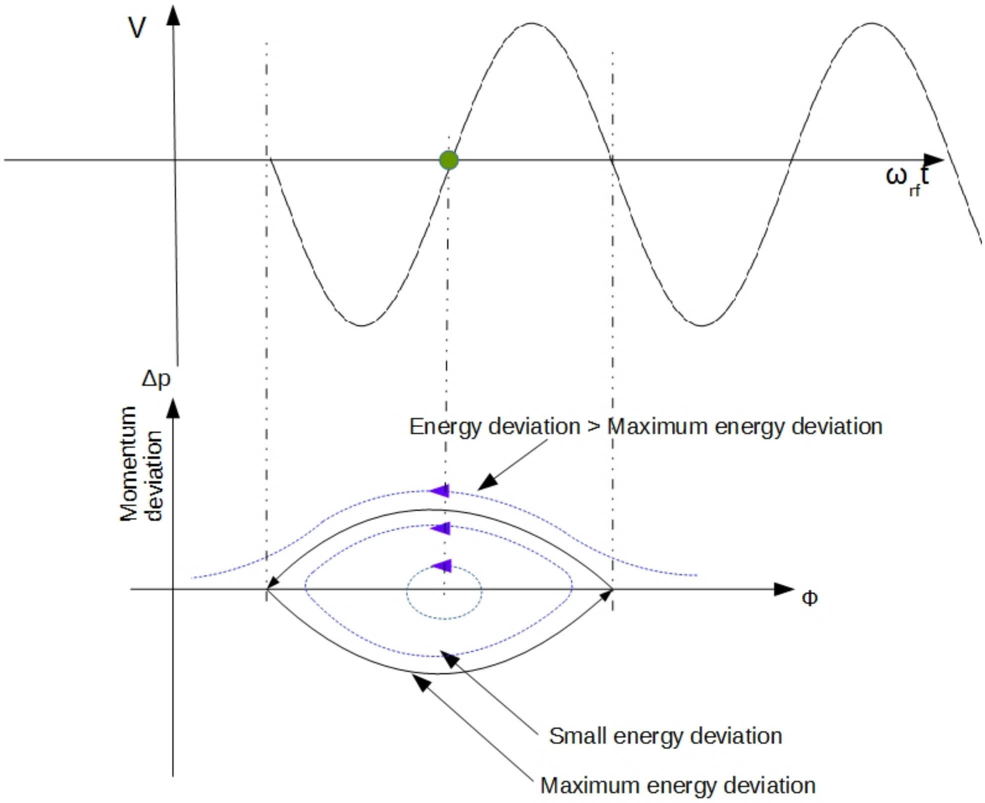

Figure 2.3: A stationary rf bucket.
The green dot represents the synchronous particle (top), the blue path orbits of asynchronous particles and the black path the boundary of a stationary rf bucket (bottom).

angular synchrotron frequency [3] ω_{syn} is [**?**]

$$\omega_{syn} = 2\pi f_{rev} \sqrt{\frac{hqV_0 |\eta \cos \phi_s|}{2\pi \beta^2 E_0}} \tag{2.13}$$

Bunches are always captured in buckets. A synchrotron can have same amount of bunches as buckets. It is also possible for a synchrotron to have less amount of bunches than buckets, e.g. only a part of buckets are filled by bunches. A train of bunches circulating along a synchrotron to be transferred to buckets is defined as a "batch".

The energy of a beam is related to the 'magnetic rigidity', which is defined as the following:

$$B\rho = \frac{p}{q} \tag{2.14}$$

where B is magnetic field, and ρ is the bending radius of a particle immersed in a magnetic field B. The ratio of p to q describes the "stiffness" of a beam, it can be considered as a measure of how much angular deflection results when a particle travels through a given magnetic field [**?**]. The relation between a rf cavity and the beam acceleration rate is

$$V_0 \sin \phi_s = 2\pi R \rho \dot{B} \tag{2.15}$$

[3]For the small-amplitude synchrotron motion.

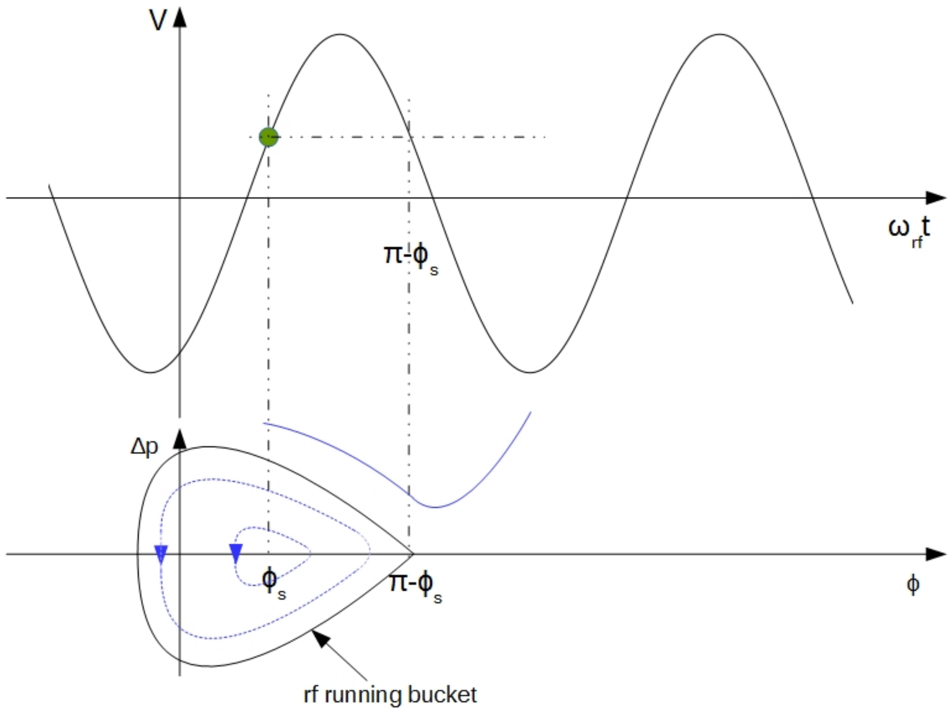

Figure 2.4: A running rf bucket.
The green dot represents the synchronous particle (top), the blue path orbits of asynchronous particles and the black path the boundary of a running rf bucket (bottom).

Bunches must be injected exactly in the center of buckets for the preservation of the longitudinal emittance, which requires the energy and phase match between bunches and buckets. Besides, the shape of bunches to be transferred must match the shape of buckets to be injected in the longitudinal phase space plane. If the source and target synchrotrons have same cavity rf frequency, buckets of the source synchrotron must have same size and height as that of the target synchrotron. The voltage mismatch between bunches and buckets will cause an emittance blow-up. Fig. 2.5 illustrates a bunch-to-bucket injection with an energy, a phase or a voltage error.

The bunch coordinates in the longitudinal phase space plane of the source synchrotron, just before transfer, must be accurately controlled, according to the bucket to be filled [**?**]. The bunch is transferred from the source to the target synchrotron with the same energy. So the beam has the same momentum for both synchrotrons. According to eq. 2.14, the magnetic rigidity of two synchrotrons must be same.

$$(B\rho)^{src} = \frac{p}{q} = (B\rho)^{trg} \tag{2.16}$$

Where the superscript of the symbol denotes the synchrotron, *src* represents the source synchrotron and *trg* the target synchrotron.

Before the B2B transfer, the revolution frequency of two synchrotrons must meet the following relation based on eq. 2.3.

$$C^{src} f_{rev}^{src} = \beta c = C^{trg} f_{rev}^{trg} \tag{2.17}$$

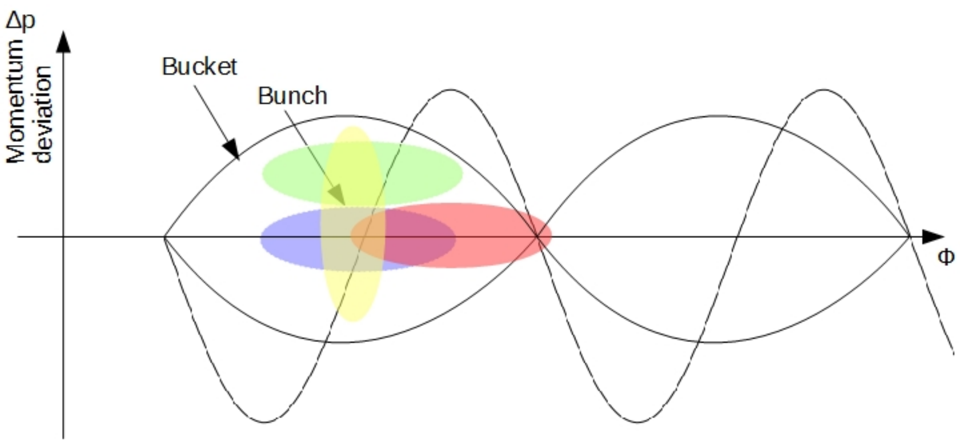

Figure 2.5: The bunch-to-bucket injection with a phase, energy or voltage error. The blue dot represents an injection without any error, the red dot an injection with a phase error, the green an injection with a energy error and the yellow an injeciton with a voltage error.

where C^X represents the circumference of a specific synchrotron. A group of new symbols are necessary to be defined. The revolution frequency and cavity rf frequency are denoted by f_{rev}^X and f_{rf}^X, the harmonic number by h^X. The superscript X could be either src or trg denoting the source or target synchrotron.

Due to the relation between the revolution frequency and cavity rf frequency, eq. 2.2, the ratio between cavity rf frequencies of two rf systems is

$$\frac{f_{rf}^{src}}{f_{rf}^{trg}} = \frac{h^{src}}{h^{trg}} \cdot \frac{f_{rev}^{src}}{f_{rev}^{trg}} = \frac{h^{src}}{h^{trg}} \cdot \frac{C^{trg}}{C^{src}} \tag{2.18}$$

The energy and voltage match will be done by machine physicists, which are out of the scope of this dissertation. The dissertation concentrates on the phase match.

2.2 Phase difference

The rf voltage of two rf systems are v_1 and v_2.

$$v_1 = V_1 \sin(2\pi f_1 t + \phi_1) \tag{2.19}$$

$$v_2 = V_2 \sin(2\pi f_2 t + \phi_2) \tag{2.20}$$

where V_1 and V_2 are the amplitude, ϕ_1 and ϕ_1 the initial phases and f_1 and f_2 are the frequencies of two rf voltages. The phase difference $\Delta\phi$ is the difference, expressed in degree, between two rf voltage sinusoidal waves referenced to the same point in time.

The phase difference between v_1 and v_1 is

$$\Delta\phi = [2\pi(f_1 - f_2)t + \phi_1 - \phi_2] \mod 2\pi \tag{2.21}$$

The phase difference $\Delta\phi$ is constant when two frequencies are same. In order to change the phase difference for the phase match between two rf voltage sinusoidal waves, the phase of either (or both) rf system can be shifted backward or forward by means of the rf frequency modulation. The frequency of one (or both) rf voltage sinusoidal wave is modulated away from the nominal value for a specified period of time and then modulated back. This is the so-called phase shift. Eq. 2.22 gives the relation between the required phase shift $\Delta\phi$ and the frequency modulation.

$$\Delta\phi = 2\pi \int_{t_0}^{t_0+T} \Delta f_{rf}(t)dt \tag{2.22}$$

The phase shift process starts at t_0. The obtainable phase shift is determined by the frequency offset Δf_{rf} and the duration of the frequency modulation T.

When two frequencies are slightly different, the phase difference $\Delta\phi$ is a periodical variation whose rate is the difference between the two frequencies. This is the so-called frequency beating. The periodically variable rate is called the "beating frequency", $\Delta f = |f_1 - f_2|$. The beating period is defined as a period of time for the periodical variation, namely $1/\Delta f$. Within one beating period, there exists a time point, which corresponds to a correct phase difference between two rf systems, namely the phase alignment.

The phase alignment is realized based on two same or two slightly different frequencies. These two frequencies are called "synchronization frequencies", denoted as f_{syn}^X. Some FAIR use cases are with an identical cavity rf frequency or slightly different cavity rf frequencies of two rf systems, so two cavity rf frequencies are chosen as the synchronization frequencies. There exists many FAIR use cases with hugely different cavity rf frequencies as well. In this scenario, two synchronization frequencies are an integral multiple of the same or slightly different derived rf frequencies, which are the division of the revolution frequencies. e.g. the division of the revolution frequency is f_{rev}^X/m and the synchronization frequency is $Y \cdot f_{rev}^X/m$, both m and Y are positive integers. The division of the the revolution frequency and the integral multiple are determined by the circumference ratio and the harmonic number of two synchrotron. Because of the technical requirement (see Chap. 4), the synchronization frequencies are impossible to have higher frequencies than cavity rf frequencies, namely $Y/m <= h^X$. Besides, m/Y is an integer for FAIR use cases, namely the revolution frequency is an integral multiple of the synchronization frequency, so the positive zero-crossings of two synchronization frequencies always indicates a specified bunch and bucket.

The calculation of the sycnhronization frequencies are explained for the different scenarios of the circumference ratio between two synchrotrons. For simplicity's sake, the following analysis is from the perspective of the large and small synchrotrons instead of the source and target synchrotrons. The superscript X of C^X, f_{rev}^X, f_{rf}^X and h^X will be either l or s denoting the large or small synchrotron. Δf represents the beating frequency, κ, m, n and Y are used to represent positive integers and λ a decimal number.

2.2.1 Circumference ratio is an integer

If the ratio of the circumference of the injection/extraction orbit of the large synchrotron to that of the small synchrotron is an integer, we have the following relation.

$$\frac{C^l}{C^s} = \kappa \tag{2.23}$$

From the circumference ratio, the revolution frequency ratio of two synchrotrons can be calculated.

$$\frac{f_{rev}^l}{f_{rev}^s} = \frac{1}{\kappa} \tag{2.24}$$

Based on eq. 2.24 and the harmonic number, the cavity rf frequency f_{rf}^X is calculated by eq. 2.25 and eq. 2.26

$$f_{rf}^s = h^s \cdot f_{rev}^s = h^s \cdot \kappa \cdot f_{rev}^l \tag{2.25}$$

$$f_{rf}^l = h^l \cdot f_{rev}^l \tag{2.26}$$

Dividing eq. 2.26 by eq. 2.25, we get

$$\frac{f_{rf}^l}{f_{rf}^s} = \frac{h^l}{h^s \cdot \kappa} \tag{2.27}$$

In this scenario, the same synchronization frequencies are f_{rf}^l/h^l and $f_{rf}^s/(h^s\kappa)$. Substituting two same synchronization frequencies into eq. 2.21, we get the constant phase difference $\Delta\phi$. Fig. 2.6 shows the constant phase difference between two same synchronization frequencies f_{rf}^l/h^l and $f_{rf}^s/(h^s\kappa)$, when $\kappa = 5$, $h^s = 1$ and $h^l = 10$.

$$\Delta\phi = (\phi_l - \phi_s) \mod 2\pi \tag{2.28}$$

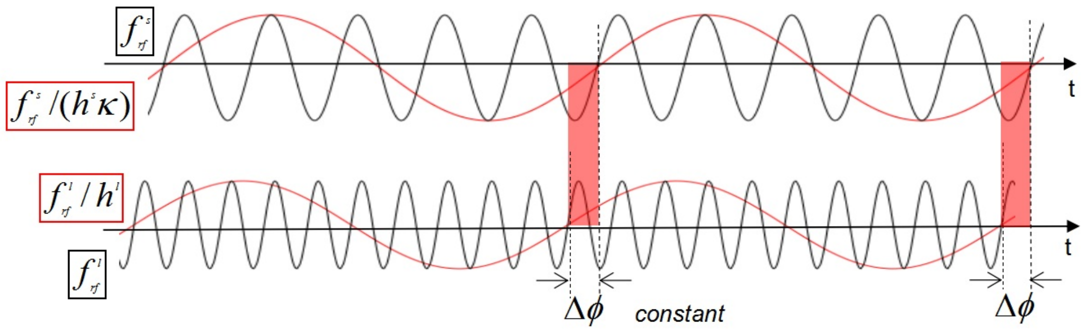

Figure 2.6: The constant phase difference between one possible pair of the synchronization frequencies when $\kappa = 5$, $h^s = 1$ and $h^l = 10$.
Red rectangles represent the constant phase difference periodically and red sinusoidal waves the synchronization frequencies. Black sinusoidal waves represent the cavity rf frequencies.

So far we get only one possible pair of the synchronization frequencies for the phase shift, but this pair is not the best one. It is easier for the LLRF system to produce synchronization frequencies closer to f_{rf}^l and f_{rf}^s. What is more, the possible pair with large frequencies reduces the period of the occurrence of the required phase difference. Hence, the pair of the synchronization frequencies with largest possible frequencies are preferred. More detailed explanation, please see Chap. 5. Two synchronization frequencies are chosen as

$$f_{syn}^l = \frac{f_{rf}^l}{h^l/Y} = Y f_{rev}^l \tag{2.29}$$

$$f_{syn}^s = \frac{f_{rf}^s}{h^s \kappa / Y} = \frac{Y}{\kappa} f_{rev}^s \tag{2.30}$$

where Y is defined as the Greatest Common Divisor (GCD) of h^l and $h^s \cdot \kappa$.

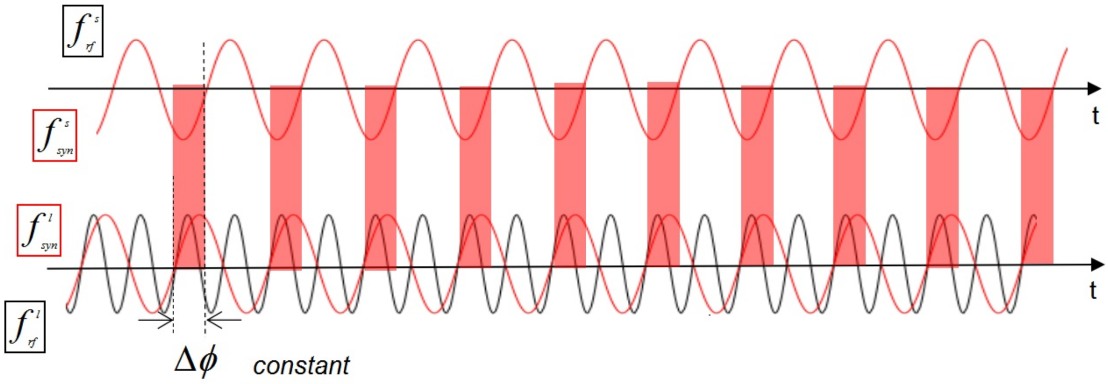

Figure 2.7: The constant phase difference between the synchronization frequencies f_{syn}^l and f_{syn}^s when $\kappa = 5$, $h^s = 1$ and $h^l = 10$.
Red rectangles represent the constant phase difference periodically and red sinusoidal waves the synchronization frequencies. Black sinusoidal waves represent the cavity rf frequencies. The sinuaoidal wave is red when the synchronization frequency and the cavity rf frequency overlap.

Fig. 2.7 illustrates two synchronization frequencies f_{syn}^l and f_{syn}^s, when $\kappa = 5$, $h^s = 1$ and $h^l = 10$. The GCD of h^l and $h^s \cdot \kappa$ is 5, namely $Y = 5$, $f_{rf}^l / f_{rf}^s = 2$, $f_{syn}^l = f_{rf}^l / 2$ and $f_{syn}^s = f_{rf}^s / 1$. This example is the FAIR use case of the H^+ B2B transfer from the SIS18 to the SIS100, which will be explained in Sec. 5.1.2.

2.2.2 Circumference ratio is close to an integer

If the ratio of the circumference of the injection/extraction orbit of the large synchrotron to that of the small synchrotron is a decimal number close to an integer. Eq. 2.23 changes to

$$\frac{C^l}{C^s} = \kappa + \lambda \tag{2.31}$$

where κ is the whole part and λ is the decimal part of the decimal number and the absolute value of λ is smaller than 0.005 for FAIR use cases. From the circumference ratio, the revolution frequency ratio of two synchrotrons can be calculated.

$$\frac{f_{rev}^l}{f_{rev}^s} = \frac{1}{\kappa + \lambda} \tag{2.32}$$

Based on eq. 2.32 and harmonic number, the f_{rf}^X are calculated by eq. 2.33 and eq. 2.34

$$f_{rf}^s = h^s \cdot f_{rev}^s = h^s \cdot (\kappa + \lambda) \cdot f_{rev}^l \tag{2.33}$$

$$f_{rf}^l = h^l \cdot f_{rev}^l \tag{2.34}$$

We could get the relation between f_{rf}^s and f_{rf}^l by dividing eq. 2.34 by eq. 2.33.

$$\frac{f_{rf}^l}{f_{rf}^s} = \frac{h^l}{h^s \cdot (\kappa + \lambda)} = \frac{h^l}{h^s \cdot \kappa + h^s \cdot \lambda} \tag{2.35}$$

In eq. 2.35, $h^s\lambda$ is much smaller than $h^s\kappa$ and h^l. Similarly as the scenario of the integral circumference ratio, two slightly different synchronization frequencies are

$$f^l_{syn} = \frac{f^l_{rf}}{h^l/Y} = Y f^l_{rev} \tag{2.36}$$

$$f^s_{syn} = \frac{f^s_{rf}}{h^s\kappa/Y} = \frac{Y}{\kappa} f^s_{rev} \tag{2.37}$$

Y is the GCD of h^l and $h^s \cdot \kappa$. Substituting two synchronization frequencies into eq. 2.21, we get the periodically variable phase difference $\Delta\phi$.

$$\Delta\phi = [2\pi(\frac{f^l_{rf}}{h^l/Y} - \frac{f^s_{rf}}{h^s\kappa/Y})t + \phi_l - \phi_s] \mod 2\pi \tag{2.38}$$

Substituting f^l_{rf} in eq. 2.35 into eq. 2.38, we get the phase difference.

$$\Delta\phi = [2\pi Y \frac{-h^s\lambda f^s_{rf}}{(h^s\kappa + h^s\lambda)h^s\kappa} t + \phi_l - \phi_s] \mod 2\pi \tag{2.39}$$

Eq. 2.39 shows that the phase difference is a periodical variable. The beating frequency is $\Delta f = |f^l_{syn} - f^s_{syn}|$. The beating frequency must not be too large in order to guarantee the precise of the phase match due to the periodical phase variable, but also not too small to satisfy the time constraint for the phase match.

Fig. 2.8 shows the periodically variable phase difference between two slightly different synchronization frequencies f^l_{syn} and f^s_{syn} when $\kappa = 2$, $\lambda = -0.003$, $h^s = 2$ and $h^l = 4$. The GCD of h^l and $h^s \cdot \kappa$ is 4, namely $Y = 4$. Hence, according to eq. 2.36 and eq. 2.37, two synchronization rf frequencies are $f^l_{syn} = f^l_{rf}$ and $f^s_{syn} = f^s_{rf}$. This example is the FAIR use case of the h=4 B2B transfer from the SIS18 to the ESR, which will be explained in Sec. 5.2.1.

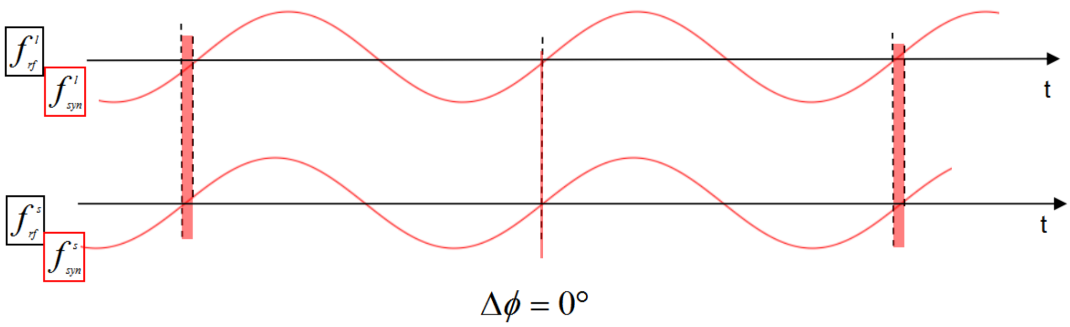

Figure 2.8: The periodically variable phase difference between two slightly different synchronization frequencies f^l_{syn} and f^s_{syn} when $\kappa = 2$, $\lambda = -0.003$, $h^s = 2$ and $h^l = 4$.
Red rectangles represent the periodical variable phase difference and red sinusoidal waves the overlap between synchronization frequencies and cavity rf frequencies.

2.2.3 Circumference ratio is far away from an integer

When the circumference ratio of the large synchrotron to that of the small synchrotron is far away from an integer, the circumference ratio is a decimal number and eq. 2.40 can be expressed as

$$\frac{C^l}{C^s} = \frac{m}{n} + \lambda \tag{2.40}$$

where m/n represents the whole and part of the decimal parts of the decimal number, λ represents the rest part of the decimal part and the absolute value of λ is smaller than 0.05 for FAIR use cases. e.g. $C^l/C^s = 2.6 - 0.003 = 26/10 - 0.003$, so $m = 26$, $n = 10$ and $\lambda = -0.003$.

Substituting κ by m/n into eq. 2.35, we could get the relation between f^s_{rf} and f^l_{rf}.

$$\frac{f^l_{rf}}{f^s_{rf}} = \frac{h^l \cdot n}{h^s \cdot m + h^s \cdot \lambda \cdot n} \tag{2.41}$$

In eq. 2.41, $h^s\lambda n$ is much smaller than $h^s m$ and $h^l n$. Similarly as the scenario of the integral circumference ratio, two slightly different synchronization frequencies are

$$f^l_{syn} = \frac{f^l_{rf}}{h^l n/Y} = \frac{Y}{n} f^l_{rev} \tag{2.42}$$

$$f^s_{syn} = \frac{f^s_{rf}}{h^s m/Y} = \frac{Y}{m} f^s_{rev} \tag{2.43}$$

Y is the GCD of $h^l n$ and $h^s m$. Substituting two synchronization frequencies into eq. 2.21, we get the periodical phase difference $\Delta\phi$.

$$\Delta\phi = [2\pi(\frac{f^l_{rf}}{h^l n/Y} - \frac{f^s_{rf}}{h^s m/Y})t + \phi_l - \phi_s] \mod 2\pi \tag{2.44}$$

Substituting f^l_{rf} in eq. 2.41 into eq. 2.44, we get the phase difference.

$$\Delta\phi = [2\pi Y \frac{-\lambda n f^s_{rf}}{(h^s m + h^s \lambda n)m} t + \phi_l - \phi_s] \mod 2\pi \tag{2.45}$$

Eq. 2.45 shows that the phase difference is a periodical variable. The beating frequency is $\Delta f = |f^l_{syn} - f^s_{syn}|$. It is possible to have various combination of m/n and λ. λ determines the beating frequency. The smaller, the more precise the phase match. $(h^l \cdot n)/Y$ and $(h^s \cdot m)/Y$ determines the two slightly different frequencies. The bigger $(h^l \cdot n)/Y$ and $(h^s \cdot m)/Y$, the smaller two synchronization rf frequencies, which has a higher requirement for LLRF systems. So we have to find a proper combination of m/n and λ.

Fig. 2.9 shows the periodically variable phase difference between two slightly different synchronization frequencies f^l_{syn} and f^s_{syn} when $m = 26$, $n = 10$, $\lambda = -0.003$, $h^s = 1$ and $h^l = 1$. $f^l_{rf}/f^s_{rf} = 1 \cdot 10/(1 \cdot 26 - 1 \cdot 10 \cdot 0.003)$. The GCD of $h^l n = 1 \cdot 10$ and $h^s m = 1 \cdot 26$ is 2, namely $Y = 2$. Hence, according to eq. 2.42 and eq. 2.43, two synchronization rf frequencies are $f^l_{syn} = f^l_{rf}/5$ and $f^s_{syn} = f^s_{rf}/13$. This example is the FAIR use case of the B2B transfer from the CR to the HESR, which will be explained in Sec. 5.3.3.

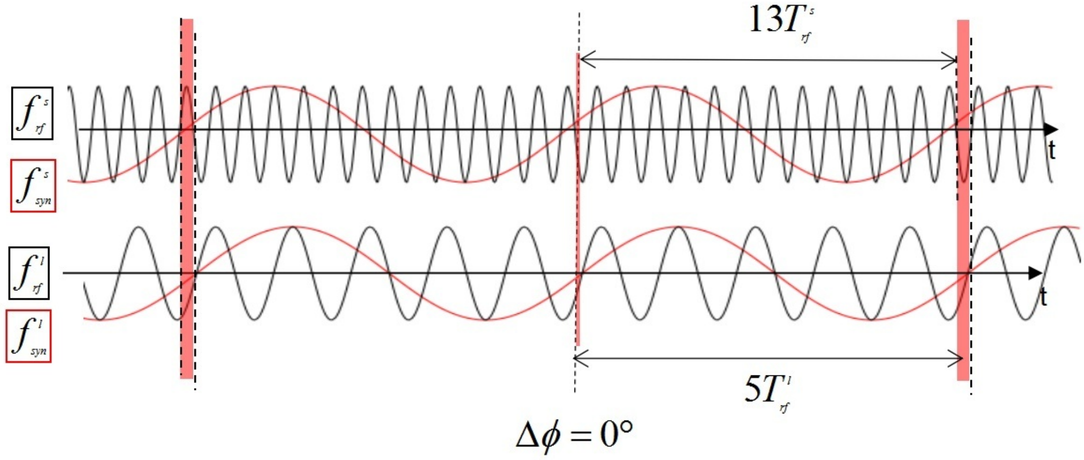

Figure 2.9: The periodically variable phase difference between two synchronization frequencies f^l_{syn} and f^s_{syn} when $m = 26$, $n = 10$, $\lambda = -0.003$, $h^s = 1$ and $h^l = 1$. Red rectangles represent the periodical variable phase difference and red sinusoidal waves the synchronization frequencies. Black sinusoidal waves represent the cavity rf frequencies.

2.3 Phase match of two rf systems

In order to guarantee a beam transfer with the required accuracy, the LLRF feedback loops used for phase corrections must be switched off before the B2B transfer starts. e.g. beam phase feedback loop [?] and bunch-by-bunch longitudinal rf feedback loop [?].

For different scenarios mentioned in Sec. 2.2, two methods available for the phase alignment of two rf systems, the phase shift and the frequency beating methods. Both methods provide a time frame for the B2B transfer, within which bunches are transferred into buckets with the bunch-to-bucket injection center mismatch smaller than the upper bound. The time frame is called the "synchronization window".

2.3.1 Phase shift method

The phase shift process must be performed slowly enough for the preservation of the longitudinal emittance. After the phase shift, bunches of the source synchrotron are phase aligned with buckets of the target synchrotron. Theoretically the synchronization window is infinitely long. In fact, the beam feedback loops on the rf system are switched off before the B2B starts, so the beam is stable for a short period of time, e.g. 10 ms. Hence, bunches must be transferred as soon as possible, causing a synchronization window with a certain length.

Fig. 6.12 illustrates an example for the phase shift method with a sinusoidal rf frequency modulation. The f^l_{syn} and f^s_{syn} are the synchronization frequencies respectively from the large and small synchrotrons. The time-of-flight between bunches and buckets is compensated here. The phase shift is done for the small synchrotron in this example. The red dashed line shows the end of the phase shift process ($\Delta\phi = 0°$) and the beginning of the synchronization window, drawn in yellow. After the phase shift, bunches match with buckets. A sinusoidal frequency modulation

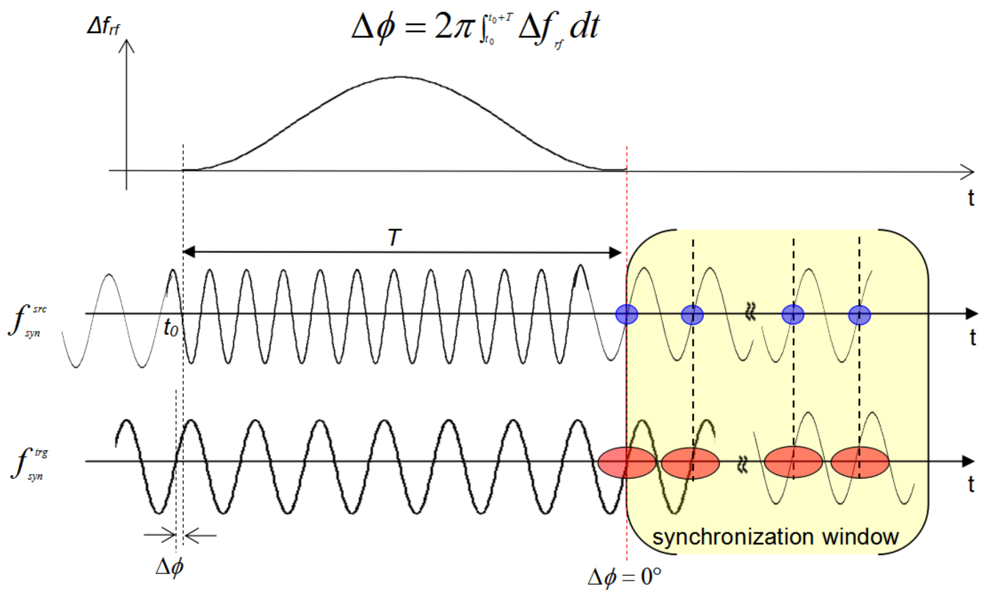

Figure 2.10: An example for the phase shift method with a sinusoidal rf frequency modulation.
Blue dots represent bunches of the source synchrotron and red dots buckets of the target synchrotron.

Δf_{rf} with a fixed duration time T is used for the rf frequency modulation.

$$\Delta f_{rf} = A[1 - \cos\frac{2\pi}{T}(t - t_0)] \tag{2.46}$$

where A is the amplitude of the sinusoidal wave. Based on eq. 2.22, the area of the sinusoidal wave equals to $\Delta\phi/2\pi$. We can calculate the amplitude A

$$A = \frac{\Delta\phi}{2\pi} \cdot \frac{1}{T} \tag{2.47}$$

A particular case of the B2B synchronization occurs, when the target synchrotron is empty, i.e. it did not capture any bunch yet, the phase jump can be done for the target synchrotron.

Now we analyze the rf frequency modulation of the phase shift from the beam dynamics perspective.

- Momentum shift and radial excursion

  A rf frequency modulation introduces the momentum shift.

$$\frac{\Delta p}{p} = \frac{1}{\frac{1}{\gamma^2} - \alpha_p} \cdot \frac{\Delta f_{rf}}{f_{rf}} \tag{2.48}$$

  Substituting $\Delta R/R$ in eq. 2.9 into eq. 2.48, we get the radial excursion due to the rf frequency modulation.

$$\frac{\Delta R}{R} = \frac{1}{\frac{1}{\alpha_p\gamma^2} - 1} \cdot \frac{\Delta f_{rf}}{f_{rf}} \tag{2.49}$$

The rf frequency modulation causes a radial excursion. There is a limit on the maximum radial excursion of every synchroton, so there is a maximum frequency offset for the rf frequency modulation.

- Shift of the synchronous phase

The beam acceleration or deceleration accompanies with the rf frequency modulation, so the synchronous phase deviates from 0° and the momentum is shifted from p to $p + \Delta p$. Based on eq. 2.14, we can get the first derivative of the magnetic rigidity

$$\dot{B\rho} = \frac{\dot{\Delta p}}{q} = B\rho\frac{\dot{\Delta p}}{p} \tag{2.50}$$

Substituting $\dot{B\rho}$ in eq. 2.50 into eq. 2.15, we get

$$V_0 \sin\phi_s = 2\pi(R + \Delta R)B\rho\frac{\dot{\Delta p}}{p} \tag{2.51}$$

Substituting $\dot{\Delta p}$ in the first derivative of eq. 2.9 into eq. 2.51, we get the simplified relation, eq. 2.52, between the change in the synchronous phase ϕ_s and the radial change rate based on the prerequisite that $\Delta R/R$ is very small and negligible. The maximum radial excursion of FAIR synchrotrons $\Delta R/R$ is in the 10^{-4} range. The full formula is listed in [**?**].

$$V_0 \sin\phi_s = \frac{2\pi B\rho}{\alpha_p}\dot{\Delta R} \tag{2.52}$$

It is clear from eq. 2.52 that when the rf frequency is modulated, ϕ_s is only determined by $\dot{\Delta R}$, since other parameters are not affected by the rf frequency modulation. ϕ_s is proportional to the radius change rate $\dot{\Delta R}$. In eq. 2.49, γ change very slowly as compared to ΔR during the rf frequency modulation. So we can get the relation between $\dot{\Delta R}$ and the rf frequency modulation rate $\dot{\Delta f}$ by the first derivative of eq. 2.49.

$$\frac{\dot{\Delta R}}{R} = \frac{1}{1/\alpha_p\gamma^2 - 1}\frac{\dot{\Delta f_{rf}}}{f_{rf}} \tag{2.53}$$

So $\dot{\Delta R}$ is proportional to $\dot{\Delta f_{rf}}$. Hence, the synchronous phase is proportional to $\dot{\Delta f_{rf}}$.

- Bucket size

At the flattop, the bucket is a stationary bucket. During the frequency modulation process, the bucket becomes a running bucket with $\phi_s \neq 0°$. The bucket area factor is calculated by eq. 2.12. Buckets must be big enough to capture bunches. Eq. 2.12 shows that the bucket area factor is in inverse proportion to the synchronous phase. The synchronous phase must be small enough to guarantee the bucket size, so $\dot{\Delta f_{rf}}$ must be small enough, namely the change of the rf frequency modulation must be slow enough.

- Adiabaticity

  A process is called "adiabatic" when the rf frequency is changed slowly enough for the beam to follow. The condition that the rf frequency varies slowly can be expressed by

$$\varepsilon = \frac{1}{\omega_{syn}^2}|\frac{d\omega_{syn}}{dt}| \ll 1 \tag{2.54}$$

  where ε is the adiabaticity parameter. For the angular synchrotron frequency, eq. 2.13, all of the other variables change very slowly compared with ϕ_s. From eq. (2.54) and eq. (2.13), the adiabaticity can be written as follows [?]:

$$\varepsilon \approx \frac{1}{2\omega_{syn\_0}}|\phi_s\dot{\phi}_s| \tag{2.55}$$

  where ω_{syn_0} is the angular synchrotron frequency with no frequency modulation, $\omega_{syn\_0} = \omega_{syn}(\phi_s = 0°)$. Form the adiabaticity eq. 2.55, ϕ_s and $\dot{\phi}_s$ must be small enough to guarantee the adiabaticity. So not only $\Delta\dot{f}_{rf}$ but also $\Delta\ddot{f}_{rf}$ must be existing and small enough. Namely, $\Delta\dot{f}_{rf}$ must be continuous and the change of $\Delta\dot{f}_{rf}$ must be slow enough.

- Tune shift

  So far the rf frequency modulation is analyzed from the longitudinal beam dynamics perspective. Because of the momentum shift, the rf frequency modulation has an influence on the transverse beam dynamics as well. The beam particle's tune $Q_{x/y}$, defined as the frequency of the horizontal/vertical oscillations, and chromaticity $Q^{`}_{x/y}$ as their horizontal/vertical dependence on particle momentum **??**. The momentum spread $\Delta p/p \neq 0$ during the phase shift process causes horizontal/vertical tune shifts $\Delta Q_{x/y}$ [?].

$$\Delta Q_{x/y} = Q^{`}_{x/y}\frac{\Delta p}{p} \tag{2.56}$$

  The momentum shift of FAIR synchrotrons $\Delta p/p$ is in the 10^{-4} range and the chromaticity is about 10 Hz. So the tune shift is relative small and has almost no influence on the transverse motion.

According to the beam dynamics analysis, there are several requirements for the rf frequency modulation. There exists a maximum rf frequency offset. $\Delta\dot{f}_{rf}$ must be not only continuous but also small enough. What is more, $\Delta\ddot{f}_{rf}$ must be small enough.

2.3.2 Frequency beating method

The frequency beating method uses two slightly different synchronization frequencies. When two synchronization frequencies are slightly different, two rf systems are beating automatically. Or the rf system of the source or the target or both synchrotrons is detuned for the achievement of beating. During the frequency dutune process, particles are not accelerated or decelerated for the energy match. The synchronization is realized when the phase difference of the two synchronization frequencies corresponds to the required phase difference. The $\Delta\phi$ is the mismatch between the bunch center and the corresponding bucket center. In principle, the B2B transfer requirement for FAIR allows a bunch-to-bucket center mismatch within the range of $\pm 1°$, which brings a symmetric time frame with respect to the time of the required phase difference. This is called the maximum synchronization window, drawn in yellow, see Fig. 2.11. The red dashed line shows the time for the required phase difference.

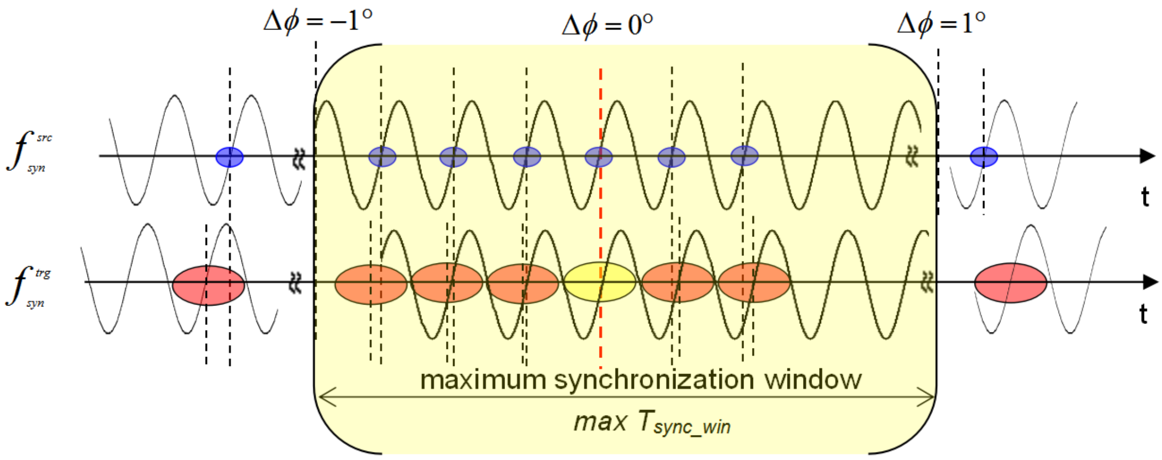

Figure 2.11: The illustration of the frequency beating method.
Blue dots represent bunches of the source synchrotron and red dots buckets of the target synchrotron.

- For one bunch to one bucket injection per B2B transfer, the bunch is "perfectly" injected into the center of the bucket. The "perfect" injection does not mean that the bunch-to-bucket center mismatch $\Delta\phi$ is 0°. It means the smallest mismatch with regard to other injection. The "perfect" injection is affected by the phase step growth $\Delta\varphi$between two synchronization frequencies, see eq. 2.57.

$$\frac{|1/(f_{syn}^{src} - f_{syn}^{trg})|}{360°} = \frac{1/f_{syn}^{trg}}{\Delta\varphi} \tag{2.57}$$

  Because the bunch-to-bucket injection center mismatch is the mismatch between the cavity rf frequencies, so it is $f_{rf}^{trg}/f_{syn}^{trg}$ times as large as the phase mismatch between two synchronization frequencies. Hence, the "perfect" injection is with the mismatch in the range between 0° and $\frac{f_{rf}^{trg}}{f_{syn}^{trg}} \cdot \Delta\varphi$, which is dependent on the initial relative relation between two rf systems.

- For more than one bunch to be transferred per B2B transfer, only one bunch is "perfectly" injected into the corresponding bucket, which is represented by the yellow dot in Fig. 2.11. Other bunches on both side of this bunch are injected into their corresponding buckets (red dots) with the mismatch due to the constant phase step growth of $\frac{f_{rf}^{trg}}{f_{syn}^{trg}} \cdot \Delta\varphi$. The maximum synchronization window T_{sync_win} is determined by the maximum tolerate bunch-to-bucket center mismatch ±1°, see eq. 2.58.

$$\frac{|1/(f_{syn}^{src} - f_{syn}^{trg})|}{360^\circ} = \frac{T_{sync\_win}}{[1^\circ - (-1^\circ)]/\frac{f_{rf}^{trg}}{f_{syn}^{trg}}} \tag{2.58}$$

The rf frequency is detuned at the end of the acceleration ramp. During the rf frequency detune process, the magnetic field and orbit react to the frequency detune in order guarantee the energy match.

- Radial excursion and magnetic field modification

  Because the momentum should not affected by the frequency detune for the energy match, namely Δp=0, we can get the general relation between the radial excursion and the rf frequency change by substituting Δp=0 into eq. 2.9.

$$\frac{\Delta R}{R} = -\frac{\Delta f_{rf}}{f_{rf}} \tag{2.59}$$

  When $\Delta p = 0$, we have the following relation between $\Delta B/B$ and the $\Delta R/R$ [?].

$$\frac{1}{\alpha_p}\frac{\Delta R}{R} = -\frac{\Delta B}{B} \tag{2.60}$$

  Substituting eq. 2.60 into eq. 2.59, we get the general relation between the magnetic field change and rf frequency change.

$$\frac{\Delta B}{B} = \frac{1}{\alpha_p}\frac{\Delta f_{rf}}{f_{rf}} \tag{2.61}$$

2.4 Synchronization of extraction and injection kicker magnets

A kicker magnet (or kicker) is a dipole magnet, which is used to rapidly switch particles between two paths. An injection kicker merges one beam into a circulating beam in a synchrotron and an extraction kicker diverts a circulating beam to leave a synchrotron. The B2B transfer needs a fast beam extraction and injection, which extracts and injects beam in a single-turn. Hence, a pulsed kicker magnet must be used with rapid rise time and fall time and the variable pulse flat-top [?]. Fig. 2.12 shows the schematic diagram of a kicker magnet. The energy storage moduleis charged with a high voltage power supply. It will be discharged via the transmission cable and the kicker magnet by switching on the pulse start switch. Before the increase of the magnetic field, there exist a preparation time for the kicker magnet. The magnet needs a certain period of time to increase from zero to a stable magnetic field, which is so-called a “kicker rise time“ (short: rise time). The length of the “kicker flat-top“ (short: flat-top) can be modified by switching on the stop switch in correlation with the pulse start switch. When the pulse stop switch is switched off, the magnet needs a certain period of time to reduce to zero magnetic field. This period is so-called a “kicker fall time“ (short: fall time) [?]. For the proper B2B transfer, the extraction and injection kickers must be synchronized with the beam. As soon as the tail of the circulating bunch passes the kicker, the start switch can be switched on. The pulse stop switch must be switched off in time in order not to affect the head of the next coming bunch in the synchrotron. The kicker control electronic produces the ignition signal to switch on/off two switches. Generally a preparation time of FAIR kickers is within the 5−10 us range. Compared with the FAIR rf frequency in the MHz range, a preparation time is not negligible, which could cause an increase of the bunch-to-bucket injection center mismatch especially for the frequency beating method. The kicker control electronic must take the preparation time into consideration, igniting kickers in advance of the preparation time.

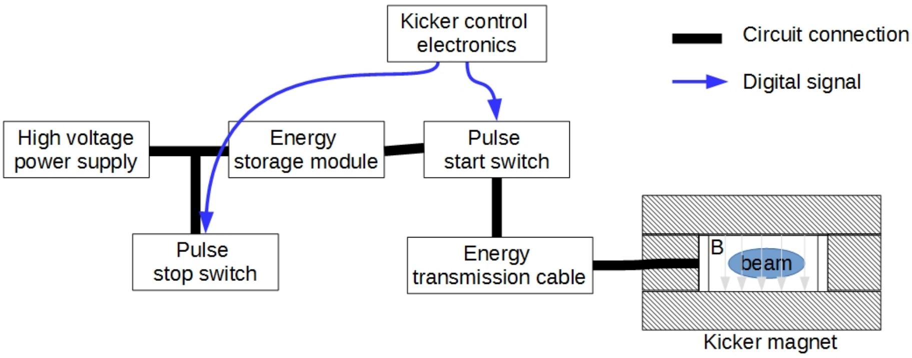

Figure 2.12: The schematic diagram of a kicker magnet.

Most commonly, an extraction kicker is used to eject all bunches. Fig. 2.13 illustrates the rise time, flat-top and fall time of an extraction kicker. The tail of the circulating bunch passes the kicker at t_0. The start switch is switched on the preparation time earlier than t_0. The rise time starts at t_0. The flat-top of the magnetic filed must be achieved before the head of the next circulating bunch passes the kicker at t_1. So the rise time of the extraction kicker must be shorter than the bunch gap. The flat-top has at least the length of bunches to be extracted. The stop switch is switched on earliest at t_2, when all bunches are extracted. Then there is no more bunch left in the synchrotron, so there is no constraint for the fall time.

For multi batches injection, see Fig. 2.14, the tail of the circulating bunch passes the kicker at t_0. The start switch is switched on the preparation time earlier than t_0. The rise time starts at t_0. The flat-top of the magnetic filed must be achieved before bunches are injected at t_1. So the rise time of the injection kicker must be shorter than the bunch gap. For a single batch injection, the rise time is not constrained. The length of the flat-top is determined by the length of bunches to be injected. The stop switch is switched on as soon as the tail of the last injected bunch passes the kicker at t_2. The magnetic field must be reduced to zero before the head of the circulating bunch passes the kicker at t_3. So the fall time must be shorter than $t_3 - t_2$.

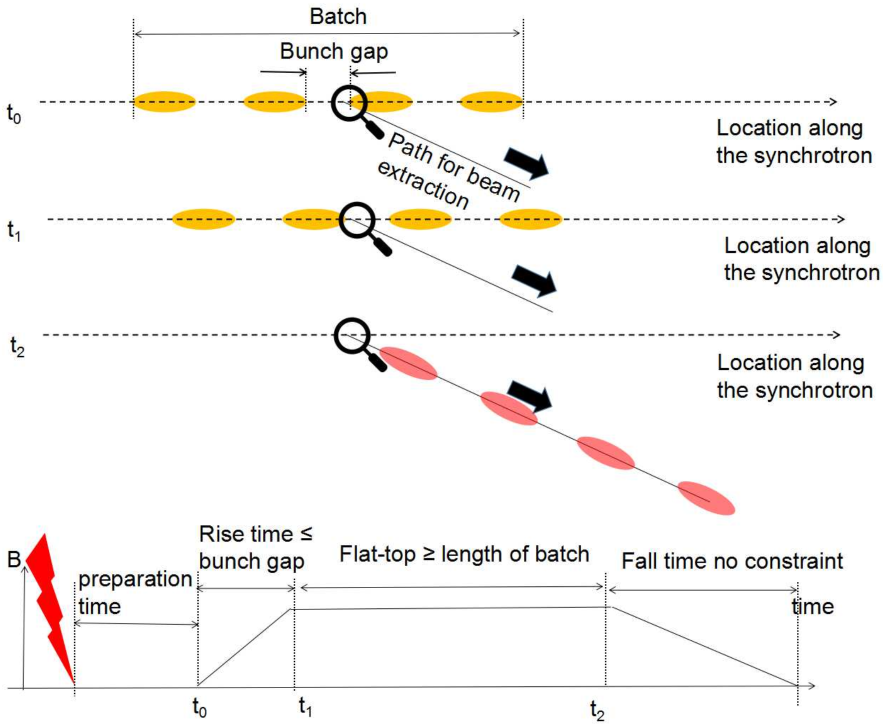

Figure 2.13: The rise time, flat-top and fall time of an extraction kicker. Yellow ellipses represent circulating bunches in the synchrotron, red ones extracted bunches and red lighting bolt the extraction kicker firing.

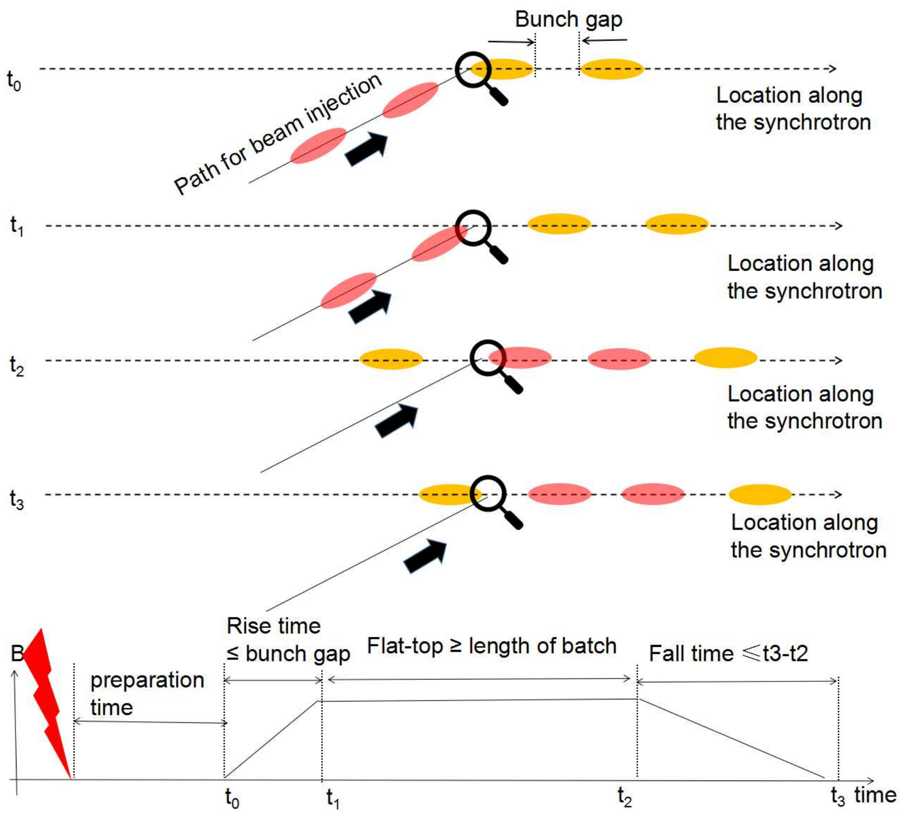

Figure 2.14: The rise time, flat-top and fall time of an injection kicker for multi batches injection.
Yellow ellipses represent circulating bunches in the synchrotron, red ones bunches to be injected and the red lighting bolt the injection kicker firing.

Chapter 3

Technical basis for the B2B transfer system

For the FAIR accelerator complex, synchronization of the B2B transfer will be realized by the FAIR control system and the Low-Level RF (LLRF) system. For the synchronization of LLRF system, the General Machine Timing (GMT) system is complemented and linked to the Bunchphase Timing System (BuTiS). Machine Protection System (MPS) protects SIS100 and subsequent accelerators or experiments from damage. Hence, the B2B transfer system for FAIR coordinates with the MPS system.

3.1 FAIR control system

The FAIR control system takes advantage of collaborations with CERN in using framework solutions like Front-End System Architecture (FESA) [?], LHC Software Architecture (LSA), White Rabbit (WR) [?]. It consists of the equipment layer, middle layer and application layer. The equipment layer consists of equipment interfaces, GMT and software representations of the equipment FESA. The middle layer provides service functionality both to the equipment layer and the application layer through the IP control system network. LSA is used for the Settings Management (SM). The application layer combines the applications for operators as GUI applications or command line tools. The application layer and the middle layer only request what the FAIR accelerator complex should do and transmit set values to the equipment layer. The SM supplies the schedule for the GMT by LSA [? ?].

3.1.1 BuTiS

Bunch Phase Timing System (BuTiS) serves as a campus-wide clocks distribution system with sub nanosecond resolution and stability over distances of several hundred meters while maintaining 100 ps per km timing stability [?]. Two BuTiS reference clocks 100 kHz P0 pulse and 10 MHz S1 phase reference signal are generated centrally in the BuTiS center. A star-shaped optical fiber BuTiS distribution system transfers these two reference clocks to the BuTiS local reference synthesizer all over the FAIR campus. The optical signal transmission delay between the BuTiS center and the different BuTiS local reference synthesizer is measured by a measurement setup in the BuTiS center. This measurement information is used to correct the phases of the signals generated in each BuTiS local reference synthesizer for the delay compensation. So at each BuTiS reference synthesizer, two delay compensated clock signals, 200 MHz C2 sine and 100 kHz T0 ident clocks, are generated from 100 kHz P0 and 10 MHz S1 reference clocks [**?** **?**]. The main task of BuTiS is the supply of the reference clock signals for Reference RF Signal RF systems, see Sec. 3.2 .

3.1.2 GMT

The GMT system is contained in the equipment layer. It does not only synchronize all timing nodes with nanosecond accuracy over the whole FAIR campus, but also distributes timing messages to all timing nodes and controls all timing nodes to execute real-time actions at a designated time [**?**]. The GMT system is a time based system. The GMT consists of the Timing Master (TM), the White Rabbit (WR) timing network and timing nodes. The timing master is a logical device, containing the data master (DM), the clock master (CM) and the management master (MM). The data master receives a schedule for the operation of the FAIR accelerator complex from the Settings Management and provides the real-time schedule by broadcasting timing messages to the WR timing network, which will be received and executed by the corresponding timing node at the designated time. The clock master is a dedicated WR switch. It is the topmost switch layer of the WR timing network and provides the grandmaster clock and timestamps which are distributed to all other timing nodes in the timing network. The clock master derives its clock from BuTiS 200 MHz C2 and 100 kHz T0 clocks and timestamps distributed are phase locked to BuTiS clocks. The GMT system could generate BuTiS T0 and C2 with any timing nodes and timing nodes are capable to timestamp clock edges. All active components including timing nodes and WR switches are registered to the MM. The MM monitors and manages the active components of the GMT system [**?** **?**].

A timing message is sent across the WR network, so it must be contained in the Ethernet frame. An Ethernet frame including one timing message has a length of 110 byte, which is called "timing frame" in this dissertation. A Virtual LAN (VLAN) [1] is a group of FECs in the WR network that is logically segmented by function or application, without regard to the physical locations of the FECs. All FECs in the WR network are assigned to the DM VLAN, within which the DM forwards broadcast timing telegrams downwards to all FECs.

3.1.3 Settings Management

The Settings Management (SM) is based on a physics model for accelerator optics, parameter space and overall relations between parameters and between accelerators. It supports off-line generation of accelerator settings, sending these settings to all involved devices, and programming the schedule for the GMT system [**?**]. The core component of SM is the LSA framework. A standardized LSA-API allows accessing data in a common way as basis for generic client applications for all accelerators. Using the LSA-API, applications can coherently modify settings [**?**]. E.g. the LSA generates timing constraints (e.g. ramp curve) as well as the equipment's data

[1] `https://en.wikipedia.org/wiki/Virtual_LAN`

settings (e.g. the current) for all devices derived from physics parameters (e.g. beam energy). For FAIR, LSA is extended to model the overall schedule of all accelerators. Beams are described as “Beam Production Chains“ to allow a description from beam source to beam target for settings organization and data correlation.

3.1.4 FESA

The FESA[2] is a framework used to fully integrate the large amount of front-end equipments into the accelerator control system. FESA was developed by CERN and has already been implemented into the CERN control system. Now it is developed further in collaboration with GSI for the FAIR project. For the FAIR project the necessary interaction with the timing nodes is realized by FESA. For a specific type of equipments, a FESA implementation accesses to the control interface of the equipments. The FESA class models the equipment as device, so the FESA output is called device class. The FEC use FESA to implement generic and equipment specific functions in form of the device classes. FESA provides JAVA based graphical user interfaces (GUI) to design, deploy, instantiate and test the device classes. Interaction with the equipment is also synchronized with the GMT system [**?**].

For time multiplexed operation of the accelerators, the FESA supports defining multiplexed properties. Before an accelerator schedule is started, the setting properties of FESA classes are pre-supplied by LSA from SM for all scheduled beams with specific settings accordingly. At runtime, FESA real time software actions are triggered by timing message, the actual beam specific data is then selected based on information carried by the timing message and send to the equipment.

3.2 LLRF system

The FAIR low-level rf (LLRF) system will be used in the existing synchrotrons SIS18 and ESR, as well as in the FAIR synchrotrons SIS100 and SIS300 and in CR, NESR, and RESR. It supports fast ramp rates and large frequency span for the acceleration of a variety of ion species, It supports different RF manipulations, including operation at different harmonic numbers, barrier bucket generation, bunch compression and longitudinal feedback. [**?**].

Each RF supply room has a Reference RF Signal distribution system shown in Fig. 3.1. The Reference RF Signals in different supply rooms are synchronized by BuTiS. BuTiS 200MHz C2 and 100kHz T0 clock signals are generated by BuTiS receivers in different supply rooms in phase. In Fig. 3.1, a number of Group Direct Digital Synthesizer (DDS) units are located in each supply room, which are synchronized by BuTiS local reference. The Group DDS signals can be routed to the different cavity systems by a Switch Matrix. All cavities in a synchrotron could be providing with the same Group DDS signal. The cavities at different harmonic numbers could be realized by using Group DDS signals with different harmonic numbers and by adjusting the harmonic number at the Cavity DDS accordingly. The Group DDS concept allows to synchronize a variety of cavities in a very flexible way [**?**].

All the cavities of the SIS18 are driven from one supply room. The SIS100 cavities will be gathered in five acceleration sections, each of them is driven by a

[2] `https://www-acc.gsi.de/wiki/FESA/WhatIsFESA`

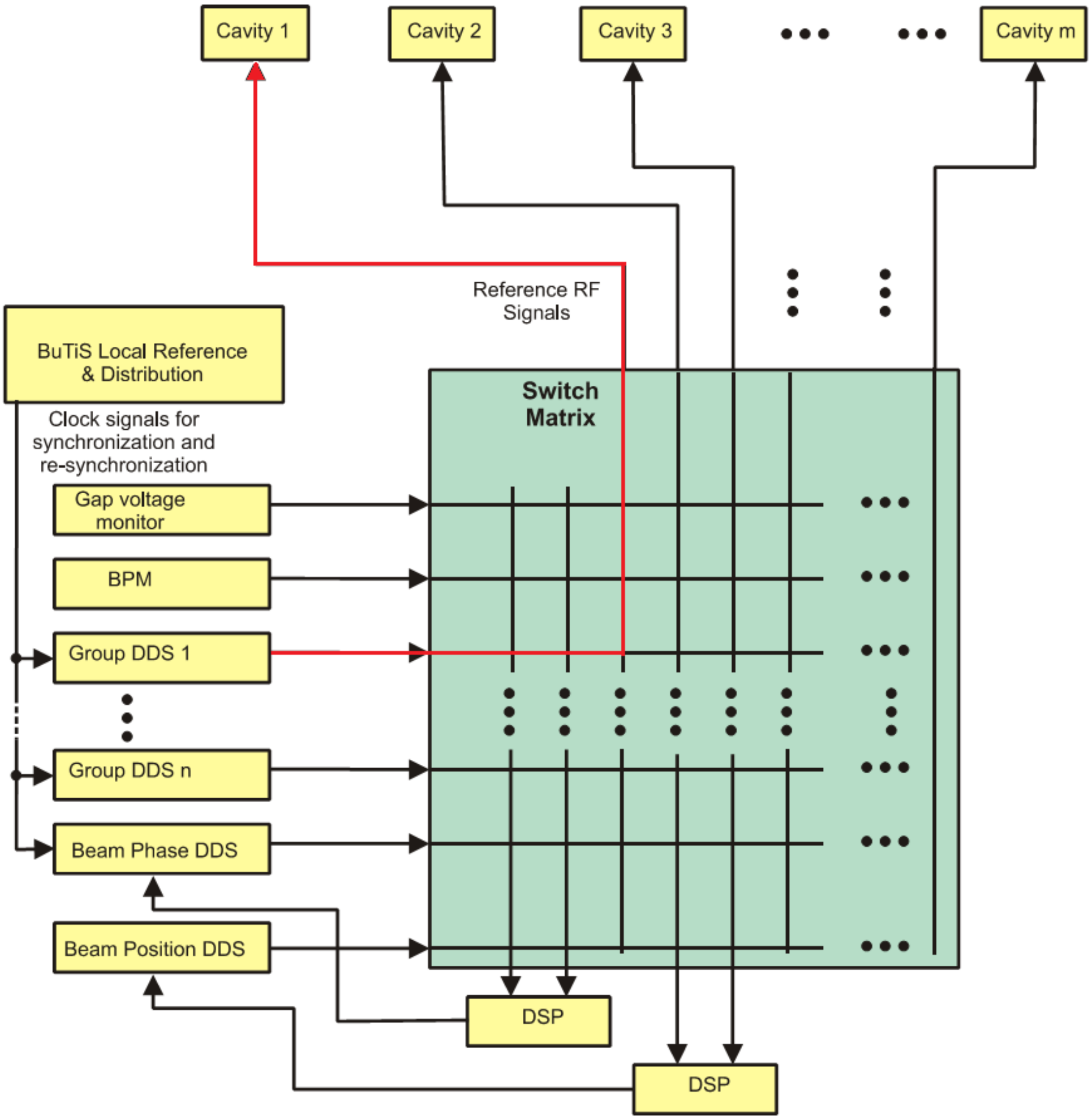

Figure 3.1: Reference RF Signal distribution system
[?]

dedicated supply room.

3.2.1 Local cavity synchronization

RF cavities are driven by one of Reference RF Signals, which are generated in each supply room . Fig. 3.2 shows the local cavity synchronization system, which synchronizes the local Cavity DDS unit to the Reference RF Signal with a specified phase offset. The cavity gets the RF signal from a local Cavity DDS unit, which receives RF Frequency Ramps from the Central Control System (CCS). A Digital Signal Processor (DSP)-System measures the phase difference between the Reference RF Signal and the gap voltage of the cavity. In the DSP system, a closed-loop control algorithm is implemented, which generates frequency corrections for the local Cavity DDS unit. This process is called local synchronization loop, which ensures that the phase of the gap voltage follows the phase of the Reference RF signal [?]. The path from the Group DDS 1 to Cavity 1 marked with the red line in Fig. 3.1 is realized by the local cavity synchronization in Fig. 3.2. The virtual rf cavity is a virtual position around the ring, to which the Reference RF Signal corresponds.

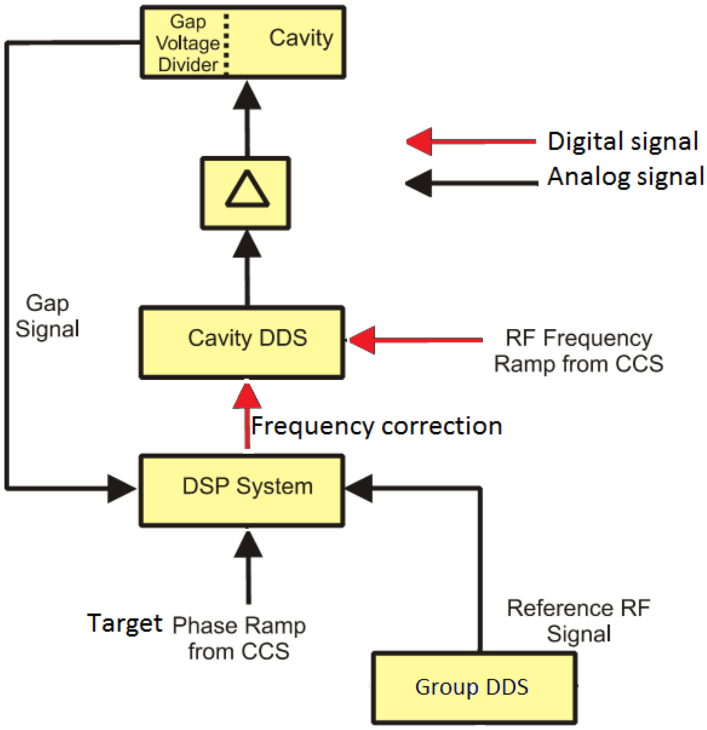

Figure 3.2: Local Cavity Synchronization
[?]

3.2.2 Longitudinal feedback system

In order to damp coherent longitudinal dipole oscillations, the beam phase control loop is used. The phase difference between the beam signal and the Reference RF Signal is fed back via an FIR filter. The beam signal is obtained by a fast current transformer or a beam position monitor. The filter output is converted in a phase-correction and forwarded to the Group DDS. The corrections are added to the phase of the frequency ramp in the Cavity DDS, which results in a change of the phase of the gap voltage and thus a feedback to the beam [?]. Unfortunately, the actual beam phase control loop in SIS18 is not able to damp incoherent longitudinal dipole oscillations. For SIS100, a bunch-by-bunch longitudinal feedback system will be developed. The bunch-by-bunch longitudinal feedback system generates a correction voltage in dedicated feedback cavities for a specified bunch [?].

3.3 MPS system

A MPS protects current accelerator and subsequent accelerators or experiments from damage or unacceptable failure, e.g. the beam position is out of tolerance, the rf cavity failure and so on. Thereby, the individual equipment is assumed self-protecting, which could triggers accelerator safety critical actions, such as an emergency beam dump [3], a shutdown of magnets or a beam injection inhibit. In case of relevant equipment failures or other inappropriate equipment states, a MPS signal is generated from this equipment [?]. The FAIR B2B transfer must coordinate with the SIS100 emergency dump signal and the beam injection inhibit signal from the MPS.

The SIS100 emergency dump signal indicates that the beam should be transferred to the emergency dump as soon as possible. If the beam injection inhibit signal is off, the B2B transfer extraction and injection kickers are allowed to be fired. If the beam injection inhibit signal is on, the injection and extraction kickers will be blocked for firing.

3.4 Comparison between the FAIR B2B transfer system and the current B2B transfer with the GSI control system

The existing GSI control system realizes the B2B transfer from the SIS18 to the ESR and from the ESR back to the SIS18. It is an event based system, that event execution will start immediately at the event receipt. Events are directly sent from a "Pulszentrale", who makes the schedule. Each accelerator has its own Pulszentrale, e.g. the ESR is equipped with the ESR-Pulszentrale and the SIS18 with the SIS-Pulszentrale. All devices are connected to distributed Equipment Controllers (EC) via field bus. ES is responsible for the receipt of the event and produces the pulse for the devices [? ?].

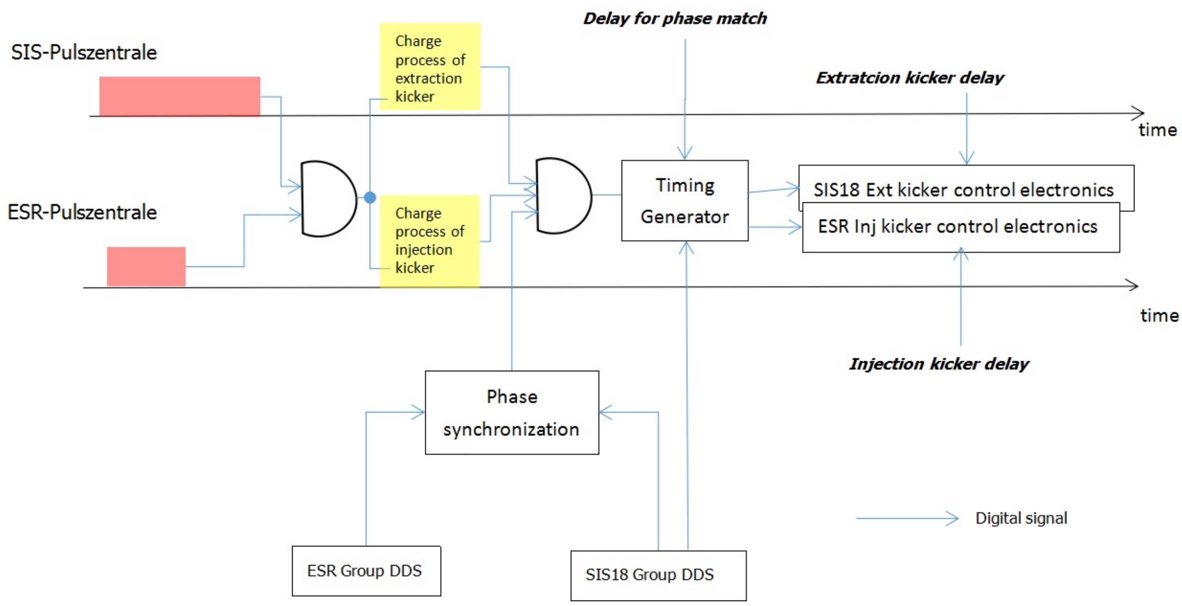

Figure 3.3: The current realization of the bunch-to-bucket transfer between the SIS18 and the ESR with GSI control system.

[3]A beam dump is a device designed to absorb the beam.

Fig. 3.3 illustrates the current realization of the B2B transfer from the SIS18 to the ESR with the GSI control system. The SIS18 needs longer time for the preparation, e.g. the beam injection and the beam acceleration, before the extraction than that of the ESR before the injection, so the ESR is earlier fully prepared for the transfer. The preparation process is represented as red rectangle in Fig. 3.3. When the SIS18 is fully prepared with bunches to be transferred, the ready signal from the ESR-Pulszentrale and the SIS-Pulszentrale are forwarded into a logic *AND* gate. When both SIS18 and ESR are prepared, namely the output of the logic *AND* gate is high, the extraction kicker charge event is sent from the SIS-Pulszentrale and the injection kicker charge event from the ESR-Pulszentrale. The charge process of kicker is represented as yellow rectangle in Fig. 3.3. When two kickers are fully charged, the ready signal of the extraction and injection kickers from the ESR-Pulszentrale and the SIS-Pulszentrale are forwarded into the second logic *AND* gate, as well as the "phase synchronization signal" from the RF system. The phase synchronization signal indicates the alignment of the zero-crossing of the Reference RF Signals from Group DDS of the SIS18 and the ESR. The output of the second *AND* gate is an indication signal, starting the delay compensation of the time-of-flight and all propagation delays on the SIS18 cavity rf signal for the correct phase match between the SIS18 and ESR rf systems, denoted as "delay for phase match" in Fig. 3.3. ESR uses the injection orbit instead of the desin orbit, so the circumference ratio between the SIS18 and the ESR is close to an interger, $C^{SIS18}/C^{ESR} = 2 - 0.003$, the SIS18 has four bunches, $h^{SIS18} = 4$ and ESR has two buckets, $h^{ESR} = 2$, so $f_{rf}^{SIS18}/f_{rf}^{ESR} = 4/(4 - 0.006)$. The phase difference between rf systems of the SIS18 and the ESR varies at the speed of the beating frequency $\Delta f = 1898\,\text{Hz}$, see Chap. 5. The required phase difference $\Delta\phi$ happens the delay for the required phase match Δt after the indication signal, see eq. 3.1.

$$\frac{1/\Delta f}{360^\circ} = \frac{\Delta t}{\Delta \phi} \tag{3.1}$$

When the delay for the required phase match is expired, trigger pulses are produced by the timing generator for both the SIS18 extraction and ESR injection kicker control electronics. Every kicker control electronics adds a separate delay to trigger pulses, denoted as "extraction kicker delay" and "injection kicker delay" in Fig. 3.3. the delay for the required phase match, extraction kicker delay and injection kicker delay are configurable by operators. The precision of the ignition signal from the kicker control electronics is 1 ns.

The existing B2B transfer with the GSI control system only supports the B2B transfer with the frequency beating method. It dose not support B2B transfer with the phase shift method. Parameters (e.g. the delay for the required phase match, the extraction kicker delay and the injection kicker delay) must be properly configured and adjusted by operators. The phase synchronization signal is delay compensated, but the transfer of the signal to the second *AND* gate is not delay compensated and with the jitter of 1 us, resulting a default bunch-to-bucket injection center mismatch of $\pm 0.68^\circ$. Besides, it does not support buckets filling by multi batches, e.g. eight out of ten SIS100 buckets are filled by four SIS18 batches, each of them has two bunches.

Compared with the current B2B transfer with the GSI control system, the FAIR B2B transfer system has many advantages. It supports both the phase shift and frequency beating methods. For the B2B transfer from the SIS18 to the ESR, it is with a smaller bunch-to-bucket injection center mismatch (see Chap. 5). The FAIR B2B transfer system is based on the GMT system, which is a time based system. All timing nodes of the GMT system are time synchronized with nano second accuracy, which achieves the smaller bunch-to-bucket injection center mismatch. Besides, the FAIR B2B transfer system is more flexible. It supports several B2B transfers running at the same time, e.g. the B2B transfer from the SIS18 to the SIS100 and B2B transfer from the ESR to the CRYRING. It is capable to transfer different species beam from one machine cycle to another without the operator's configuration. It is capable to transfer the beam between two synchrotrons via a FRS, Pbar or Super FRS. It can achieve various complex bucket pattern. What is more, the FAIR B2B transfer system coordinates with the MPS system, which protects SIS100/SIS300 from unacceptable failure or situation.

Chapter 4

Concept of the FAIR B2B transfer system

In this Chapter, the basic idea of the FAIR B2B transfer system is presented in Sec. 4.1. The standard procedure of the system is defined and described in Sec. 4.2. Sec. 4.3 illustrates how the basic functionalities of the system are realized. In Sec. 4.4, the data flow of the system is described.

4.1 Basic idea of the FAIR B2B transfer system

The basic idea of the B2B transfer is simple. First of all, two rf systems of the source and target synchrotrons must be phase aligned. Secondly, the trigger for the extraction and injection kickers must be calculated. In the end, the actual beam injection must be indicated for the beam instrumentation and diagnostics, which shows the properties and the behavior of the beam.

4.1.1 Phase alignment

The phase alignment is one of the most important prerequisites for the B2B transfer. It makes sure that there must be buckets to be filled by extracted bunches at the correct time. The phase alignment is based on the synchronization frequencies, see Sec. 2.2. When two rf systems have an identical cavity rf frequency or slightly different cavity rf frequencies, two cavity rf frequencies are chosen as the synchronization frequencies. When two rf systems have hugely different cavity rf frequencies, two synchronization frequencies are an integral multiple of the same or slightly different derived rf frequencies, which are the division of the revolution frequencies. More details about the calculation of the synchronization frequencies, see Sec. 2.2. If two synchronization frequencies of two rf systems are same, the phase difference between two rf systems is constant. The phase difference can be adjusted by the phase shift method or the frequency beating method with the frequency detune on one (or both) rf system. If two synchronization frequencies of two rf systems are slight different, the phase difference is adjusted automatically because of the beating frequency.

For the phase alignment, the following idea must be followed.

1. The measurement of the phase of the rf system and the corresponding timestamp in each synchrotron.

2. The exchange of the measured phase and the timestamp.
3. The phase comparison between two rf systems.
4. The adjustment of the phase on one (or both) rf system, when the phase shift method is used.
5. The calculation of the time for the phase alignment of two rf systems.

4.1.2 Calculation of the trigger time for the extraction and injection kickers

For the proper B2B transfer, not only the relative position of bunches and buckets, but also the firing of the extraction and injection kickers must be precisely controlled. The extraction kicker must kick the bunch exactly the time-of-flight between two rings before a specific bucket passes the injection kicker. For the calculation of the trigger time for the extraction and injection kickers, the following idea must be followed.

1. The kicker firing requires the B2B injection center phase mismatch in the range between $\pm 1°$, which defines a "coarse synchronization".
2. The bucket counting requires the kicker firing based on the revolution frequency f_{rev}^{trg} or the synchronization frequency f_{syn}^{trg} of the target synchrotron (see Sec. 4.3.5). With the help of the bucket counting, bunches are injected into correct buckets. This process is called the "fine synchronization".

Before the detailed idea of the calculation is explained, some basic concepts and their symbols are introduced, see Fig. 4.1.

- The bucket pattern t_{bucket}.
- The Time-Of-Flight (TOF) between two synchrotrons t_{TOF}.
- The Time-Of-Flight between the virtual rf cavity and the extraction/injection kicker, t_{v_ext} and t_{v_inj}.
- The sum of the preparation time and rise time of an extraction kicker and an injection kicker, t_{ext} and t_{inj}.

Fig. 4.1 illustrates the B2B transfer from the SIS18 to the SIS100. The the SIS18 U^{28+} super cycle consists of four the SIS18 cycles. Each cycle produces two U^{28+} bunches. From the SIS18, four batches, each of two bunches, are injected into eight out of ten buckets of the SIS100. The the SIS18 H^+ super cycle consists of four the SIS18 cycles. Each cycle produces one H^+ bunch. From the SIS18, four batches, each of one bunch, are injected into four out of ten buckets of the SIS100 [? ?]. The the SIS18 and the SIS100 revolution frequency markers (black bars on the first time axis and bars on the second/third time axis in Fig. 4.1) indicate the time when the first bunch or the first bucket pass by the virtual rf cavity (black bars correspond to 1^{st} and $\sharp 1$). The extraction and injection kicker firing (red lighting bolts) have a delay with respect to the first bars of the SIS100 revolution frequency marker at

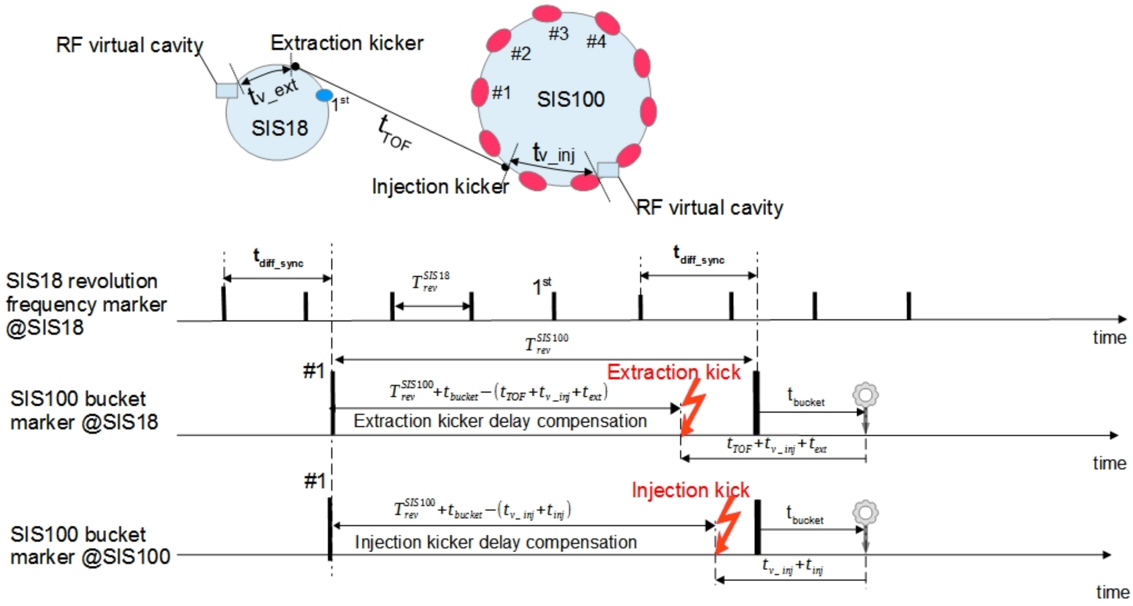

Figure 4.1: The illustration of the B2B transfer from the SIS18 to the SIS100. The blue dot represents bunch, red ones buckets, red lighting bolts the extraction and injection kicker firing and gray gears the bucket pattern.

the SIS18 and the SIS100. This delay is called the extraction/injection kicker delay compensation. The mentioned four instances of time are related to the second bars of the SIS100 revolution frequency marker. T_{rev}^{X} represents the revolution period of the synchrotron X, e.g. the SIS18 revolution period is T_{rev}^{SIS18}. T_{rf}^{X} represents the rf period of the cavity rf frequency of the synchroton X, e.g. the SIS18 rf period of the cavity rf frequency is T_{rf}^{SIS18}. After the rf phase alignment, the time difference between the SIS18 and the SIS100 revolution frequency markers is represented by t_{diff_sync}, e.g. t_{diff_sync}=$t_{v\_ext} + t_{TOF} + t_{v\_inj}$ for U^{28+} and H^{+} odd bucket injection, t_{diff_sync}=$t_{v\_ext} + t_{TOF} + t_{v\_inj} - T_{rf}^{SIS100}$ for H^{+} even bucket injection. The phase alignment for the odd or even bucket injection is informed by the "extra phase shift" from the SM. More details about the use cases of the B2B transfer from the SIS18 to the SIS100, please see Sec. 5.1.1 and Sec. 5.1.2. More details about the parameters of the B2B transfer system from SM, please see Appendix ??.

The kicker magnet must have zero magnetic field when bunches pass by it and the kicker magnet only can be switched on during bunch gaps. Bunch gaps depend on the cavity rf frequency, the bucket pattern and the bunch length.

- Extraction kick

  In order to inject into specific buckets, the extraction kicker delay compensation for the first bar of the SIS100 revolution frequency marker is $T_{rev}^{SIS100} + t_{bucket}$, see the gray gear at the SIS100 revolution frequency marker at the SIS18. For example, when two U^{28+} bunches of the SIS18 are to be injected into buckets ♯3 and ♯4 of the SIS100, $t_{bucket} = 1 \cdot T_{rev}^{SIS18}$. The extraction kicker must be fired $t_{v\_inj} + t_{TOF} + t_{ext}$ earlier as the bucket passes the virtual rf cavity, so the extraction kicker delay compensation is $T_{rev}^{SIS100} + t_{bucket} - (t_{TOF} + t_{v\_inj} + t_{ext})$, see the red lighting bolt at the SIS100 revolution frequency marker at the SIS18.

- Injection kick

  With the consideration of the bucket pattern, the injection kicker delay compensation for the first bar of the SIS100 revolution frequency marker is $T_{rev}^{SIS100} + t_{bucket}$, see the gray gear at the SIS100 revolution frequency marker at the SIS100. The injection kicker must be fired $t_{v\_inj} + t_{inj}$ time earlier as the bucket passes the virtual rf cavity, so the injection kicker delay compensation is $T_{rev}^{SIS100} + t_{bucket} - (t_{v\_inj} + t_{inj})$, see the red lighting bolt at the SIS100 revolution frequency marker at the SIS100.

4.2 Basic procedure of the FAIR B2B transfer system

Fig. 4.2 illustrates the basic procedure of the B2B transfer with two different synchronization scenarios. The yellow region shows the synchronization window. The purple region shows the valid time for the emergency kicker. The emergency kickers can be triggered at any time during the acceleration cycle by the MPS.

The B2B transfer process basically needs to follow the six steps [**?**]:

1. The DM announces the B2B transfer and requests the switch off of the beam feedback loops on the rf system, when required.

2. Two synchrotrons measure the rf phase locally.

3. The source synchrotron receives the measured rf phase from the target synchrotron.

4. The source synchrotron calculates the synchronization window and sends it to both synchrotrons and to the DM. Besides, the bucket label signal is reproduces at the source and target synchrotrons for the indication of the bucket pattern.

   The source synchrotron generally accomplishes the phase alignment in case of the phase shift method. A particular case is the empty target synchrotron. The phase alignment can be achieved very fast and simple by the phase jump at the target synchrotron. Although the synchronization window is theoretically infinite for the phase shift method, bunches should be transferred as soon as the phase shift is done, in order to guarantee the stability of the beam. For both synchronization methods, the synchronization window has a certain length.

5. The trigger signals are generated for the kickers with the delay compensation.

6. The kicker electronic fire the kickers. The actual beam injection time and the B2B transfer status are send from the source synchrotron to the DM and the DM sends them further to the beam instrumentation.

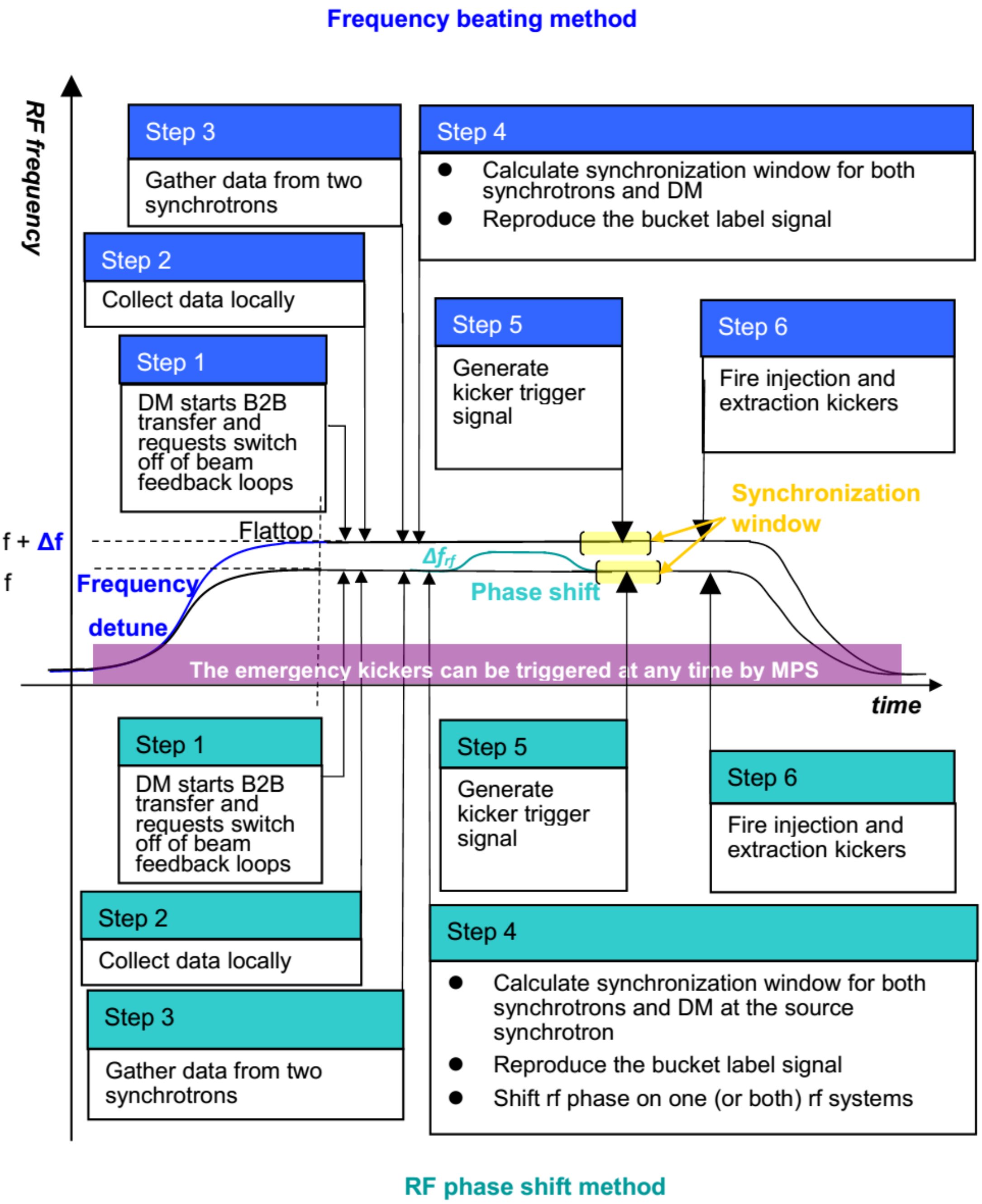

Figure 4.2: The procedure for the B2B transfer within one acceleration cycle. Shown are with the frequency beating method (blue, top) and with the phase shift method (green, bottom).

4.3 Realization of the FAIR B2B transfer system

This section describes the realization of the FAIR B2B transfer system based on the FAIR control system and LLRF system introduced in Chap. 3.

4.3.1 Phase measurement and corresponding timestamp of each rf system

The rf frequency in the source and target synchrotron need to be stable constant during the B2B transfer process. The phase measurement of each rf system follows the principles as shown below.

1. The measurement of the actual phase values.
2. The extrapolation of the phase value in the future based on the measured phase values.
3. The timestamp for the extrapolated phase values.

4.3.1.1 Measurement of actual phase values of each rf system

The phase measurement of each rf system is achieved by measuring the phase advance between a dedicated Reference RF Signal of a synchrotron and a shared reference sinusoidal signal. The phase advance has a linear relationship with time, whose range is from $-180°$ to $+180°$.

A dedicated Reference RF Signal of a synchrotron has its synchronization frequency, see Sec. 2.2. A shared reference signal (which is called "Synchronization Reference Signal") is used in the source and target synchrotrons in order to determine the phase difference between two rf systems. It has a fixed frequency and always in phase at two synchrotrons. It is a sinusoidal wave, whose frequency is a multiple of BuTiS T0 100 kHz and whose positive zero-crossings are always aligned with the first positive zero-crossings of C2 clocks after T0 edges [**?** **?**]. Thus, the Synchronization Reference Signal is synchronous in different supply rooms by definition. The frequency of the Synchronization Reference Signal f_{syn}^{REF} is calculated by

$$f_{syn}^{REF} = round(f_{syn}^{X}/100\,\text{kHz}) \cdot 100\,\text{kHz} \tag{4.1}$$

The function *round* rounds $f_{syn}^{X}/100\,\text{kHz}$ up or down to an integer value, which is closest to $f_{syn}^{X}/100\,\text{kHz}$. When $|f_{syn}^{X}/100\,\text{kHz}| < 1$, $f_{syn}^{REF} = 100\,\text{kHz}$. e.g. $f_{syn}^{X} = 988.388\,\text{kHz}$, $f_{syn}^{X}/100\,\text{kHz} = 0.988388$, so $round(f_{syn}^{X}/100\,\text{kHz}) = 10$ and $f_{syn}^{REF} = 1\,\text{MHz}$. This is the FIAR use case of the h=1 B2B transfer from the SIS18 to the ESR, more details, please see Chap. 5. For the detailed realization of the Synchronization Reference Signal, please see "Development of the LLRF system for a deterministic Bunch-to-Bucket transfer for FAIR".

Fig. 4.3 shows the phase measurement of the rf system at a dedicated synchrotron. The red sinusoidal wave represents the Synchronization Reference Signals (e.g 100 kHz) in two supply rooms and the black wave the Reference RF Signals (e.g. 1000/3 kHz) from the Group DDS. Although the relation between the Synchronization Reference Signal and the Reference RF Signal in Fig. 4.3 does not comply with eq. 4.1, the principle for the measurement of the phase advance is same and they are used for the easy observation of the process. The phase advance between the Reference RF Signal and the Synchronization Reference Signal $\Delta\varphi^{src}$ is measured by the Phase Advance Measurement (PAM) module at the source synchrotrons and $\Delta\varphi^{trg}$ at the target synchrotron. $\Delta\varphi^{X}$ represents the measured phase advance of

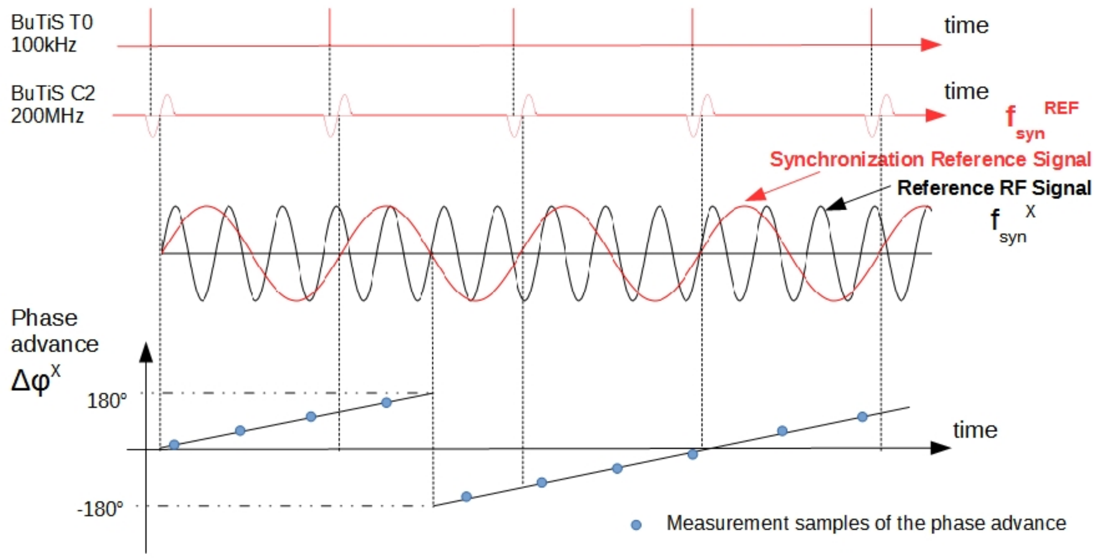

Figure 4.3: The realization of the phase advance measurement at one synchrotron

the synchrotron X. The phase advance measurement is performed asynchronously to an internal clock, which is represented by the blue dots. For more details about the implementation and realization of the PAM module, please see "Development of the LLRF system for a deterministic Bunch-to-Bucket transfer for FAIR" [?].

4.3.1.2 Phase extrapolation of each rf system

The phase advance can be extrapolated due to the linear relationship between time and the phase advance. Based on a series of the phase advance measurements, the phase advance at the first positive zero-crossings of C2 clocks after T0 edges ψ^{src} and ψ^{trg} are extrapolated at the source and target synchrotrons by the Phase Advance Prediction (PAP) Module. ψ^X represents the extrapolated phase advance of the synchrotron X. The extrapolated phase advance, ψ^{src} and ψ^{trg} at the source and target synchrotron, is represented by red diamonds in Fig. 4.4. Because the phase advance extrapolation is synchronized with the first positive zero-crossings of C2 clocks after T0 edges and the Synchronization Reference Signal is zero phase aligned with the first positive zero-crossings of C2 clocks after T0 edges, ψ^{src} and ψ^{trg} are the phase of the Reference RF Signals of the virtual rf cavitis of two synchrotrons (represented as black dots in Fig. 4.4). For more details about the implementation and realization of the PAP module, please see "Development of the LLRF system for a deterministic Bunch-to-Bucket transfer for FAIR" [?].

4.3.1.3 Timestamp the extrapolated phases

The timestamp of the first positive zero-crossings of C2 clocks after T0 edges corresponds to the extrapolated phases.

The timing nodes, the B2B source and target SCUs [? ?], are equiped in the source and target synchrotrons. The PAP module is as a SCU slave [1] in the B2B

[1] `https://en.wikipedia.org/wiki/Master/slave_(technology)`

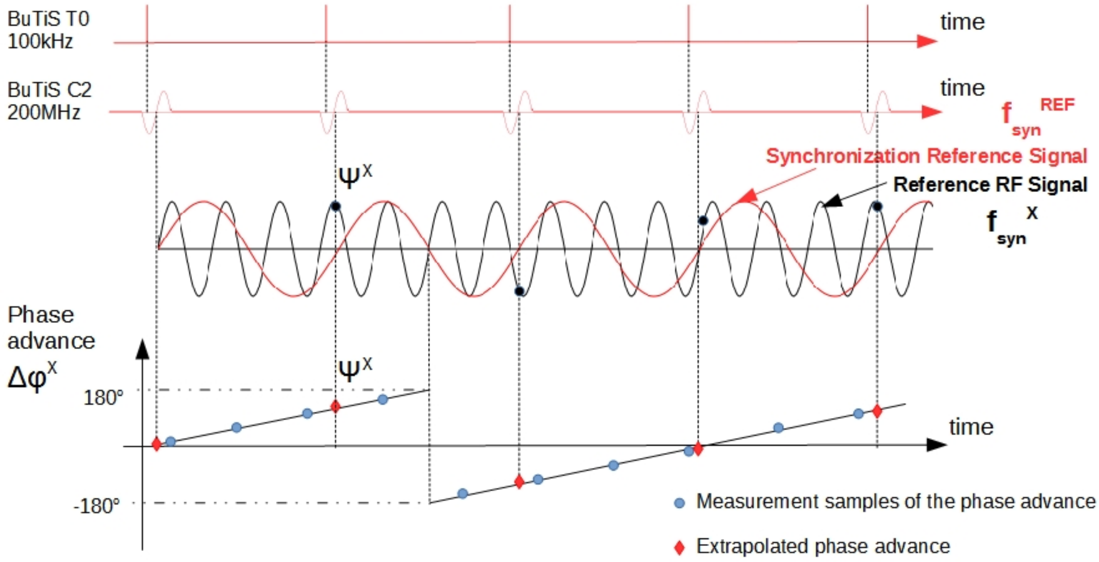

Figure 4.4: The realization of the phase advance extrapolation at one synchrotron

source and target SCU, see Fig. 4.5. Both the B2B source and target SCUs could get the timestamp of positive zero-crossings of BuTiS C2 clocks.

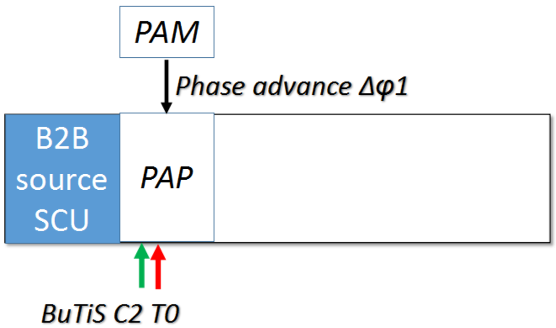

Figure 4.5: Implementation of the Phase Advance Prediction Module in the B2B source SCU

Fig. 4.6 illustrates the synchronization of the extrapolated phase to the timestamp. The DM broadcasts the timing frame of CMD_START_B2B to the WR network. This timing frame will be received by the B2B source SCU and the B2B target SCU. The B2B source and target SCUs start the B2B process at the designated time, the first positive zero-crossings of C2 clock after a specified T0 edge (represented as the pink dot in Fig. 4.6). They need maximum 1 µs to inform the PAP modules to start the phase advance extrapolation respectively. The PAP modules needs approximate 500 µs for the phase extrapolation and updates the extrapolated phase value at the first positive zero-crossings of C2 clocks after T0 edges. After 500 µs, the B2B source and target SCUs need another maximum 1 µs to get the extrapolated phase ψ^X (represented as the red diamond in Fig. 4.6) from the PAP modules and they also get the timestamp of the first positive zero-crossing of C2 clock after T0 edge t_{ψ^X} which corresponds to the extrapolated phase, as well as the slope of the phase advance k^X. The B2B source SCU obtains ψ^{src}, $t_{\psi^{src}}$ and k^{src}

at the source synchrotron and the B2B target SCU obtains ψ^{trg}, $t_{\psi^{trg}}$ and k^{trg} at the target synchrotron.

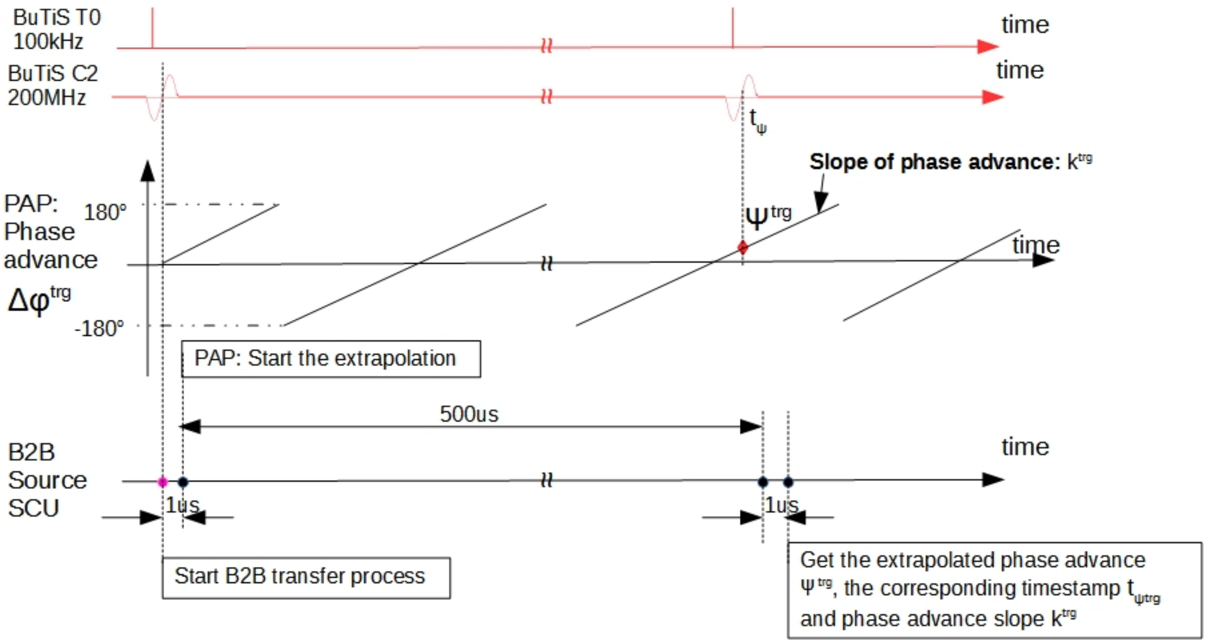

Figure 4.6: The synchronization of the extrapolated phase to the timestamp in one synchrotron

4.3.2 Exchange of the measured data

For the B2B transfer, there is a “B2B transfer master“, which is responsible for the data collection of two synchrotrons, the data calculation, the data redistribution and the B2B transfer status check. The data of the source and target synchrotron must be transferred to the “B2B transfer master“ via the deterministic WR network in the format of the timing frame.

For the simplicity, the B2B source SCU works as the “B2B transfer master“, so the extrapolated phase ψ^{trg}, the corresponding timestamp $t_{\psi^{trg}}$ and the phase advance slope k^{trg} are transferred by the B2B target SCU to the B2B source SCU via the WR network. The transfer of the data is achieved by the timing frame TGM _PHASE _TIME. The B2B transfer involves a certain amount of timing frames. More details about the B2B timing frames, please see Appendix A. The timing frames are not sent via the DM in order to reduce the traffic of the WR network and reduce the timing frame transfer delay on the WR network [?], so a specified VLAN, B2B VLAN, is defined for the B2B timing frames. All SCUs for the B2B transfer are assigned to the B2B VLAN. Fig. 4.7 illustrates an example of the transfer path of the B2B timing frames in the WR network. The frames are transferred along the path with orange color instead of the path with blue color.

4.3.3 Rf synchronization

The FAIR B2B transfer system is available for both the phase shift and frequency beating methods, see Sec. 2.3. The rf synchronization of two synchrotrons can be

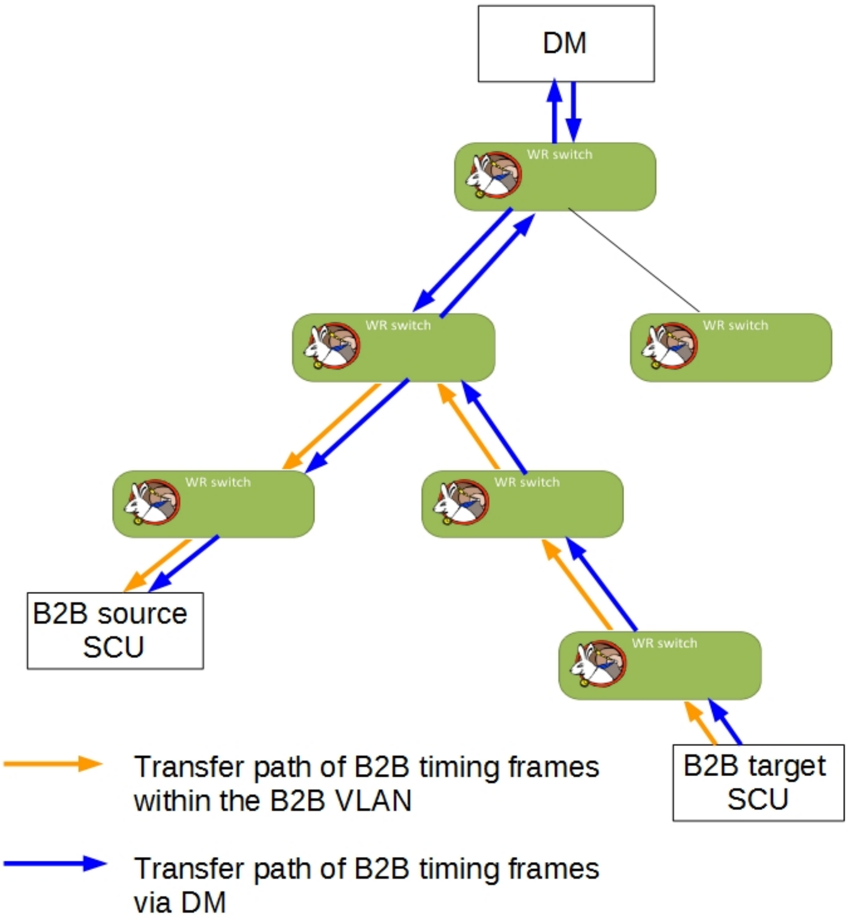

Figure 4.7: One example of the transfer path of the B2B timing frames in the WR network

realized based on the measurement of the phase difference between the Reference RF Signals of two rf systems. With the phase shift method, a frequency modulation with a fixed duration is applied to the Reference RF Signal of one (or both) rf system. With the frequency beating method, the phase difference varies at the rate of the synchronization frequency difference between two rf systems.

- Rf synchronization with the phase shift method

  Eq. 2.22 gives the relation between the required phase shift and the frequency modulation. The phase shift must be executed adiabatically, see Sec. 2.3. For the rf synchronization, the maximum required phase shift of the synchronization frequency is 360°. In order to accomplish the phase alignment as fast as possible, the phase shift will be conducted backward or forward. Therefore a phase shift of up to ±180° will be implemented on the synchronization frequency for the rf frequency modulation. A normalized frequency modulation profile $f_{normalized}$ for 180° can be precalculated, which guarantees the adiabaticity. The actual frequency modulation profile f_{actual} is decided by the normalized frequency modulation profile and the required phase shift, see eq. 4.2. The B2B source SCU calculates the required phase shift, $\Delta\phi$, according to the phase difference with the help of the required phase difference between two rf system. The SM provides the required phase difference with the consideration of the extra phase shift. If the SIS100 odd buckets need to be injected by one the SIS18 H^+ bunch, the extra phase shift equals to 0°, If the SIS100 even buckets need to be injected by one the SIS18 H^+ bunch, the extra phase shift equals to π.

$$\frac{\Delta\phi}{180^\circ} = \frac{f_{actual}}{f_{normalized}} \tag{4.2}$$

Fig. 4.8 shows an example of a normalized and several actual frequency modulation profiles and the corresponding phase shift profiles. The magenta profile is the normalized profile $f_{normalized}$ with the phase shift of 180°. The blue one is $1/2 f_{normalized}$ with the phase shift of 90° and the green one is $1/3 f_{normalized}$ with 60°.

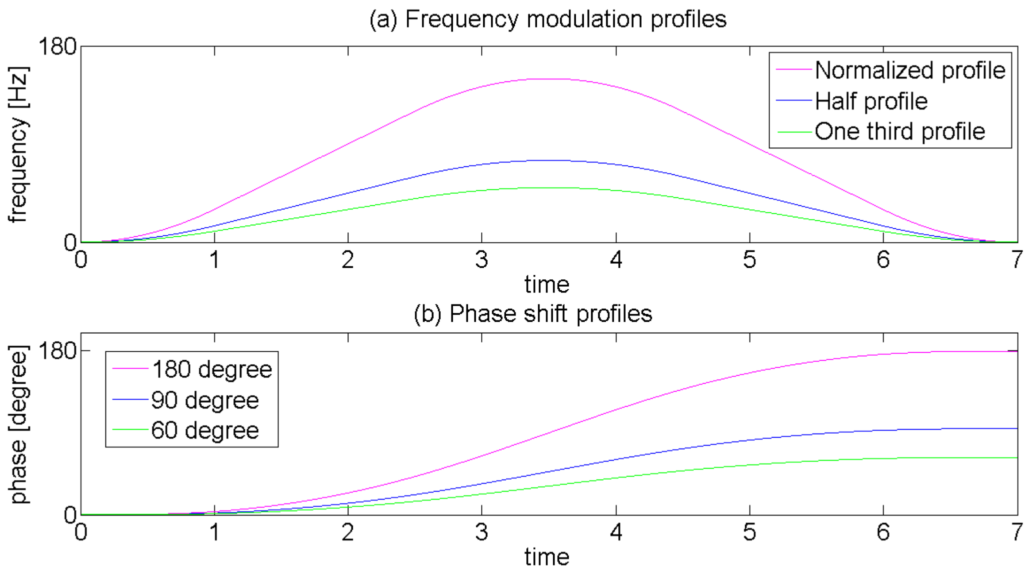

Figure 4.8: The normalized frequency and phase modulation profile and the actual profiles

Fig. 4.9 shows the implementation of the Phase Shift Module (PSM) in the B2B source SCU. The B2B source SCU sends the required phase shift to the PSM, which controls the phase shift of the Reference RF Signal of Group DDS by means of either the frequency modulation (Fig. 4.8 (a)) or the phase modulation (Fig. 4.8 (b)). The required phase shift is distributed star-shaped to all the Group DDS of the synchrotron. The Reference RF Signal is routed to the different cavity systems by a Switch Matrix to realize the phase shift of all cavities on the synchrotron. For more details about the implementation and realization of the PSM module, please see "Development of the LLRF system for a deterministic Bunch-to-Bucket transfer for FAIR" [**?**].

A particular case of the B2B synchronization occurs, when the target synchrotron is empty, i.e. it does not capture any bunch yet, the phase shift can be done for the target synchrotron without adiabatical consideration (e.g. the phase jump is possible). In this case, the B2B source SCU sends the timing frame TGM_PHASE_JUMP to the B2B target SCU, which contains the required phase jump. After the B2B target SCU receives the timing frame, it

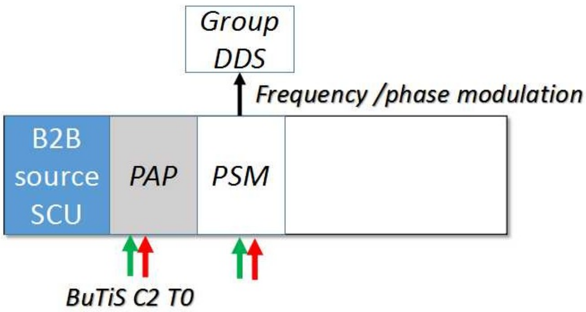

Figure 4.9: Implementation of the Phase Shift Module in the B2B source SCU

sends the value to the PSM for the phase jump of the Group DDS of the target synchrotron.

- Rf synchronization with the frequency beating method

  The circumference ratio between many pair of machines in FAIR is not an integer, the synchronization frequencies of two synchrotrons begin beating automatically. For the pairs with an integral circumference ratio, the synchronization frequency of the source synchrotron is detuned. The Group DDS produces the detuned Reference RF Signal.

4.3.4 Coarse synchronization

The coarse synchronization is achieved by the synchronization window with a certain length. Within this window, bunches are transferred into buckets with the center mismatch smaller than the upper bound[2]. The length of the synchronization window T_{sync_win} is two rf periods of the reproduced signal for the bucket label, see Sec. 4.3.5. For the phase shift method, the bunch-to-bucket injection center mismatch within the synchronization window is almost 0°. For the frequency beating method, the maximum bunch-to-bucket injection center mismatch $\Delta\phi$ within the synchronization window is calculated by

$$\frac{T_{sync\_win}}{1/\Delta f} = \frac{\Delta\phi}{360°} \tag{4.3}$$

The B2B source SCU obtains the delay compensation for the TOF, all propagation delays and kicker preparation time from the SM. It calculates the synchronization window, taking the delay compensation into consideration and transfers the timestamp of the start of the synchronization window, TGM_SYNCH_WIN, to the DM and the source and target Trigger SCUs via the WR network. The Trigger SCUs are used to produce the kicker trigger signals.

4.3.5 Bucket label

The bucket label is realized based on the indication signal for the first bucket plus a fixed delay for the indication of the correct buckets to be filled. The indication signal indicates the passing time of the first bucket of the target synchrotron, when it is

[2]B2B transfer from the SIS18 to the SIS100: upper bound of the bunch-to-bucket center mismatch is ±1°

correct phase aligned with the rf system of the source synchrotron for the bunch-to-bucket injection. The first bucket of the target synchrotron is indicated by f_{rev}^{trg}. The correct phase alignment of the rf system of the target synchrotron with the rf system of the source synchrotron is indicated directly by f_{syn}^{trg} for the phase shift method (black bars on the second x-axis of Fig. 4.10 (a)) and indirectly by f_{syn}^{trg} for the frequency beating method (black bars on the second x-axis of Fig. 4.10 (b)). Hence, the rising edges of the bucket label signal occurs, when the positive zero-crossings of f_{rev}^{trg} overlap that of f_{syn}^{trg}, see Fig. 4.10. In Fig. 4.10, the bunch length is not taken into consideration. (a) is the FAIR use case of the U^{28+} B2B transfer from the SIS18 to the SIS100 and (b) is the FAIR use case of the h=4 B2B transfer from the SIS18 to the ESR, more details, please see Chap. 5.

The indication signal is either with the revolution frequency or the synchronization frequency of the target synchrotron. It is dependent on the relation between the revolution frequency and the synchronization frequency of the target synchrotron. When $f_{syn}^{trg} >= f_{rev}^{trg}$, namely the rf period of the synchronization frequency is equal to or less than the revolution period, the rf period of the synchronization frequency is not long enough to include all buckets. In this case, the indication signal is with the revolution frequency of the target synchrotron and the synchronization window is two times long as the revolution period, namely $T_{sync\_win} = 2 \cdot T_{rev}^{trg}$. Oppositly, the indication signal is with the synchronization frequency of the target synchrotron and the synchronization window is two times long as the rf period of the synchronization frequency, namely $T_{sync\_win} = 2 \cdot T_{syn}^{trg}$. T_{syn}^{X} is denoted as the rf period of the synchronization frequency of the synchrotron X. Because the phase advance of the Reference RF Signal complies with the linear relation with time, see eq. 4.4, its evolution of the target synchrotron can be calculated.

$$\psi^X = k^X t + \psi_0^X \tag{4.4}$$

Where ψ^{trg} and $t_{\psi^{trg}}$ coincidence with the linear relationship, so ψ_0^X, the initial phase advance, can be calculated as $\psi^{trg} - kt_{\psi^{trg}}$.

The indication signal can be corrected exactly in phase with the frequency of f_{rev}^{trg} or f_{syn}^{trg} by the evolution of the phase advance of the Reference RF Signal. The indication signal is exactly a copy of the revolution frequency or the synchronization frequency of the target synchrotron, so it is called the "reproduced signal", or the “bucket label signal“ from the functional perspective. The reproduced signal could be reproduced campus-wide. A specific bucket is just a certain number of the cavity rf periods of the target synchrotron delay based on the reproduced signal.

The FAIR B2B transfer system needs the bucket label not only at the rf flattop, but also during the whole acceleration cycle. The bucket label at the rf flattop is used for the normal extraction and injection and the bucket label during the whole acceleration cycle is used for the emergency dump. For the SIS100 emergency kick, the reproduced signal has always the same frequency and is always in phase with the SIS100 revolution signal, so it is called the "real-time reproduced signal". The delay based on the real-time reproduced signal always indicates the bunch gap.

The bucket label is realized by the Trigger SCU, the Signal Reproduction (SR) module and the Phase Correction Module (PCM), see Fig. 4.11. The reproduced signal is produced by SR module. The Trigger SCU is responsible for the receipt of the phase correction value from the B2B source SCU and the transfer of this value to the PCM. The PCM module is used to correct the phase of the reproduced

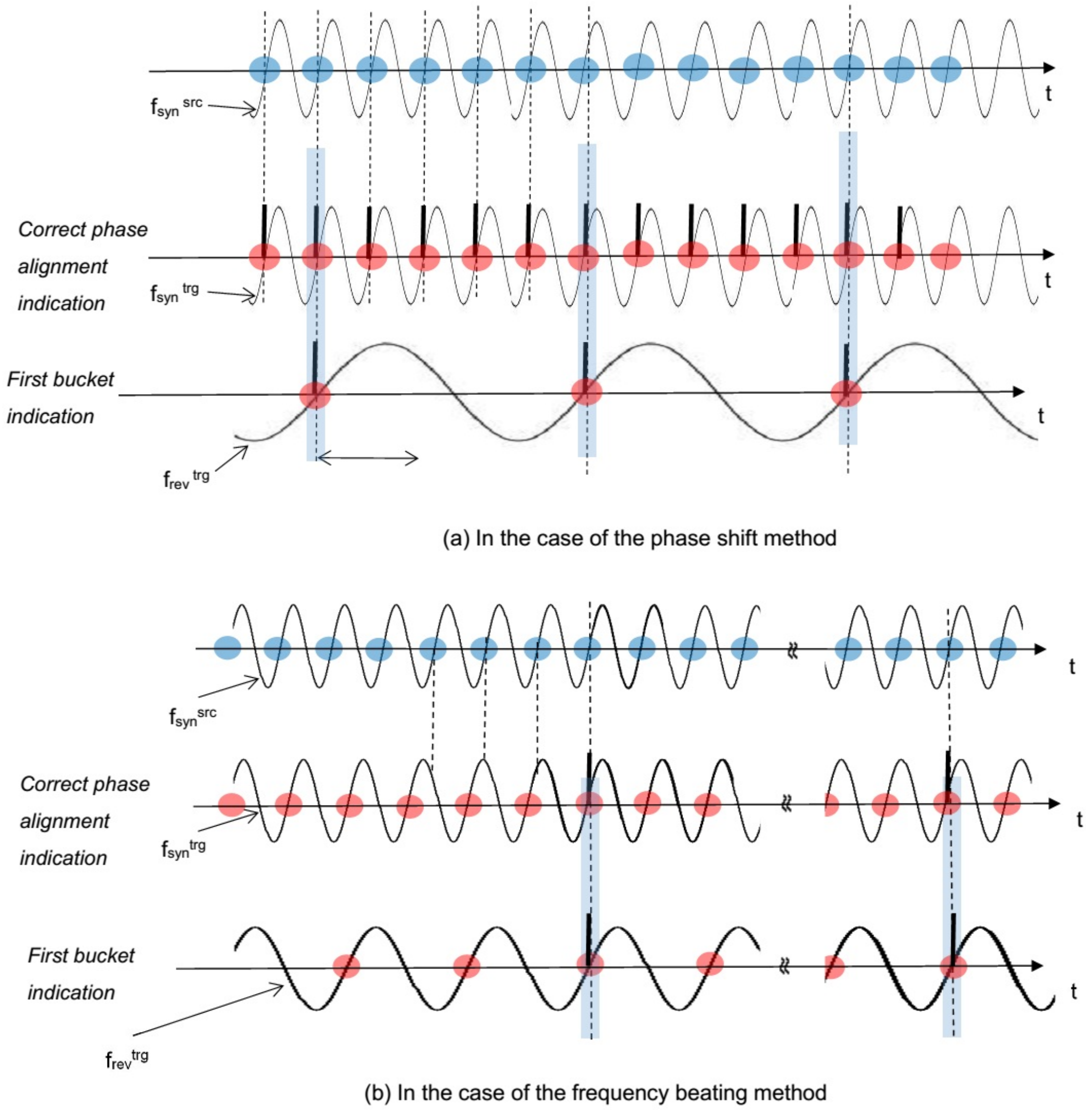

Figure 4.10: The occurrence of the rising edges of the bucket label signal. Red dots represent buckets and blue ones represent bunches of the source synchrotron. The occurrence of the rising edges of the bucket label signal are at the positive zero-crossings chosen by blue rectangles. The phase of two rf systems in this example is correct phase aligned with $\Delta\phi = 0°$. (a) In the case of the phase shift method. (b) In the case of the frequency beating method.

signal. The PCM module is as a SCU salve in the Trigger SCU. The SR module produces the bucket label signal in the format of the pulse wave, whose rising edges are aligned with the positive zero-crossings of the rf signal of the revolution frequency or the synchronization frequency. For more details about the implementation and realization of the PCM and the SR module, please see "Development of the LLRF system for a deterministic Bunch-to-Bucket transfer for FAIR" [?].

- Bucket label for the normal extraction and injection

  For the bucket label for the normal extraction and injection, three steps are necessary. Fig. 4.12 shows these three steps for the reproduction of the bucket

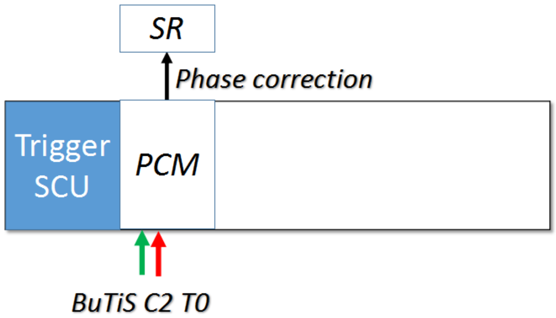

Figure 4.11: Implementation of the Phase Correction Module in the Trigger SCU

label. Here the B2B transfer from the SIS18 to the SIS100 is taken as an example.

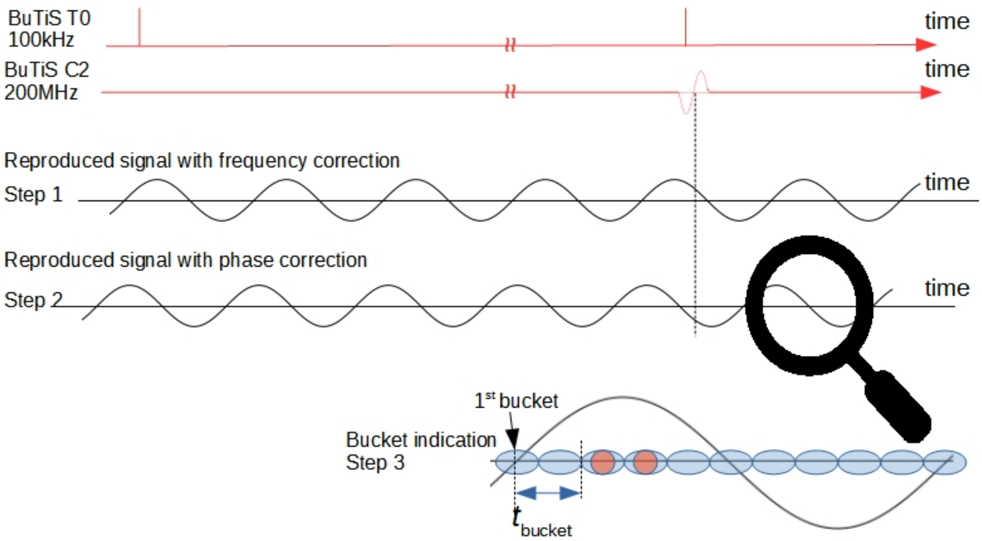

Figure 4.12: The realization of the bucket label for the normal extraction and injection.

- Step 1. Frequency correction

  The SR module produces the "reproduced signal" with the same frequency as the revolution frequency or the synchronization frequency of the target synchrotron. The positive zero-crossing of the reproduced signal always indicates the start of the 1st bucket.

- Step 2. Phase correction

  The reproduced signal must do the phase correction at a specified first positive zero-crossing of C2 clock after T0 edge. The phase correction value is calculated by the B2B source SCU and transferred by the timing frame TGM _PHASE _CORRECTION to the Trigger SCU. Then the Trigger SCU gives the phase correction value to the SR module via the PCM.

- Step 3. Bucket indication

  The SM considers the bucket pattern t_{bucket} within the kicker delay compensation, see Sec. 4.1.2. In Fig. 4.12, the reproduced signal is with the SIS100 revolution frequency and the 3rd and 4th buckets of ten buckets will be filled with $t_{bucket} = 1 \cdot T_{rev}^{SIS18}$.

- Bunch gap label for the emergency extraction

  Only for the SIS100 emergency procedure, the bunch gap label is important during the whole acceleration cycle. There are two steps for the realization of the bunch gap label, see Fig. 4.13.

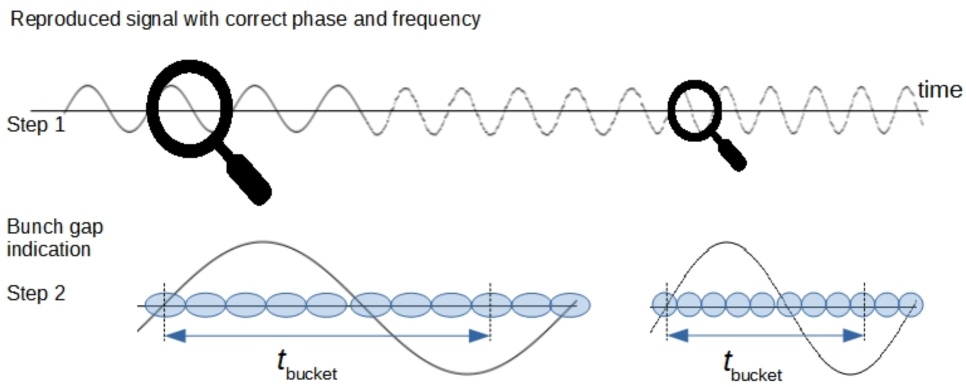

Figure 4.13: The realization of the bunch gap for the emergency extraction.

- Step 1. Reproduced signal synchronized with the Reference RF Signal of the revolution frequency

  The real-time reproduced signal is directly distributed from the switch matrix, which synchronizes with the Reference RF Signal of the revolution frequency in frequency and phase.

- Step 2. Bunch gap indication

  The SM considers the bunch gap t_{bucket} within the kicker delay compensation. In Fig. 4.13, the real-time reproduced signal is with the SIS100 revolution frequency and the 9th and 10th buckets of ten buckets are taken as an example as the bunch gap. The $t_{bucket} = 4 \cdot T_{rev}^{SIS18}$.

4.3.6 Fine synchronization of the extraction and injection kicker

After the synchronization of the rf systems between two synchrotrons, the TOF, all propagation and kicker preparation delays are compensated. Now, the extraction and injection kickers must be fired at the calculated trigger time within the bunch gap before the specific bunch or bucket passes the kickers.

This is the task of the Trigger Decision (TD) module in the Trigger SCU. The TD receives the synchronization window in the form of an enable signal. The fine synchronization will be accomplished by the pulse of the reproduced signal plus the extraction or injection kicker delay compensation from the SM. This achieves the fine synchronization of the B2B transfer. The TD transmits the kicker pulse directly to the kicker electronic.

In case of fatal errors or considerable damage, the emergency kicker must kick the beam immediately but within the bunch gap into the emergency dump.

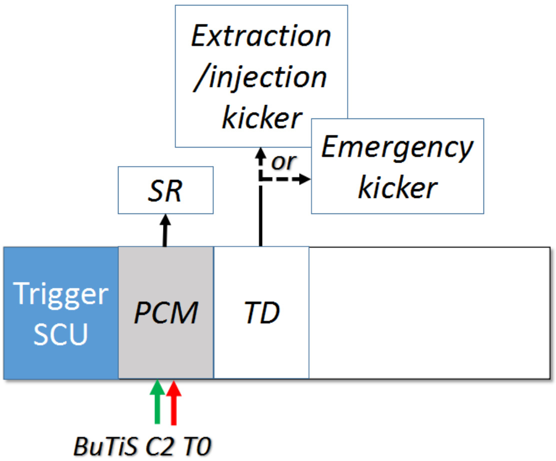

Figure 4.14: Implementation of the Trigger Decision module in the Trigger SCU

Fig. 4.14 shows the implementation of the Trigger Decision (TD) module in the Trigger SCU. The TD module is responsible for the production of triggers for the kickers.

The kicker triggering is realized based on the first rising edge of the bucket label signal within the synchronization window plus the kicker delay compensation. For the normal B2B extraction/injection, the synchronization window is received by the source and target Trigger SCUs from the WR network by TGM_SYNCH_WIN. The extraction kick delay compensation is $T_{rev}^{SIS100} + T_{rev}^{SIS18}$ -(t_{TOF} +t_{v_inj}+ t_{ext}) and the injection kicker delay compensation is $T_{rev}^{SIS100} + T_{rev}^{SIS18} - (t_{v\_inj} + t_{inj})$ in the example in Fig. 4.1, when the bucket label signal has the frequency of f_{rev}^{trg}.

For FAIR use cases, that the bucket label signal has the frequency of f_{syn}^{trg}, there is always only one bucket in the target synchrotron. In this case, the bucket pattern is not taken into consideration. The extraction kick delay compensation is $T_{syn}^{trg} - (t_{TOF} + t_{v\_inj} + t_{ext})$ and the injection kicker delay compensation is $T_{syn}^{trg} - (t_{v\_inj} + t_{inj})$, see Fig. 4.15.

Both extraction and injection kick delay compensation values are preloaded from the SM to the Trigger SCU and the Trigger SCU gives these values to the TD module. When the beam injection inhibit signal from the MPS is on, the TD module will block the extraction/injeciton trigger.

For the SIS100 emergency kick, the extraction delay compensation is calculated by $T_{rev}^{SIS100} + t_{bucket} - (t_{v\_emg} + t_{emg})$, where t_{v_emg} is the time delay between the virtual rf cavity and the emergency extraction position and t_{emg} the emergency kicker delay. The emergency extraction delay compensation values are preloaded from the SM to the Trigger SCU and the Trigger SCU gives these values to the TD module. The kicker delay compensation is applied to the real-time reproduced signal by TD module. Only when the emergency dump signal from MPS is valid, the emergency kicker will be triggered by the TD module.

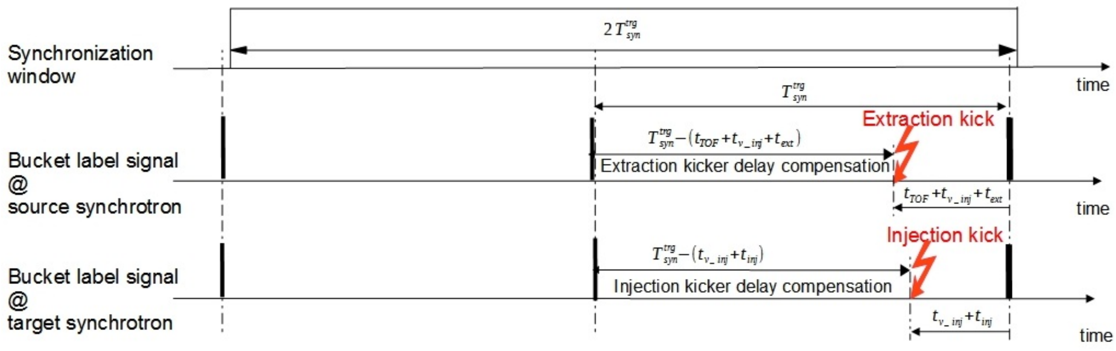

Figure 4.15: The illustration of the kicker delay compensation when the bucket label signal has the frequency of f_{syn}^{trg}.
Red lighting bolts represent the extraction and injection kicker firing.

4.3.7 B2B transfer status check

The B2B transfer status must be known by the DM. The B2B source SCU, the B2B transfer master, is responsible for the status check. The B2B source SCU receives the trigger time of the extraction kicker and actual beam extraction time, TGM _KICKER _TRIGGER _TIME _S, from the source Trigger SCU via the WR network and also the trigger time of the injection kicker and actual beam injection time, TGM _KICKER _TRIGGER _TIME _T, from the target Trigger SCU via the WR network. The Trigger SCU collects the kicker trigger time and the beam extraction/injection time. The B2B source SCU examines the status of the B2B transfer system and transfers the status and the actual beam injection time, TGM _B2B _STATUS, to the DM. If all components of the B2B transfer system work correctly and the B2B transfer process is successful. Otherwise it is failed.

4.4 Data flow of the FAIR B2B transfer system

In this section, the procedure for the B2B transfer is explained from the perspective of the data flow, which follows the basic six steps in Fig. 4.2. Fig. 4.16 shows the data flow in the source and target synchrotrons and between two synchrotrons. The rectangle with the different color represents the basic six steps. The left part in each rectangle presents the data flow in the source synchrotron and the right part the data flow in the target synchrotron.

1. The DM sends the timing frame CMD_START_B2B to the B2B source and target SCUs for the start of the B2B transfer via the WR network. Besides, it requests the switch-off of the feedback loop.

2. After receiving CMD_START_B2B, the B2B source and target SCUs start the PAM module to measure the phase advance $\Delta\varphi^X$ with the help of the PAP module locally and the PAP module extrapolates the phase advance in the future. After a period of time, the B2B source and targtet SCU reads the extrapolated phase advance ψ^X and the slope of the phase advance k^{trg} from the PAP module locally, timestamping the ψ^X.

3. The B2B target SCU sends the extrapolated phase ψ^{trg}, the corresponding timestamp $t_{\psi^{trg}}$ and the slope k^{trg} in the format of the timing frame TGM _PHASE _TIME to the B2B source SCU via the WR network.

4. When the B2B source SCU receives the timing frame TGM _PHASE _TIME, it calculates the synchronization window and transfers the timestamp of the start of the window to the DM in the format of the timing frame TGM _SYNCH _WIN, as well as to the Trigger SCUs at the source and target synchrotrons. The B2B source SCU calculates the phase correction value and transfers it to all Trigger SCUs via the WR network in the format of the timing frame TGM _PHASE _CORRECTION. Then the Trigger SCUs transfer the phase correction value to its PCM. The PCM starts the phase correction of the SR module.

   Only for the phase shift method, the B2B source SCU calculates the required shifted phase $\Delta\phi$ and transfers it to the PSM. Then the PSM transfers the phase or frequency modulation profile to the Group DDS.

5. When the source and target Trigger SCUs receive the timing frame TGM _SYNCH _WIN, they produces the synchronization window pulse for the TD module. With the help of the reproduced signal from the SR module, the kicker delay compensation from the Trigger SCU and the indication signals (the emergency dump signal and the beam injection inhibit signal) from the MPS, the TD module produces the normal extraction/injection trigger signals or the emergency kick trigger for the kicker.

6. The extraction and injection kickers or emergency kicker are fired. After that, the source Trigger SCU gets the actual beam extraction time and the timestamp of the extraction trigger signal from the TD module and transfers them to the source B2B SCU in the format of the timing frame TGM _KICKER _TRIGGER _TIME _S. The target Trigger SCU gets the timestamp of actual beam injection time and the timestamp of the injection trigger signal from the TD module and transfers them to the source B2B SCU in the format of the timing frame TGM _KICKER _TRIGGER _TIME _T. Then the B2B source SCU checks the B2B transfer status and transfers the status together with the beam injection time to the DM in the format of the timing frame TGM _B2B _STAUS (represented as the red line in the rectangle of step 6 in Fig. 4.16).

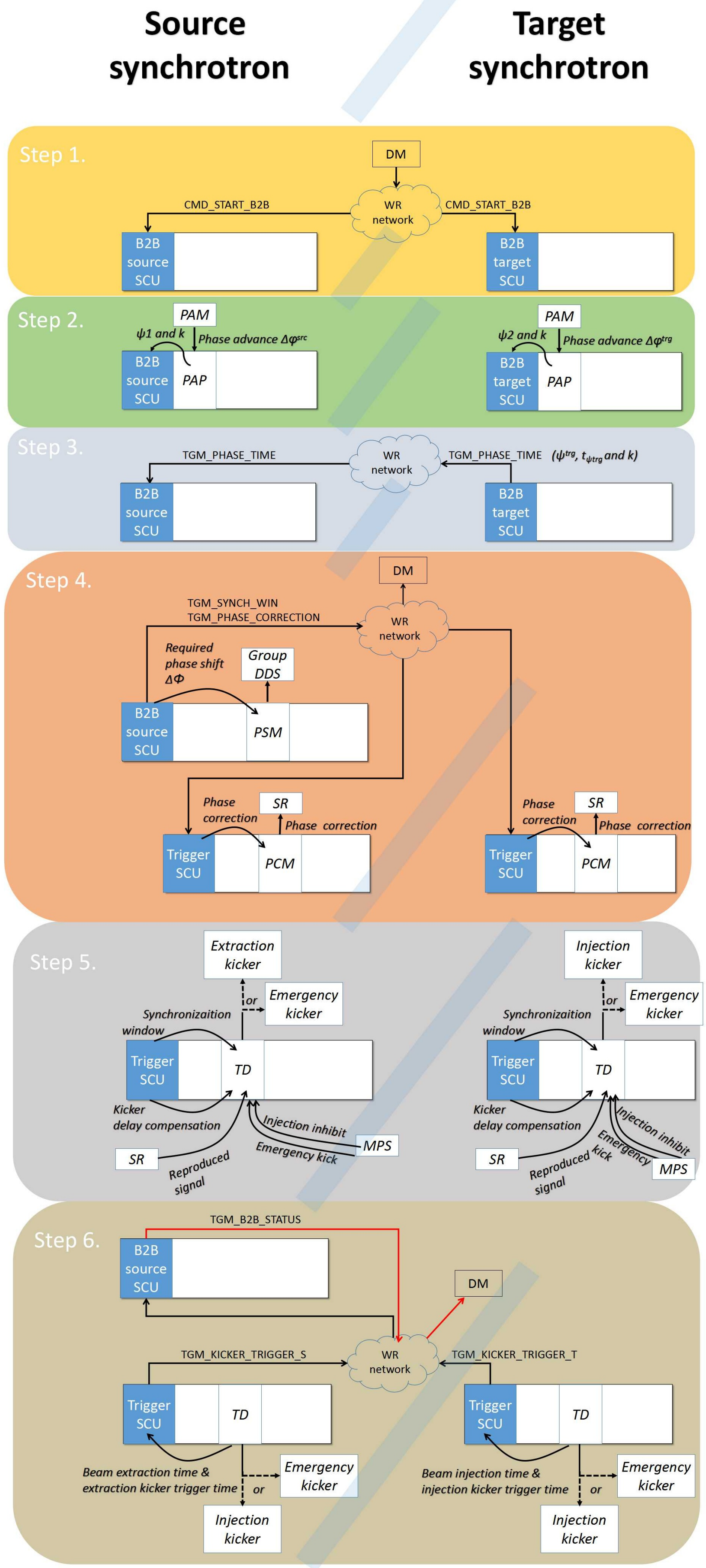

Figure 4.16: The data flow of the B2B transfer system

Chapter 5

Application of the FAIR B2B transfer system for FAIR accelerators

The phase shift method must be executed slowly enough to preserve the beam emittance, which needs much longer time than the frequency beating method. Besides, many FAIR accelerator pairs are beating automatically due to the non integer ratio of the circumference between two synchrotrons. So there is a preference for FAIR to use the frequency beating method. In this chapter all FAIR use cases with the frequency beating method will be discussed in details. Based on the circumference ratio, there are three scenarios of the B2B transfer for FAIR with the frequency beating method.

- The circumference ratio between the large and small synchrotrons is an integer.
  - The U^{28+} B2B transfer from the SIS18 to the SIS100
  - The H^{+} B2B transfer from the SIS18 to the SIS100
- The circumference ratio between the large and small synchrotrons is close to an integer.
  - The h=4 B2B transfer from the SIS18 to the ESR
  - The h=1 B2B transfer from the SIS18 to the ESR
  - The B2B transfer from the ESR to the CRYRING
- The circumference ratio between the large and small synchrotrons is far away from an integer.
  - The B2B transfer from the CR to the HESR

Besides, FAIR has many use cases of B2B transfers that the extraction and injection beam have different energy because of targets installed between two synchrotrons (e.g. a Pbar, FRS or Super FRS). In this situation, the beam revolution frequency ratio between the small and large synchrotrons is equivalent to the circumference ratio between the large and small synchrotrons.

- The revoluiton frequency ratio between the small and large synchrotrons is far away from an integer.

- The H^+ B2B transfer from the SIS100 to the CR via a Pbar
- The rare isotope beams (RIB) B2B transfer from the SIS100 to the CR via a Super FRS
- The B2B transfer from the SIS18 to the ESR via a FRS

Tab. 5.1 lists all FAIR use cases of the B2B transfer. m, n and κ are integers.

Table 5.1: FAIR B2B transfer use cases

Circumference ratio	C^l/C^s	$\frac{f^s_{rev}}{f^l_{rev}}$	Use cases of FAIR accelerators
$C^l/C^s = \kappa$ an integer	5		U^{28+} B2B transfer from the SIS18 to the SIS100
	5		H^+ B2B transfer from the SIS18 to the SIS100
$C^l/C^s = \kappa + \lambda$ or $frev^s/frev^l = \kappa + \lambda$ close to an integer ($\lvert\lambda\rvert <= 0.005$)	2-0.003		h=4 B2B transfer from the SIS18 to the ESR
	2-0.003		h=1 B2B transfer from the SIS18 to the ESR
	2+0.003		B2B transfer from the ESR to the CRYRING
$C^l/C^s = m/n + \lambda$ or $frev^s/frev^l = m/n + \lambda$ far away from an integer ($\lvert\lambda\rvert <= 0.05$)	not applicable	4.8-0.039	H^+ B2B transfer from the SIS100 to the CR via a Pbar
	not applicable	4.4-0.0046	RIB B2B transfer from the SIS100 to the CR via a Super FRS
	2.6-0.003		B2B transfer from the CR to the HESR
	not applicable	1.8+0.036	B2B transfer from the SIS18 to the ESR via a FRS

5.1 Circumference ratio is an integer

When the circumference ratio of the large synchrotron to that of the small synchrotron is an integer, there exists the following relation between two rf frequencies.

$$\frac{f^l_{rf}}{f^s_{rf}} = \frac{h^l}{h^s \cdot \kappa} \tag{5.1}$$

Two synchronization rf frequencies are

$$f^l_{syn} = \frac{f^l_{rf}}{h^l/Y} = Y f^l_{rev} \tag{5.2}$$

$$f_{syn}^{s} = \frac{f_{rf}^{s}}{h^{s}\kappa/Y} = \frac{Y}{\kappa} f_{rev}^{s} \tag{5.3}$$

Y is the GCD of h^l and $h^s \cdot \kappa$. More details, please see Sec. 2.2.1.

f_{syn}^{l} and f_{syn}^{s} are chosen for the phase shift method. There is a constant phase difference between two synchroniation frequencies. The phase shift can be implemented either for the rf system of the large or small synchrotron, because the rf frequency modulation only depends on the ion species and the required phase shift. Only when the target synchrotron is empty, the phase will be shifted for the target synchrotron by the phase jump. For the frequency beating method, two slightly different frequencies is based on f_{syn}^{l} and f_{syn}^{s} by detuning one of them. Generally the rf system of the source synchrotron is preferred to be detuned, which is easy to be achieved during or after the acceleration ramp.

The frequency of the bucket label signal depends on the relation between f_{syn}^{trg} and f_{rev}^{trg}.

When the large synchrotron is the target, there exists $f_{syn}^{l} = Y f_{rev}^{l} >= f_{rev}^{l}$. The revolution period is Y times as long as the period of f_{syn}^{l}. The period of f_{syn}^{l} is not long enough to contain all buckets. So the bucket label signal is with the frequency of f_{rev}^{l} for this case and the length of the synchronization window is two times as long as the revolution period of the large synchrotron.

When the small synchrotron is the target, the relation between $f_{syn}^{s} = f_{rev}^{s} \frac{Y}{\kappa}$ and f_{rev}^{s} is not fixed. If $f_{syn}^{s} >= f_{rev}^{s}$, namely $\frac{Y}{\kappa} >= 1$, the revolution period is $\frac{Y}{\kappa}$ times long as the period of f_{syn}^{s}. Hence, the bucket label signal is with the frequency of f_{rev}^{s} and the length of the synchronization window is two times as long as the revolution period of the small synchrotron. Oppositly, if $f_{syn}^{s} < f_{rev}^{s}$, namely $\frac{Y}{\kappa} < 1$, the period of f_{syn}^{s} is $\frac{\kappa}{Y}$ times as long as the revolution period. Hence, the rf frequency with f_{syn}^{s} is used as the bucket label signal and the length of the synchronization window is two times as long as the rf period of the synchronization frequency of the small synchrotron.

In fact, two synchronization frequencies could be a fraction (between $1/Y$ and 1) times of f_{syn}^{X}. The bunch-to-bucket injection center mismatch is the mismatch between the cavity rf frequencies within the synchronization window, so it is $f_{rf}^{trg}/f_{syn}^{trg}$ times as large as the phase mismatch between two synchronization frequencies within the synchronization window. When we use one of two synchronization frequencies as the frequency of the bucket label signal, the synchronization window is two times as long as the rf period of the synchronization frequency of the target synchrotron, so the phase mismatch between two synchronization frequencies within the synchronization window is a constant. The longer the synchronization window, namely the smaller the synchronization frequency, the larger the bunch-to-bucket injection center mismatch. When we use one of two revolution frequencies as the bucket label signal, the length of the synchronization window is constant. Hence, the bunch-to-bucket injection center mismatch within the synchronization window is also constant. In conclusion, f_{syn}^{X} is chosen as the synchronization frequencies.

Tab. 5.2 shows the formulas for the frequency of the bucket label signal, two slightly different frequencies for the beating, the frequency of the Synchronization Reference Signal, the length of the synchronization window and the bunch and bucket center mismatch when the large synchrotron is the target. Tab. 5.3 shows the formulas when the small synchrotron is the target.

Table 5.2: Synchronization when the circumference ratio is an integer and the large synchrotron is the target

	Large synchrotron is target synchrotron
Frequency of bucket label	f^l_{rev}
synchronization frequencies	$f^s_{syn} + \Delta f$ and f^l_{syn}
Frequency of Synchronization Reference Signal	$f^{REF}_{syn} = round(f^l_{syn}/100\,\mathrm{kHz}) \cdot 100\,\mathrm{kHz}$
Length of synchronization window	$2/f^l_{rev}$
Bunch-to-bucket injection center mismatch	$\pm\frac{1}{2} \cdot \frac{2/f^l_{rev}}{1/\Delta f} \cdot 360° \cdot \frac{f^l_{rf}}{f^l_{syn}}$

Table 5.3: Synchronization when the circumference ratio is an integer and the small synchrotron is the target

	Small synchrotron is target synchrotron	
Cases	$f^s_{syn} >= f^s_{rev}$ $(\frac{Y}{\kappa} >= 1)$	$f^l_{syn} < f^s_{rev}$ $(\frac{Y}{\kappa} < 1)$
Frequency of bucket label	f^s_{rev}	f^s_{syn}
synchronization frequencies	$f^l_{syn} + \Delta f$ and f^s_{syn}	
f^{REF}_{syn}	$round(f^s_{syn}/100\,\mathrm{kHz}) \cdot 100\,\mathrm{kHz}$	
Length of synchronization window	$2/f^s_{rev}$	$2/f^s_{syn}$
Bunch-to-bucket injection center mismatch	$\pm\frac{1}{2} \cdot \frac{2/f^s_{rev}}{1/\Delta f} \cdot 360° \cdot \frac{f^s_{rf}}{f^s_{syn}}$	$\pm\frac{1}{2} \cdot \frac{2/f^s_{syn}}{1/\Delta f} \cdot 360° \cdot \frac{f^s_{rf}}{f^s_{syn}}$

5.1.1 Use case of the U^{28+} B2B transfer from the SIS18 to the SIS100

The use case of the U^{28+} B2B transfer from the SIS18 to the SIS100 belongs to this scenario. Four batches of U^{28+} at 200 MeV/u are injected into continuous eight out of ten buckets of the SIS100. Each batch consists of two bunches [? ?]. The large synchroton is the SIS100 and the small one the SIS18. $\kappa = 5$, $h^{SIS100} = 10$ and $h^{SIS18} = 2$. The GCD of $h^{SIS100} = 10$ and $h^{SIS18} \cdot \kappa = 2 \cdot 5 = 10$ is 10, namely $Y = 10$. Substituting these values into eq. 2.27, we get

$$\frac{f_{rf}^{SIS100}}{f_{rf}^{SIS18}} = \frac{h^{SIS100}}{h^{SIS18} \cdot \kappa} = \frac{10}{2 \cdot 5} = \frac{10}{10} \tag{5.4}$$

Because the SIS100 is the large synchrotron and the target, substituting h^X, κ, f_{rf}^X, f_{rev}^X and Y into formulas in Tab. 5.2, the synchronization of the U^{28+} B2B transfer from the SIS18 to the SIS100 with the frequency beating method is obtained, see Tab. 5.4. Here we assume that the SIS18 is detuned with 200 Hz.

Table 5.4: Synchronization of the U^{28+} B2B transfer from the SIS18 to the SIS100 with the frequency beating method

	Large synchrotron (the SIS100) is target synchrotron
Frequency of bucket label	f_{rev}^{SIS100}
synchronization frequencies	$f_{syn}^{s} + \Delta f = f_{rf}^{SIS18} + 200\,\text{Hz}$=1.572 536 MHz+200 Hz and $f_{syn}^{l} = f_{rf}^{SIS100}$=1.572 536 MHz
f_{syn}^{REF}	1.6 MHz
Length of synchronization window	$2/f_{rev}^{SIS100} = 12.718\,\text{us}$
Bunch-to-bucket injection center mismatch	$\pm\frac{1}{2} \cdot \frac{2/frev^{SIS100}}{1/200} \cdot 360° \cdot 1 = \pm 0.5°$

After the synchronization, the phase difference between the SIS18 and SIS100 synchronization frequenciy markers equals to the sum of t_{v_inj}, t_{v_ext} and t_{TOF}. The SIS100 revolution frequency marker works for the bucket label. When the 1st and 2nd buckets are to be filled, $t_{pattern}$=0. When the 3rd and 4th buckets are to be filled, $t_{pattern}$=T_{rev}^{SIS18}. When the 5th and 6th buckets are to be filled, $t_{pattern}$= $2 \cdot T_{rev}^{SIS18}$. When the 7th and 8th buckets are to be filled, $t_{pattern}$= $3 \cdot T_{rev}^{SIS18}$. Detailed parameters of the U^{28+} B2B transfer from the SIS18 to the SIS100, please see Appendix ??.

5.1.2 Use case of the H^+ B2B transfer from the SIS18 to the SIS100

Four batches of H^+ at 4 GeV/u are injected into continuous four out of ten buckets of the SIS100. Each batch consists of one bunch [? ?]. The large synchrotron is the SIS100 and the small one the SIS18. $\kappa = 5$, $h^{SIS100} = 10$ and $h^{SIS18} = 1$. The

GCD of $h^{SIS100} = 10$ and $h^{SIS18} \cdot \kappa = 1 \cdot 5$ is 5, namely $Y = 5$. Substituting these values into eq. 2.27, we get

$$\frac{f_{rf}^{SIS100}}{f_{rf}^{SIS18}} = \frac{h^{SIS100}}{h^{SIS18} \cdot \kappa} = \frac{10}{1 \cdot 5} = \frac{2}{1} \tag{5.5}$$

Because the SIS100 is the large synchrotron and the target, substituting h^X, κ, f_{rf}^X, f_{rev}^X and Y into formulas in Tab. 5.2, the synchronization of the H^+ B2B transfer from the SIS18 to the SIS100 with the frequency beating method is obtained, see Tab. 5.5. Here we assume that the SIS18 is detuned with 200 Hz for the frequency beating method.

Table 5.5: Synchronization of the H^+ B2B transfer from the SIS18 to the SIS100 with the frequency beating method

	Large synchrotron (the SIS100) is target synchrotron
Frequency of bucket label	f_{rev}^{SIS100}
synchronization frequencies	$f_{syn}^s + \Delta f = f_{rf}^{SIS18} + 200\,\text{Hz}$=1.359 358 MHz+200 Hz and $f_{syn}^l = f_{rf}^{SIS100}/2$=1.359 358 MHz
f_{syn}^{REF}	1.4 MHz
Length of synchronization window	$2/f_{rev}^{SIS100} = 7.356$ us
Bunch-to-bucket injection center mismatch	$\pm\frac{1}{2} \cdot \frac{2/f_{rev}^{SIS100}}{1/200} \cdot 360° \cdot 2 = \pm 0.6°$

The the SIS100 revolution frequency marker works for the bucket label. In order to inject into the odd and even number buckets, there are two scenarios of the phase difference between the SIS18 and SIS100 synchronization frequency markers after the synchronization.

- Injection into odd number buckets

  The phase difference between the SIS18 and SIS100 synchronization frequency markers equals to t_{v_ext}+t_{v_inj}+ t_{TOF}. When the 1st bucket is to be filled, $t_{pattern}$=0. When the 3rd bucket is to be filled, $t_{pattern}$=1 $\cdot$ T_{rev}^{SIS18}.

- Injection into even number buckets

  The phase difference between the SIS18 and SIS100 synchronization frequency markers equals to t_{v_ext}+t_{v_inj}+t_{TOF}- T_{rf}^{SIS100}. When the 2nd bucket is to be filled, $t_{pattern}$=0. When the 4th bucket is to be filled, $t_{pattern}$=1 $\cdot$ T_{rev}^{SIS18}.

Detailed parameters of the H^+ B2B transfer from the SIS18 to the SIS100, please see Appendix **??**.

5.2 Circumference ratio is close to an integer

When the circumference ratio of the large synchrotron to that of the small synchrotron is very close to an integer, there exists the relation between two rf frequencies.

$$\frac{f^l_{rf}}{f^s_{rf}} = \frac{h^l}{h^s \cdot (\kappa + \lambda)} = \frac{h^l}{h^s \cdot \kappa + h^s \cdot \lambda} \tag{5.6}$$

Besides, it is also grouped to this scenario, that the revolution frequency ratio between the small and large synchrotrons is close to an integer when the beam passes a target (e.g. a FRS, a Pbar) between two synchrotrons. The ratio between two revolution frequencies can be expressed as

$$\frac{f^s_{rev}}{f^l_{rev}} = \kappa + \lambda \tag{5.7}$$

The relation between two cavity rf frequencies is same as eq. 5.6. Two synchronization frequencies are

$$f^l_{syn} = \frac{f^l_{rf}}{h^l/Y} = Y f^l_{rev} \tag{5.8}$$

$$f^s_{syn} = \frac{f^s_{rf}}{h^s\kappa/Y} = \frac{Y}{\kappa} f^s_{rev} \tag{5.9}$$

Y is the GCD of h^l and $h^s \cdot \kappa$.

Two synchronization frequencies are beating automatically. The choice of the frequency for the bucket label signal and the calculation of the synchronization window are same as that of the integral circumference ratio scenario. Tab. 5.6 shows the formulas for the frequency beating method when the large synchrotron is the target and Tab. 5.7 shows the formulas when the small synchrotron is the target.

5.2.1 Use case of the h=4 B2B transfer from the SIS18 to the ESR

Continuous two of four bunches are injected into two buckets of the injection orbit of the ESR [**?**]. The beam is accumulated in the ESR. The large synchrotron is the SIS18 and the small one is the ESR. $h^{SIS18} = 4$ and $h^{ESR} = 2$. Substituting the circumference of the SIS18 and the ESR into eq. 2.31, we get

$$\frac{C^l}{C^s} = \kappa + \lambda = 2 - 0.003 \tag{5.10}$$

The GCD of $h^{SIS18} = 4$ and $h^{ESR} \cdot \kappa = 2 \cdot 2 = 2$ is 4, namely $Y = 4$. Substituting h^{SIS18}, h^{ESR}, κ and λ into eq. 2.35, we get

$$\frac{f^{SIS18}_{rf}}{f^{ESR}_{rf}} = \frac{h^{SIS18}}{h^{ESR} \cdot (\kappa + \lambda)} = \frac{4}{2 \cdot (2 - 0.003)} \tag{5.11}$$

The ESR is the small synchrotron and the target and there exists $Y/\kappa > 1$,so substituting h^X, κ, λ, f^X_{rf} and Y into formulas in the second column in Tab. 5.7, the

Table 5.6: Synchronization when the circumference ratio is close to an integer and the large synchrotron is the target

	Large synchrotron is target synchrotron
Frequency of bucket label	f^l_{rev}
synchronization frequencies	$f^s_{syn} = \frac{f^s_{rf}}{(h^s \cdot \kappa)/Y}$ and $f^l_{syn} = \frac{f^l_{rf}}{h^l/Y}$
Frequency of Synchronization Reference Signal	$f^{REF}_{syn} = round(f^l_{syn}/100\,\text{kHz}) \cdot 100\,\text{kHz}$
Beating frequencies	$\Delta f = \lvert f^s_{syn} - f^l_{syn} \rvert$
Length of synchronization window	$2/f^l_{rev}$
Bunch-to-bucket injection center mismatch	$\pm\frac{1}{2} \cdot \frac{2/f^l_{rev}}{1/\Delta f} \cdot 360° \cdot \frac{f^l_{rf}}{f^l_{syn}}$

synchronization of the h=4 B2B transfer from the SIS18 to the ESR is obtained, see Tab. 5.8. Here we use the 30 MeV/u heavy ion as an example.

Detailed parameters of the $h = 4$ B2B transfer from the SIS18 to the ESR, please see Appendix **??**. After the synchronization, the phase difference between the SIS18 and ESR synchronization frequency markers depends on the accumulation method.

5.2.2 Use case of the h=1 B2B transfer from the SIS18 to the ESR

One bunch is injected into one bucket of the injection orbit of the ESR. The beam is accumulated in the ESR. The large synchrotron is the SIS18 and the small one is the ESR. $h^{SIS18} = 1$ and $h^{ESR} = 1$. Substituting the circumference of the SIS18 and the ESR into eq. 2.31, we get

$$\frac{C^l}{C^s} = \kappa + \lambda = 2 - 0.003 \tag{5.12}$$

The GCD of $h^{SIS18} = 1$ and $h^{ESR} \cdot \kappa = 1 \cdot 2 = 2$ is 1, namely $Y = 1$. Substituting h^{SIS18}, h^{ESR}, κ and λ into eq. 2.35, we get

$$\frac{f^{SIS18}_{rf}}{f^{ESR}_{rf}} = \frac{h^l}{h^s \cdot (\kappa + \lambda)} = \frac{1}{1 \cdot (2 - 0.003)} \tag{5.13}$$

The ESR is the target and there exists $Y/\kappa < 1$, so substituting h^X, κ, λ, f^X_{rf} and Y into formulas in the last column in Tab. 5.7, the synchronization of the h=1

Table 5.7: Synchronization when the circumference ratio is close to an integer and the small synchrotron is the target

	Small synchrotron is target synchrotron	
Cases	$f^s_{syn} >= f^s_{rev}$ $(\frac{Y}{\kappa} >= 1)$	$f^s_{syn} < f^s_{rev}$ $(\frac{Y}{\kappa} < 1)$
Frequency of bucket label	f^s_{rev}	f^s_{syn}
synchronization frequencies	$f^l_{syn} = \frac{f^l_{rf}}{h^l/Y}$ and $f^s_{syn} = \frac{f^s_{rf}}{(h^s \cdot \kappa)/Y}$	
Frequency of Synchronization Reference Signal	$f^{REF}_{syn} = round(f^s_{syn}/100\,\text{kHz}) \cdot 100\,\text{kHz}$	
Beating frequencies	$\Delta f = \lvert f^s_{syn} - f^l_{syn} \rvert$	
Length of synchronization window	$2/f^s_{rev}$	$2/f^s_{syn}$
Bunch-to-bucket injection center mismatch	$\pm\frac{1}{2} \cdot \frac{2/f^s_{rev}}{1/\Delta f} \cdot 360° \cdot \frac{f^s_{rf}}{f^s_{syn}}$	$\pm\frac{1}{2} \cdot \frac{2/f^s_{syn}}{1/\Delta f} \cdot 360° \cdot \frac{f^s_{rf}}{f^s_{syn}}$

Table 5.8: Synchronization of the h=4 B2B transfer from the SIS18 to the ESR with the frequency beating method

	Small synchrotron (the ESR) is target synchrotron
Frequency of bucket label	f^{ESR}_{rev}
synchronization frequencies	$f^l_{syn} = f^{SIS18}_{rf} = 1.373\,201\,\text{MHz}$ and $f^s_{syn} = f^{ESR}_{rf} = 1.371\,302\,\text{MHz}$
f^{REF}_{syn}	1.4 MHz
Beating frequencies	1899 Hz
Length of synchronization window	$2/f^{ESR}_{rev} = 2.917$ us
Bunch-to-bucket injection center mismatch	$\pm\frac{1}{2} \cdot \frac{2/f^{ESR}_{rev}}{1/1899} \cdot 360° \cdot 1 = \pm 1.0°$

Table 5.9: Synchronization of h=1 B2B transfer from the SIS18 to the ESR with the frequency beating method

	Small synchrotron (the ESR) is target synchrotron
Frequency of bucket label	f^s_{syn}
synchronization frequencies	$f^l_{syn} = \frac{f^{SIS18}_{rf}}{1} = 989.756\,\text{kHz}$ and $f^s_{syn} = \frac{f^{ESR}_{rf}}{2} = 988.388\,\text{kHz}$
f^{REF}_{syn}	$1\,\text{MHz}$
Beating frequencies	$1368\,\text{Hz}$
Length of synchronization window	$2/f^s_{syn} = 2.034\,\text{us}$
Bunch-to-bucket injection center mismatch	$\pm\frac{1}{2} \cdot \frac{2/f^s_{syn}}{1/1368} \cdot 360° \cdot 2 = \pm 1.0°$

B2B transfer from the SIS18 to the ESR is obtained, see Tab. 5.9. Here we use the 400 MeV/u proton as an example.

Detailed parameters of the $h = 1$ B2B transfer from the SIS18 to the ESR, please see Appendix **??**. After the synchronization, the phase difference between the SIS18 and ESR synchronization frequency markers depends on the accumulation method.

5.2.3 Use case of the B2B transfer from the ESR to the CRYRING

Only one bunch is injected into one bucket of the CRYRING [**?** **?**]. The large synchrotron is the SIS18 and the small one is the CRYRING. $h^{ESR} = 1$ and $h^{CRYRING} = 1$. Substituting the circumference of the ESR and the CRYRING into eq. 2.31, we get

$$\frac{C^l}{C^s} = \kappa + \lambda = 2 + 0.003 \tag{5.14}$$

The GCD of $h^{ESR} = 1$ and $h^{CRYRING} \cdot \kappa = 1 \cdot 2$ is 1, namely $Y = 1$. Substituting h^{ESR}, $h^{CRYRING}$, κ and λ into eq. 2.35, we get

$$\frac{f^{ESR}_{rf}}{f^{CRYRING}_{rf}} = \frac{h^l}{h^s \cdot (\kappa + \lambda)} = \frac{1}{1 \cdot (2 + 0.003)} \tag{5.15}$$

The CRYRING is the target and there exists $Y/\kappa < 1$, so substituting h^X, κ, λ, f^X_{rf} and Y into formulas in the last column in Tab. 5.7, the synchronization of the B2B transfer from the ESR to the CRYRING is obtained, see Tab. 5.10. Here we use the 30 MeV/u proton as an example.

The CRYRING synchronization frequency marker works for the bucket label. The phase difference between the ESR and CRYRING synchronization frequency

Table 5.10: Synchronization of the B2B transfer from the ESR to the CRYRING with the frequency beating method

	Small synchrotron (the CRYRING) is target synchrotron
Frequency of bucket label	f^s_{syn}
synchronization frequencies	$f^l_{syn} = f^{ESR}_{rf} = 0.685\,651\,\text{MHz}$ and $f^s_{syn} = \frac{f^{CRYRING}_{rf}}{2} = 0.686\,600\,\text{MHz}$
f^{REF}_{syn}	$0.7\,\text{MHz}$
Beating frequencies	$949\,\text{Hz}$
Length of synchronization window	$2/f^s_{syn} = 2.912\,\text{us}$
Bunch-to-bucket injection center mismatch	$\pm\frac{1}{2} \cdot \frac{2/f^s_{syn}}{1/949} \cdot 360° \cdot 2 = \pm 1.0°$

markers equals to $t_{v\_ext}+t_{v\_inj}+t_{TOF}$ after the synchronization. Detailed parameters of the B2B transfer from the ESR to the CRYRING, please see Appendix ??.

5.3 Circumference ratio is far away from an integer

When the circumference ratio of the large synchrotron to that of the small synchrotron is far away from an integer, there exists the relation between two rf frequencies.

$$\frac{f^l_{rf}}{f^s_{rf}} = \frac{h^l \cdot n}{h^s \cdot m + h^s \cdot \lambda \cdot n} \tag{5.16}$$

Besides, it is also grouped to this scenario, that the revolution frequency ratio between the small and large synchrotrons is far away from an integer when the beam passes a target between two synchrotrons. The revolution frequency ratio can be expressed as

$$\frac{f^s_{rev}}{f^l_{rev}} = \frac{m}{n} + \lambda \tag{5.17}$$

The relation between two cavity rf frequencies is same as eq. 5.16. Two synchronization frequencies are

$$f^l_{syn} = \frac{f^l_{rf}}{h^l n/Y} = \frac{Y}{n} f^l_{rev} \tag{5.18}$$

$$f^s_{syn} = \frac{f^s_{rf}}{h^s m/Y} = \frac{Y}{m} f^s_{rev} \tag{5.19}$$

Y is the GCD of $h^l \cdot n$ and $h^s \cdot m$.

Two synchronization frequencies are beating automatically. When the large synchrotron is the target, the frequency of the bucket label signal depends on the relation between f^s_{syn} and f^s_{rev}. When $f^l_{syn} >= f^l_{rev}$, namely $\frac{Y}{n} >= 1$, the synchronization period is not long enough to indicate all buckets. Hence, the frequency of the bucket label signal is f^s_{rev}. Or the bucket label signal with the frequency of f^l_{syn}. Tab. 5.11 shows the formulas when the large synchrotron is the target.

Table 5.11: Synchronization when the circumference ratio is far away from an integer and the large synchrotron is the target

	Large synchrotron is target synchrotron	
Cases	$f^l_{syn} >= f^l_{rev}$ $(\frac{Y}{n} >= 1)$	$f^l_{syn} < f^l_{rev}$ $(\frac{Y}{n} < 1)$
Frequency of bucket label	f^l_{rev}	f^l_{syn}
synchronization frequencies	$f^s_{syn} = \frac{f^s_{rf}}{(h^s \cdot m)/Y}$ and $f^l_{syn} = \frac{f^l_{rf}}{(h^l \cdot n)/Y}$	
Frequency of Synchronization Reference Signal	$f^{REF}_{syn} = round(f^l_{syn}/100\,\text{kHz}) \cdot 100\,\text{kHz}$	
Beating frequencies	$\Delta f = \lvert f^l_{syn} - f^s_{syn} \rvert$	
Length of synchronization window	$2/f^l_{rev}$	$2/f^l_{syn}$
Bunch-to-bucket injection center mismatch	$\pm\frac{1}{2} \cdot \frac{2/f^l_{rev}}{1/\Delta f} \cdot 360° \cdot \frac{f^l_{rf}}{f^l_{syn}}$	$\pm\frac{1}{2} \cdot \frac{2/f^l_{syn}}{1/\Delta f} \cdot 360° \cdot \frac{f^l_{rf}}{f^l_{syn}}$

When the small synchrotron is the target, the frequency of the bucket label signal depends on the relation between f^s_{syn} and f^s_{rev}. When $f^s_{syn} >= f^s_{rev}$, namely $\frac{Y}{m} >= 1$, the frequency of the bucket label signal is f^s_{rev}. Or the bucket label signal with the frequency of f^s_{syn}. Tab. 5.12 shows the formulas when the small synchrotron is the target.

There are various combination of $\frac{m}{n}$ and λ, λ determines the beating frequency. The smaller, the more precise bunch-to-bucket injection. $(h^l \cdot n)/Y$ and $(h^s \cdot m)/Y$ determines two synchronization frequencies. The bigger $(h^l \cdot n)/Y$ and $(h^s \cdot m)/Y$, the smaller two synchronization frequencies, which has higher requirement for the LLRF system. So we have to find a balance between the precision of the bunch-to-bucket injection and two synchronization frequencies for the beating.

Table 5.12: Synchronization when the circumference ratio is far away from an integer and the small synchrotron is the target

	Small synchrotron is target synchrotron	
Cases	$f^s_{syn} >= f^s_{rev}$ $(\frac{Y}{m} >= 1)$	$f^s_{syn} < f^s_{rev}$ $(\frac{Y}{m} < 1)$
Frequency of bucket label	f^s_{rev}	f^s_{syn}
synchronization frequencies	$f^s_{syn} = \frac{f^s_{rf}}{(h^s \cdot m)/Y}$ and $f^l_{syn} = \frac{f^l_{rf}}{(h^l \cdot n)/Y}$	
Frequency of Synchronization Reference Signal	$f^{REF}_{syn} = round(f^s_{syn}/100\,\text{kHz}) \cdot 100\,\text{kHz}$	
Beating frequencies	$\Delta f = \lvert f^s_{syn} - f^l_{syn} \rvert$	
Length of synchronization window	$2/f^s_{rev}$	$2/f^s_{syn}$
Bunch-to-bucket injection center mismatch	$\pm\frac{1}{2} \cdot \frac{2/f^s_{rev}}{1/\Delta f} \cdot 360° \cdot \frac{f^s_{rf}}{f^s_{syn}}$	$\pm\frac{1}{2} \cdot \frac{2/f^s_{syn}}{1/\Delta f} \cdot 360° \cdot \frac{f^s_{rf}}{f^s_{syn}}$

5.3.1 Use case of the H^+ B2B transfer from the SIS100 to the CR

Only one out of five bunches of proton is extracted from the SIS100 and goes to a Pbar, then antiprotons are produced and injected into one bucket of the CR [?]. The large synchrotron is the SIS100 and the small one is the CR, $h^{SIS100} = 5$ and $h^{CR} = 1$. Here we take an example, that the proton energy before the Pbar is 28.8 GeV/u and the antiproton energy after the Pbar is 3 GeV/u. Substituting the extraction and injection revolution frequencies into eq. 5.17, we get

$$\frac{f^{CR}_{rev}}{f^{SIS100}_{rev}} = 4.8 - 0.039 = \frac{m}{n} + \lambda = \frac{24}{5} - 0.039 \tag{5.20}$$

The GCD of $h^{SIS100} \cdot n = 5 \cdot 5 = 25$ and $h^{CR} \cdot m = 1 \cdot 24 = 24$ is 1, namely $Y = 1$. Substituting h^{SIS100}, h^{CR}, m, n and λ into eq. 5.16, we get

$$\frac{f^{SIS100}_{rf}}{f^{CR}_{rf}} = \frac{h^{SIS100} \cdot n}{h^{CR} \cdot m + h^{CR} \cdot \lambda \cdot n} = \frac{5 \cdot 5}{1 \cdot 24 - 1 \cdot 0.039 \cdot 5} \tag{5.21}$$

The CR is the small synchrotron and the target and there exists $\frac{Y}{m} = 1/24 < 1$, so substituting h^X, m, n, λ, f^X_{rf} and Y into formulas in the last column in Tab. 5.12, the synchronization of the H^+ B2B transfer from the SIS100 to the CR is obtained, see Tab. 5.13.

Table 5.13: Synchronization of the H^+ B2B transfer from the SIS100 to the CR with the frequency beating method

	Small synchrotron (the CR) is target synchrotron
Frequency of bucket label	f^s_{syn}
synchronization frequencies	$f^l_{syn} = \frac{f^{SIS100}_{rf}}{25} = 55.316\,\text{kHz}$ and $f^s_{syn} = \frac{f^{CR}_{rf}}{24} = 54.866\,\text{kHz}$
f^{REF}_{syn}	100 kHz
Beating frequencies	450 Hz
Length of synchronization window	$2/f^s_{syn} = 36.452\,\text{us}$
Bunch-to-bucket injection center mismatch	$\pm\frac{1}{2} \cdot \frac{2/f^s_{syn}}{1/450} \cdot 360° \cdot 24 = \pm 70.9°$

There exists an inherent big bunch-to-bucket injection center mismatch. If this mismatch is not acceptable, the phase jump of the CR is a solution, because the CR is empty before the injection. The difficulty is how to precisely synchronize the phase jump with the beam transfer, which is beyond the scope of this dissertation. Detailed parameters of the H^+ B2B transfer from the SIS100 to the CR , please see Appendix **??**.

5.3.2 Use case of the RIB B2B transfer from the SIS100 to the CR

Only one out of two bunches is extracted from the SIS100 and goes to a Super FRS, then the RIB is produced and injected into one bucket of the CR. The large synchrotron is the SIS100 and the small one is the CR. $h^{SIS100} = 2$ and $h^{CR} = 1$. Here we take an example, that the energy of the heavy ion beam before the Super FRS is 1.5 GeV/u and the RIB energy after the Super FRS is 740 MeV/u. Substituting the extraction and injection revolution frequencies into eq. 5.17, we get

$$\frac{f^{CR}_{rev}}{f^{SIS100}_{rev}} = 4.4 - 0.0046 = \frac{m}{n} + \lambda = \frac{22}{5} - 0.0046 \tag{5.22}$$

Substituting h^{SIS100}, h^{CR}, m, n and λ into eq. 5.16, we get

$$\frac{f^{SIS100}_{rf}}{f^{CR}_{rf}} = \frac{h^{SIS100} \cdot n}{h^{CR} \cdot m + h^{CR} \cdot \lambda \cdot n} = \frac{2 \cdot 5}{1 \cdot 22 - 1 \cdot 0.0046 \cdot 5} \tag{5.23}$$

The GCD of $h^{SIS100} \cdot n = 2 \cdot 5 = 10$ and $h^{CR} \cdot m = 1 \cdot 22 = 22$ is 2, namely $Y = 2$. the CR is the small synchrotron and the target and there exists $\frac{Y}{m} = 1/11 < 1$, so substituting h^X, m, n, λ, f^X_{rf} and Y into formulas in the last column in Tab. 5.12, the synchronization of the RIB B2B transfer from the SIS100 to the CR is obtained, see Tab. 5.14.

Table 5.14: Synchronization of the RIB B2B transfer from the SIS100 to the CR with the frequency beating method

	Small synchrotron (the CR) is target synchrotron
Frequency of bucket label	f^s_{syn}
synchronization frequencies	$f^l_{syn} = \frac{f^{SIS100}_{rf}}{5} = 102.326\,\text{kHz}$ and $f^s_{syn} = \frac{f^{CR}_{rf}}{11} = 102.218\,\text{kHz}$
f^{REF}_{syn}	$100\,\text{kHz}$
Beating frequencies	$108\,\text{Hz}$
Length of synchronization window	$2/f^s_{syn} = 19.558\,\text{us}$
Bunch-to-bucket injection center mismatch	$\pm\frac{1}{2} \cdot \frac{2/f^s_{syn}}{1/108} \cdot 360° \cdot 11 = \pm 4.2°$

Detailed parameters of RIB B2B transfer from the SIS100 to the CR, please see Appendix ??.

5.3.3 Use case of the B2B transfer from the CR to the HESR

One bunch of the CR is injected into one bucket of the HESR. The beam is accumulated in the HESR [?]. The large synchrotron is the HESR and the small one is the CR. $h^{HESR} = 1$ and $h^{CR} = 1$. Substituting the circumference of the HESR and the CR to eq. 2.40, we have

$$\frac{C^{HESR}}{C^{CR}} = 2.6 - 0.003 = \frac{m}{n} + \lambda = \frac{13}{5} - 0.003 \tag{5.24}$$

The GCD of $h^{HESR} \cdot n = 1 \cdot 5 = 5$ and $h^{CR} \cdot m = 1 \cdot 13 = 13$ is 1, namely $Y = 1$. Substituting h^{HESR}, h^{CR}, m, n and λ into eq. 2.41, we get

$$\frac{f^{HESR}_{rf}}{f^{CR}_{rf}} = \frac{h^{HESR} \cdot n}{h^{CR} \cdot m + h^{HESR} \cdot \lambda \cdot n} = \frac{1 \cdot 5}{1 \cdot 13 - 1 \cdot 0.003 \cdot 5} \tag{5.25}$$

The HESR is the large synchrotron and the target and there exists $\frac{Y}{n} = 1/5 < 1$, so substituting h^X, m, n, λ, f^X_{rf} and Y into formulas in the last column in Tab. 5.11, the synchronization of the B2B transfer from the CR to the HESR is obtained. Tab. 5.15 shows two operations for antiproton and HESR.

Table 5.15: Synchronization of the B2B transfer from the CR to the HESR with the frequency beating method

	Larger synchrotron (the HESR) is target synchrotron
Frequency of bucket label	f^l_{syn}
	3 GeV/u antiproton
synchronization frequencies	$f^s_{syn} = \frac{f^{CR}_{rf}}{13} = 101.290\,\mathrm{kHz}$ and $f^l_{syn} = \frac{f^{HESR}_{rf}}{5} = 101.426\,\mathrm{kHz}$
f^{REF}_{syn}	100 kHz
Beating frequencies	136 Hz
Length of synchronization window	$2/f^l_{syn} = 19.719$ us
Bunch-to-bucket injection center mismatch	$\pm\frac{1}{2} \cdot \frac{2/f^l_{syn}}{1/136} \cdot 360° \cdot 5 = \pm 2.4°$
	740 MeV/u RIB
synchronization frequencies	$f^s_{syn} = \frac{f^{CR}_{rf}}{13} = 86.493\,\mathrm{kHz}$ and $f^l_{syn} = \frac{f^{HESR}_{rf}}{5} = 86.608\,\mathrm{kHz}$
f^{REF}_{syn}	100 kHz
Beating frequencies	113 Hz
Length of synchronization window	$2/f^l_{syn} = 23.090$ us
Bunch-to-bucket injection center mismatch	$\pm\frac{1}{2} \cdot \frac{2/f^l_{syn}}{1/113} \cdot 360° \cdot 5 = \pm 2.4°$

After the synchronization, the phase difference between two synchronization frequency markers depends on the accumulation method. Detailed parameter about the B2B transfer from the CR to the HESR, please see Appendix **??**.

5.3.4 Use case of the B2B transfer from the SIS18 to the ESR via a FRS

Only one bunch is extracted from the SIS18 and goes to a FRS, then a RIB is produced and injected into one bucket of the ESR. The large synchrotron is the SIS18 and the small one is the ESR. $h^{SIS18} = 1$ and $h^{ESR} = 1$. Here we take an applied case as an example, that the energy of the heavy ion beam before the FRS is 550 MeV/u and the RIB energy after the FRS is 400 MeV/u. Substituting the extraction and injection revolution frequencies into eq. 5.17, we get

$$\frac{f_{rev}^{ESR}}{f_{rev}^{SIS18}} = 1.8 + 0.036 = \frac{m}{n} + \lambda = \frac{9}{5} + 0.036 \tag{5.26}$$

Substituting h^{SIS18}, h^{ESR}, m, n and λ into eq. 2.41, we get

$$\frac{f_{rf}^{SIS18}}{f_{rf}^{ESR}} = \frac{h^{SIS18} \cdot n}{h^s \cdot m + h^{ESR} \cdot \lambda \cdot n} = \frac{1 \cdot 5}{1 \cdot 9 + 1 \cdot 0.036 \cdot 5} \tag{5.27}$$

The GCD of $h^{SIS18} \cdot n = 1 \cdot 5 = 5$ and $h^s \cdot m = 1 \cdot 9 = 9$ is 1, namely $Y = 1$. The ESR is the small synchrotron and the target and there exits $\frac{Y}{m} = 1/9 < 1$, so substituting h^X, m, n, λ, f_{rf}^X and Y into formulas into formulas in the last column in Tab. 5.12, the synchronization of the B2B transfer from the SIS18 to the ESR via a FRS is obtained, see Tab. 5.16.

Table 5.16: Synchronization of the B2B transfer from the SIS18 to the ESR via a FRS with the frequency beating method

	Small synchrotron (the ESR) is target synchrotron
Frequency of bucket label	f_{syn}^s
synchronization frequencies	$f_{syn}^l = \frac{f_{rf}^{SIS18}}{5} = 215.393\,\text{kHz}$ and $f_{syn}^s = \frac{f_{rf}^{ESR}}{9} = 219.642\,\text{kHz}$
f_{syn}^{REF}	200 kHz
Beating frequencies	4.249 kHz
Length of synchronization window	$2/f_{syn}^s = 9.106\,\text{us}$
Bunch-to-bucket injection center mismatch	$\pm\frac{1}{2} \cdot \frac{2/f_{syn}^s}{1/4249} \cdot 360° \cdot 9 = \pm 62.28°$

There exists an inherent big bunch-to-bucket injection center mismatch. If this mismatch is not acceptable, the phase jump of the ESR is a solution, because the ESR is empty before the injection. The difficulty is how to precisely synchronize the phase jump with the beam transfer, which is beyond the scope of this dissertation. More parameters about the B2B transfer from the SIS18 to the ESR via a FRS, please see Appendix **??**.

5.4 Summary of the synchronization for different scenarios

In this section, all the formulas are summarized. Tab. 5.17 summarizes the formulas when the large synchrotron is the target. Tab. 5.18 summarizes the formulas when the small synchrotron is the target and the revolution period is longer than the rf period of the synchronization period of the target synchrotron. Tab. 5.19 summarizes the formulas when the small synchrotron is the target and the revolution period is shorter than the rf period of the synchronization period of the target synchrotron.

Table 5.17: Summary of the formulas for the frequency beating method when the large synchrotron is the target

Circumference ratio	Rf cavity frequency ratio f^l_{rf}/f^s_{rf}	Frequency of bucket label	Frequency beating Two slightly different frequencies	Frequency beating bunch-to-bucket center mismatch
$C^l/C^s = \kappa$ Integer	$\frac{h^l}{h^s \cdot \kappa}$ $Y = GCD(h^l, h^s \cdot \kappa)$	f^l_{rev}	$f^l_{syn} = \frac{f^l_{rf}}{h^l/Y}$ and $f^s_{syn} = \frac{f^s_{rf}}{(h^s \cdot \kappa)/Y} + \Delta f$ or $f^l_{syn} = \frac{f^l_{rf}}{h^l/Y} + \Delta f$ and $f^s_{syn} = \frac{f^s_{rf}}{(h^s \cdot \kappa)/Y}$	$\pm\frac{1}{2} \cdot \frac{2/f^l_{rev}}{1/\Delta f} \cdot 360° \cdot \frac{f^l_{rf}}{f^l_{syn}}$
$C^l/C^s = \kappa + \lambda$ or $frev^s/frev^l = \kappa + \lambda$ close to integer	$\frac{h^l}{h^s \cdot (\kappa+\lambda)}$ $Y = GCD(h^l, h^s \cdot \kappa)$	f^l_{rev}	$f^l_{syn} = \frac{f^l_{rf}}{h^l/Y}$ and $f^s_{syn} = \frac{f^s_{rf}}{(h^s \cdot \kappa)/Y}$ $\Delta f = \lvert f^l_{syn} - f^s_{syn} \rvert$	$\pm\frac{1}{2} \cdot \frac{2/f^l_{rev}}{1/\Delta f} \cdot 360° \cdot \frac{f^l_{rf}}{f^l_{syn}}$
$C^l/C^s = m/n + \lambda$ or $frev^s/frev^l = m/n + \lambda$ far away from integer	$\frac{h^l}{h^s \cdot (m/n+\lambda)}$[1] Y=GCD $(h^l \cdot n, h^s \cdot m)$	if $Y/n < 1, f^l_{syn}$ if $Y/n >= 1, f^l_{rev}$	$f^l_{syn} = \frac{f^l_{rf}}{(h^l \cdot n)/Y}$ and $f^s_{syn} = \frac{f^s_{rf}}{(h^s \cdot m)/Y}$ $\Delta f = \lvert f^l_{syn} - f^s_{syn} \rvert$	$\pm\frac{1}{2} \cdot \frac{2/f^l_{syn}}{1/\Delta f} \cdot 360° \cdot \frac{f^l_{rf}}{f^l_{syn}}$ $\pm\frac{1}{2} \cdot \frac{2/f^l_{rev}}{1/\Delta f} \cdot 360° \cdot \frac{f^l_{rf}}{f^l_{syn}}$

[1] $\frac{f_r f^l}{f_{rf} s} = \frac{h^l f_r ev^l}{h^s f^s_{rev}} = \frac{h^l C^s}{h^s C_l} = \frac{h^l}{h^s(m/n+\lambda)} = \frac{h^l \cdot n}{h^s \cdot m + h^s \cdot \lambda \cdot n}$

Table 5.18: Summary of the formulas for the frequency beating method when the small synchrotron is the target and the revolution period is longer than the rf period of the synchronization frequency of the target synchrotron

Circumference ratio	rf cavity frequency ratio f^l_{rf}/f^s_{rf}	Frequency of bucket label	Frequency beating Two slightly different frequencies	Frequency beating bunch-to-bucket center mismatch
$C^l/C^s = \kappa$ Integer	$\frac{h^l}{h^s \cdot \kappa}$ $Y = GCD(h^l, h^s \cdot \kappa)$	$Y/\kappa >= 1, f^s_{rev}$	$f^l_{syn} = \frac{f^l_{rf}}{h^l/Y}$ and $f^s_{syn} = \frac{f^s_{rf}}{(h^s \cdot \kappa)/Y} + \Delta f$ or $f^l_{syn} = \frac{f^l_{rf}}{h^l/Y} + \Delta f$ and $f^s_{syn} = \frac{f^s_{rf}}{(h^s \cdot \kappa)/Y}$	$\pm\frac{1}{2} \cdot \frac{2/f^s_{rev}}{1/\Delta f} \cdot 360° \cdot \frac{f^s_{rf}}{f^s_{syn}}$
$C^l/C^s = \kappa + \lambda$ or $frev^s/frev^l = \kappa + \lambda$ close to integer	$\frac{h^l}{h^s \cdot (\kappa + \lambda)}$ $Y = GCD(h^l, h^s \cdot \kappa)$	$Y/\kappa >= 1, f^s_{rev}$	$f^l_{syn} = \frac{f^l_{rf}}{h^l/Y}$ and $f^s_{syn} = \frac{f^s_{rf}}{(h^s \cdot \kappa)/Y}$ $\Delta f = \lvert f^l_{syn} - f^s_{syn} \rvert$	$\pm\frac{1}{2} \cdot \frac{2/f^s_{rev}}{1/\Delta f} \cdot 360° \cdot \frac{f^s_{rf}}{f^s_{syn}}$
$C^l/C^s = m/n + \lambda$ or $frev^s/frev^l = m/n + \lambda$ far away from integer	$\frac{h^l}{h^s \cdot (m/n + \lambda)}$ Y=GCD $(h^l \cdot n, h^s \cdot m)$	$Y/m >= 1, f^s_{rev}$	$f^l_{syn} = \frac{f^l_{rf}}{(h^l \cdot n)/Y}$ and $f^s_{syn} = \frac{f^s_{rf}}{(h^s \cdot m)/Y}$ $\Delta f = \lvert f^l_{syn} - f^s_{syn} \rvert$	$\pm\frac{1}{2} \cdot \frac{2/f^s_{rev}}{1/\Delta f} \cdot 360° \cdot \frac{f^s_{rf}}{f^s_{syn}}$

Table 5.19: Summary of the formulas for the frequency beating method when the small synchrotron is the target and the revolution period is shorter than the rf period of the synchronization frequency of the target synchrotron

Circumference ratio	rf cavity frequency ratio f^l_{rf}/f^s_{rf}	Frequency of bucket label	Frequency beating Two slightly different frequencies	Frequency beating bunch-to-bucket center mismatch
$C^l/C^s=\kappa$ Integer	$\frac{h^l}{h^s\cdot\kappa}$ $Y=GCD(h^l,h^s\cdot\kappa)$	$Y/\kappa<1, f^s_{syn}$	$f^l_{syn}=\frac{f^l_{rf}}{h^l/Y}$ and $f^s_{syn}=\frac{f^s_{rf}}{(h^s\cdot\kappa)/Y}+\Delta f$ or $f^l_{syn}=\frac{f^l_{rf}}{h^l/Y}+\Delta f$ and $f^s_{syn}=\frac{f^s_{rf}}{(h^s\cdot\kappa)/Y}$	$\pm\frac{1}{2}\cdot\frac{2/f^s_{syn}}{1/\Delta f}\cdot 360°\cdot\frac{f^s_{rf}}{f^s_{syn}}$
$C^l/C^s=\kappa+\lambda$ or $frev^s/frev^l=\kappa+\lambda$ close to integer	$\frac{h^l}{h^s\cdot(\kappa+\lambda)}$ $Y=GCD(h^l,h^s\cdot\kappa)$	$Y/\kappa<1, f^s_{syn}$	$f^l_{syn}=\frac{f^l_{rf}}{h^l/Y}$ and $f^s_{syn}=\frac{f^s_{rf}}{(h^s\cdot\kappa)/Y}$ $\Delta f=\lvert f^l_{syn}-f^s_{syn}\rvert$	$\pm\frac{1}{2}\cdot\frac{2/f^s_{syn}}{1/\Delta f}\cdot 360°\cdot\frac{f^s_{rf}}{f^s_{syn}}$
$C^l/C^s=m/n+\lambda$ or $frev^s/frev^l=m/n+\lambda$ far away from integer	$\frac{h^l}{h^s\cdot(m/n+\lambda)}$ Y=GCD $(h^l\cdot n,h^s\cdot m)$	$Y/m<1, f^s_{syn}$	$f^l_{syn}=\frac{f^l_{rf}}{(h^l\cdot n)/Y}$ and $f^s_{syn}=\frac{f^s_{rf}}{(h^s\cdot m)/Y}$ $\Delta f=\lvert f^l_{syn}-f^s_{syn}\rvert$	$\pm\frac{1}{2}\cdot\frac{2/f^s_{syn}}{1/\Delta f}\cdot 360°\cdot\frac{f^s_{rf}}{f^s_{syn}}$

Chapter 6

Realization and systematic investigation of the FAIR B2B transfer system

!!!!!!!!!!!!!!!please check List of symbol and abbrevation ... for chapter 5 and 6.

This chapter concentrates on the realization and systematic investigation of the B2B transfer system. In Sec. 6.1, both the phase shift and frequency beating synchronization methods are analyzed from the beam dynamic viewpoint. The WR network is investigated for the B2B transfer and the calculation of the synchronization window are presented in Sec. 6.2. The B2B transfer system for FAIR focuses first of all on SIS18 to SIS100 transfer, so the trigger possibility of the SIS18 extraction and SIS100 injection kicker is systematically investigated in Sec. 6.3. Besides, the test setup from the timing aspect is built in Sec. 6.4.

6.1 Investigation of two synchronization methods for U^{28+} B2B transfer from SIS18 to SIS100 from the beam dynamics viewpoint

This section analyzes the phase shift and frequency beating methods from the beam-dynamics viewpoint for the synchronization of SIS18 with SIS100. In this chapter, the circumference of SIS18 and SIS100 are denoted by C^{SIS18} and C^{SIS100}, the revolution frequency by $f_{h=1}^{SIS18}$ and $f_{h=1}^{SIS100}$ and the rf frequency by $f_{h=2}^{SIS18}$ and $f_{h=10}^{SIS100}$. Since SIS18 and SIS100 harmonic number are 2 and 10, the relationship between the revolution and rf frequencies are $f_{h=2}^{SIS18} = 2f_{h=1}^{SIS18}$ and $f_{h=10}^{SIS100} = 10f_{h=1}^{SIS100}$. Since C^{SIS100} is five times as long as C^{SIS18}, we could get the relation $f_{h=1}^{SIS18}{=}5f_{h=1}^{SIS100}$ and $f_{h=10}^{SIS100}{=}f_{h=2}^{SIS18}$.

6.1.1 Phase shift method

To achieve a required phase shift, the rf frequency is modulated away from the nominal value for a period of time and modulated back [?]. Let $\Delta\phi_{shift}$ be the phase shift to be achieved and Δf_{rf} the RF frequency variation to accomplish it;

then,

$$\Delta\phi_{shift} = 2\pi \int_{t_0}^{t_0+T} \Delta f_{rf}(t)dt \tag{6.1}$$

where T is the period of frequency modulation and t_0 is the time at which the modulation begins. To make the frequency modulation effective, the stabilization system, beam-phase feedback loop, must be frozen before the modulation begins.

The following four examples of frequency modulation are analyzed. Case (1) trapezoid modulation, Case (2) triangular modulation, Case (3) sinusoidal modulation and Case (4) parabolic modulation. Here I assume the phase shift must be achieved within 7ms. These frequency modulations are shown in Fig. 6.1. All the four modulations give the same phase shift, $\Delta\phi_{shift} = \pi$, which is proved by substituting each form of $\Delta f_{rf}(t)$ into eq. 6.1 and performing integration.

Case (1)

$$\Delta f_{rf}(t) = \begin{cases} 50Hz/ms \cdot (t - t_0) & t_0 + 0 < t \le t_0 + 2ms \\ 100Hz & t_0 + 2 < t \le t_0 + 5ms \\ 100Hz - 50Hz/ms \cdot (t - t_0) & t_0 + 5ms < t \le t_0 + 7ms \end{cases} \tag{6.2}$$

Case (2)

$$\Delta f_{rf}(t) = \begin{cases} \frac{10^3}{7 \cdot 3.5} Hz/ms \cdot (t - t_0) & t_0 + 0 < t \le t_0 + 3.5ms \\ \frac{10^3}{7} Hz - \frac{10^3}{7 \cdot 3.5} Hz/ms \cdot (t - t_0 - 3.5ms) & t_0 + 3.5ms < t \le t_0 + 7ms \end{cases} \tag{6.3}$$

Case (3)

$$\Delta f_{rf}(t) = \frac{10^3}{14} Hz \cdot (1 - cos(\frac{2\pi}{7} rad/ms \cdot (t - t_0))) \quad t_0 + 0 < t \le t_0 + 7ms \tag{6.4}$$

Case (4)

$$\Delta f_{rf}(t) = \frac{20}{21} \cdot \begin{cases} 30Hz/ms^2 \cdot (t - t_0)^2 & t_0 + 0 < t \le t_0 + 1ms \\ 30Hz + 60Hz/ms \cdot (t - t_0 - 1ms) & t_0 + 1ms < t \le t_0 + 2.5ms \\ 30Hz/ms^2 \cdot [5ms^2 - (t - t_0 - 3.5ms)^2] & t_0 + 2.5ms < t \le t_0 + 4.5ms \\ 30Hz + 60Hz/ms \cdot [6ms - (t - t_0)] & t_0 + 4.5ms < t \le t_0 + 6ms \\ 30Hz/ms^2 \cdot [7ms^2 - (t - t_0)]^2 & t_0 + 6ms < t \le t_0 + 7ms \end{cases} \tag{6.5}$$

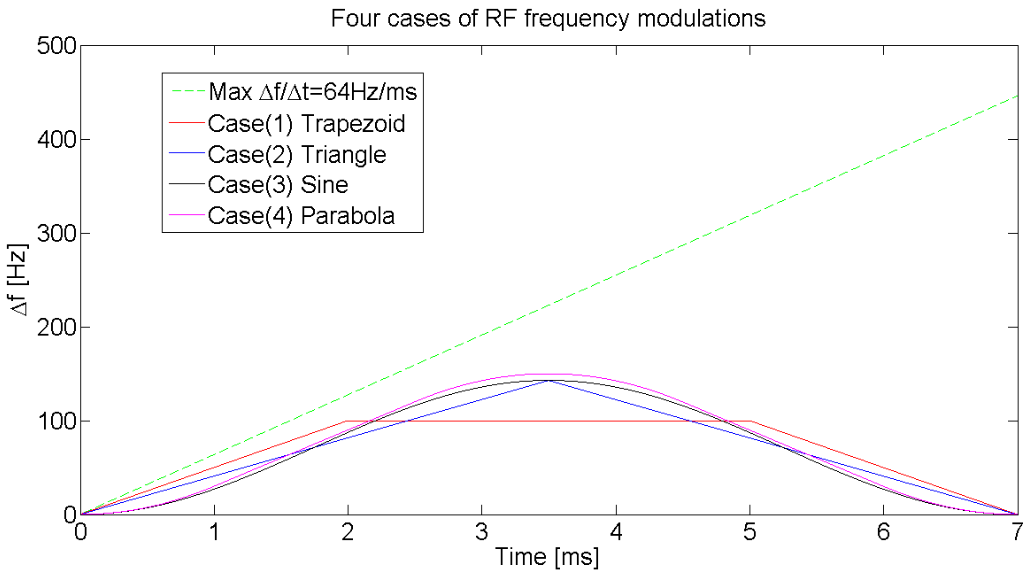

Figure 6.1: Examples of RF frequency modulation.

Fig. 6.2 shows the time derivation of four rf frequency modulations, which are smaller than the maximum time derivative of rf frequency during the acceleration ramp 64Hz/ms for the adiabaticity consideration. The acceleration ramp is an adiabatical process.

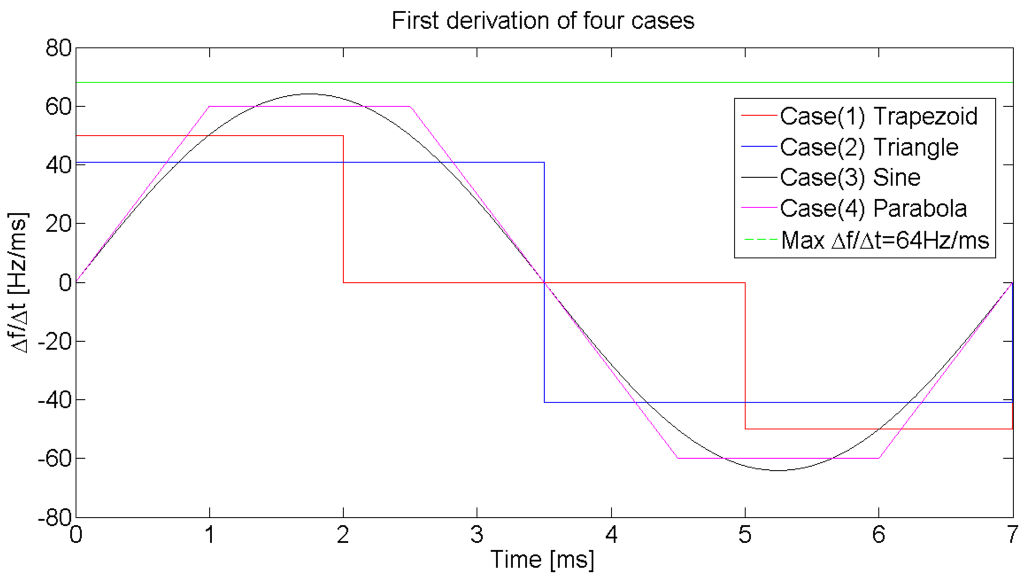

Figure 6.2: Time derivation of four modulations

Fig. 6.3 shows the corresponding phase shift modulation of four cases.

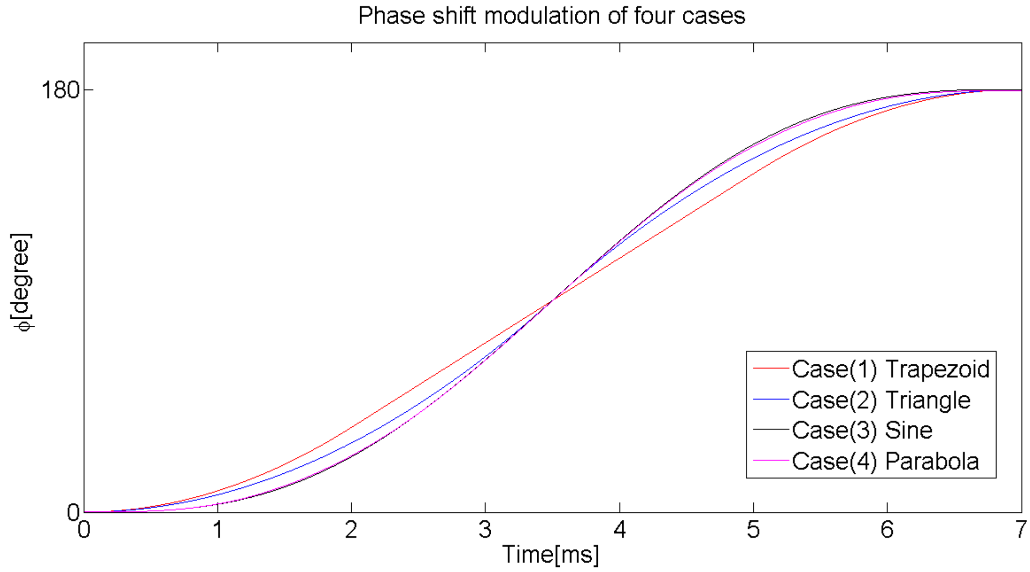

Figure 6.3: The phase shift modulation of four cases

6.1.1.1 Longitudinal dynamic analysis for the simulation

In this section, the average radial excursion, the relative momentum shift, synchronous phase, bucket size and adiabaticity of four rf frequency modulations are analyzed.

- Average radial excursion

  The average radial excursion is calculated for the four cases of rf frequency modulations by eq. (2.49). Fig. 6.4 shows the calculation result [**?**].

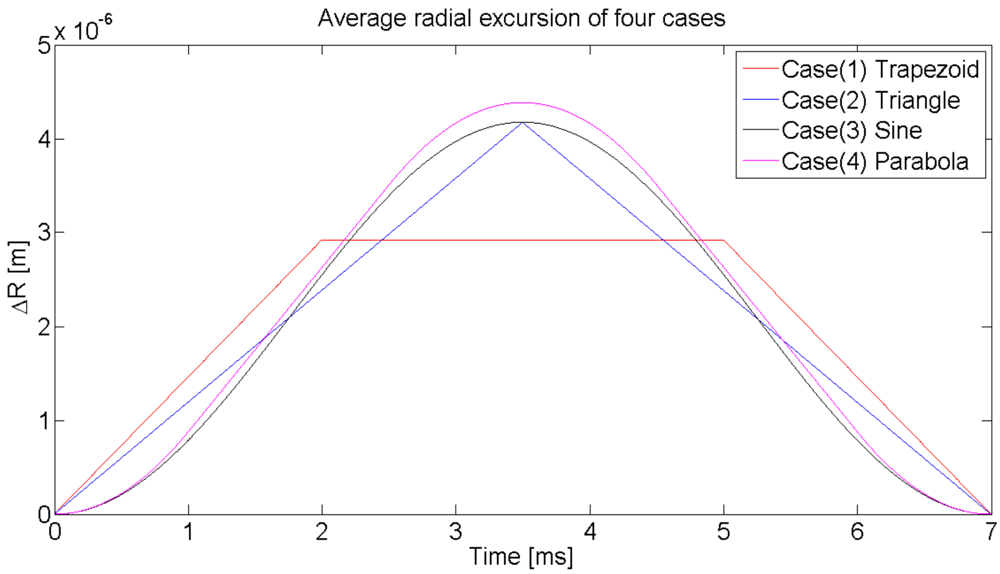

Figure 6.4: Average radial excursions of four cases.

Table 6.1: The maximum average radial excursion of four cases

	Case (1)	Case (2)	Case (3)	Case (4)
Max avg radial excursion	$2.93 \cdot 10^{-6}$	$4.17 \cdot 10^{-6}$	$4.18 \cdot 10^{-6}$	$4.38 \cdot 10^{-6}$
Time	flat	3.5 ms	3.5 ms	3.5 ms

Tab. 6.1 shows the maximum average radial excursion and the time for four cases. The maximum tolerable radial excursion of SIS18 is $\pm 2.4 \cdot 10^{-4}$. For all cases, the average radial excursion is within the acceptable range. Hence, all cases are applicable.

- Relative momentum shift

  The relative momentum shift is calculated for the four cases of rf frequency modulations by eq. (??). Fig. 6.5 shows the calculation result.

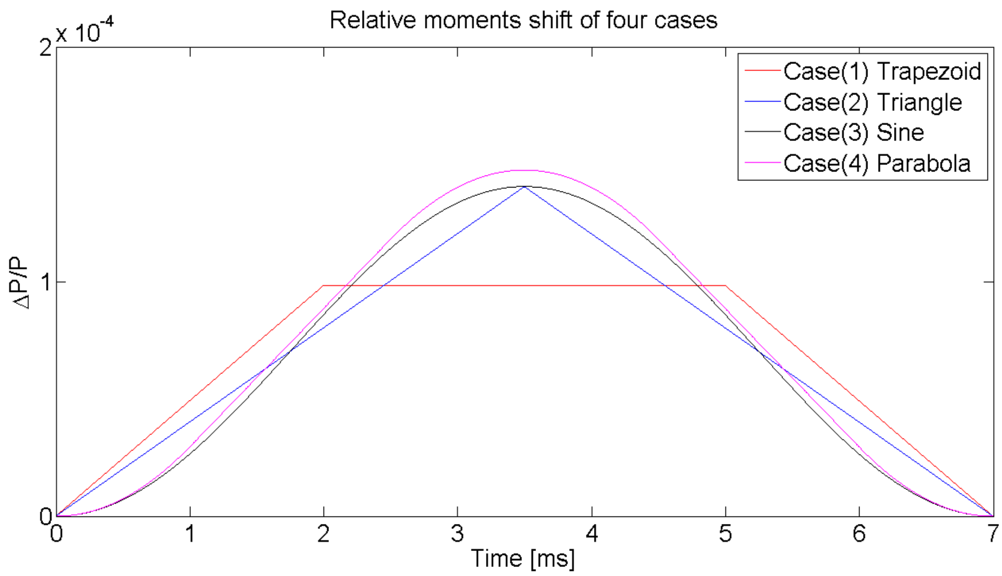

Figure 6.5: Relative momentum shift of four cases.

Table 6.2: The maximum relative momentum shift of four cases

	Case (1)	Case (2)	Case (3)	Case (4)
Max relative momentum shift	$9.83 \cdot 10^{-5}$	$1.38 \cdot 10^{-4}$	$1.40 \cdot 10^{-4}$	$1.48 \cdot 10^{-4}$
Time	flat	3.5 ms	3.5 ms	3.5 ms

Tab. 6.2 shows the maximum relative momentum shift and the time for four cases. The maximum tolerable relative momentum shift of SIS18 is ± 0.008. For all cases, the maximum relative momentum shift is within the acceptable range. Hence, all cases are applicable.

- Synchronous phase

The rf frequency modulations make the synchronous phase deviate from the nominal value 0°. Fig. 6.6 shows the changes in the synchronous phase, $\Delta\phi_s$(t). It is calculated by substituting values into eq. **??**. For case (1), the phase jumps in $\Delta\phi_s$ appear at the start and end of the frequency modulation, and at two points where the slope of modulation changes from upward to flat and from flat to downward. For case (2), the phase jumps in $\Delta\phi_s(t)$ appear at the start and end of the frequency modulation, and at the midpoint where the slope of modulation changes from upward to downward. For case (3) and (4), the synchronous phase $\Delta\phi_s(t)$ during the modulations are continuous. The phase jumps endanger the beam stability. Hence, only case (3) and (4) are applicable.

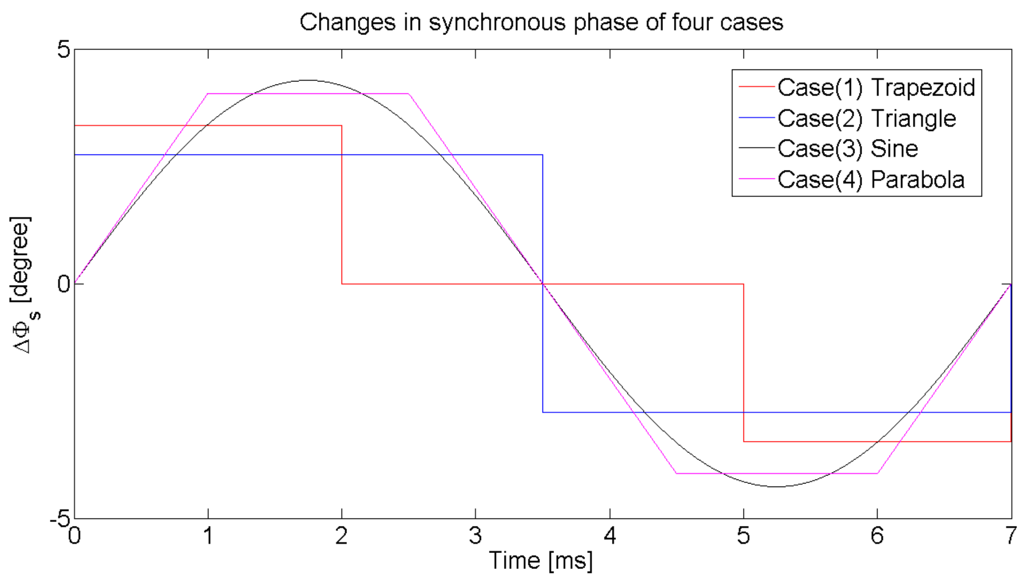

Figure 6.6: Changes in synchronous phase of four cases

- Bucket size

The bucket area factor α_b varies during rf frequency modulations. Before the modulations, the synchronous phase ϕ_s=0° and $\alpha_b(0°) = 1$. By substituting the changes in synchronous phase into eq. (6.6), we get the ratio of bucket areas of a running bucket to the stationary bucket for four cases, see Fig. (6.7).

$$\alpha_b(\phi_s) \approx \frac{1 - sin\phi_s}{1 + sin\phi_s} \tag{6.6}$$

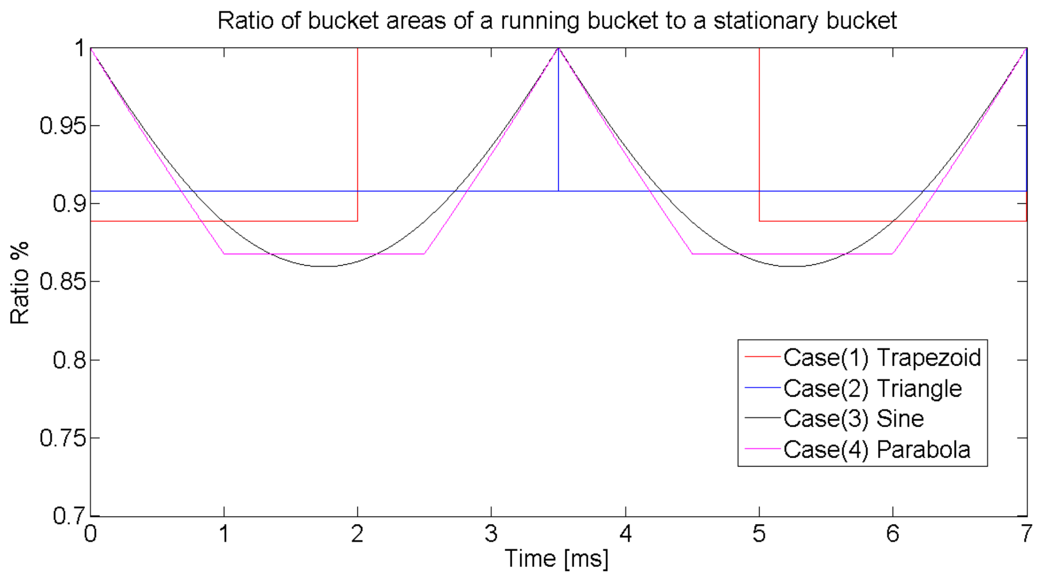

Figure 6.7: Ratio of bucket areas of a running bucket to the stationary bucket of four cases

Tab. 6.3 shows the bucket area factor for four cases. For all cases, the running bucket area factor is larger than 85%. Hence, all cases are applicable.

Table 6.3: The minimum bucket area factor of four cases

	Case (1)	Case (2)	Case (3)	Case (4)
Min bucket area factor	88%	90%	86%	86%

- Adiabaticity

By substituting the values of $d\Delta\phi_s(t)/dt$ obtained from Fig. 6.6 and the other appropriate values into eq. 2.55, we can calculate the adiabaticity parameter, ε, for the case (3) and (4), see Fig. 6.8. Because $d\Delta\phi_s(t)$ changes discontinuously for case (1) and (2), this abrupt change gives rise to a coherent bunch oscillation at a synchrotron frequency, resulting in emittance dilution. So the rf frequency modulations of case (1) and (2) are not applicable.

For case (4), the maximum of ε, 0.000059, occurs at 1ms, 2.5ms, 4.5ms and 6ms. From Fig. 6.6, we could see the change of the synchronous phase $d\Delta\phi_s(t)/dt$ at these time points is big but smoothly. For case (3), the maximum of ε is 0.000030. So the frequency modulation is adiabatical for case (3) and (4).

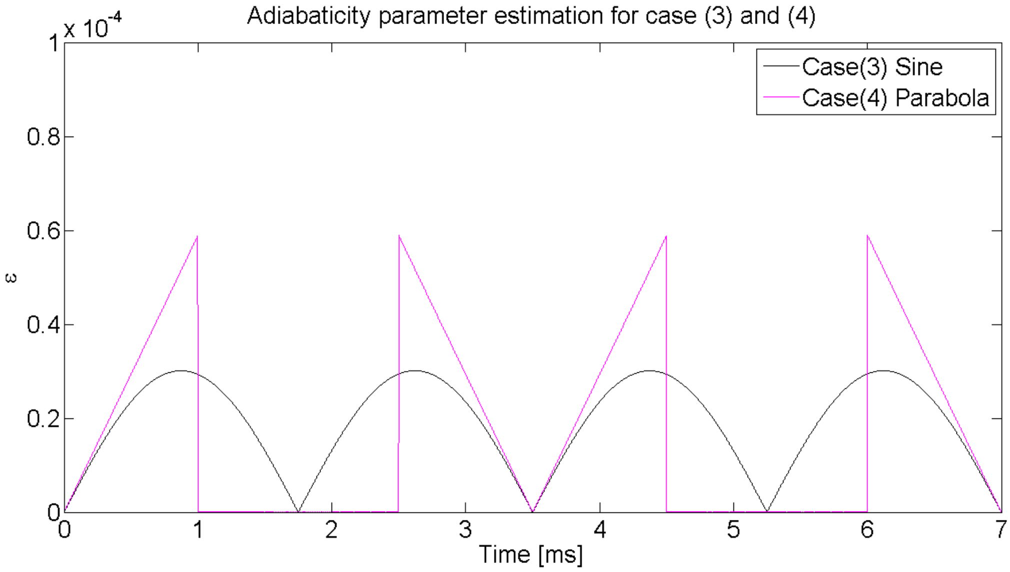

Figure 6.8: Adiabaticity parameter estimation of case (3) and (4)

6.1.1.2 Transverse dynamics analysis for the simulation

For SIS18, the chromaticity $Q_x^{`}$ and $Q_y^{`}$ is 4.17 and 3.4. Substituting chromaticity and maximum momentum shift (see. Tab. 6.2) into eq. **??**. The chromatic tune shift ΔQ_x and ΔQ_y during rf modulations for four cases can be calculated.

Case (1)

$$\Delta Q_x = 4.17 \cdot 9.83 \cdot 10^{-5} = 4.10 \cdot 10^{-4} \tag{6.7}$$

$$\Delta Q_y = 3.4 \cdot 9.83 \cdot 10^{-5} = 3.34 \cdot 10^{-4} \tag{6.8}$$

Case (2)

$$\Delta Q_x = 4.17 \cdot 1.38 \cdot 10^{-4} = 5.75 \cdot 10^{-4} \tag{6.9}$$

$$\Delta Q_y = 3.4 \cdot 1.38 \cdot 10^{-4} = 4.69 \cdot 10^{-4} \tag{6.10}$$

Case (3)

$$\Delta Q_x = 4.17 \cdot 1.40 \cdot 10^{-4} = 5.84 \cdot 10^{-4} \tag{6.11}$$

$$\Delta Q_y = 3.4 \cdot 1.40 \cdot 10^{-4} = 4.76 \cdot 10^{-4} \tag{6.12}$$

Case (4)

$$\Delta Q_x = 4.17 \cdot 1.48 \cdot 10^{-4} = 6.17 \cdot 10^{-4} \tag{6.13}$$

$$\Delta Q_y = 3.4 \cdot 1.48 \cdot 10^{-4} = 5.03 \cdot 10^{-4} \tag{6.14}$$

The chromatic tune shift for four cases are significantly small, which could be negligible.

6.1.2 Frequency beating method

In the case of the frequency beating method, we guarantee the extraction and injection energy always match, which means that the momentum is not affected by the frequency detune, namely $\Delta p = 0$, So the frequency beating method has no influence on the transverse dynamics.

6.1.2.1 Longitudinal dynamics analysis of the frequency beating for SIS18

For the frequency beating method, the rf frequency de-tune is done accompanying with the RF ramp. Accepting to decentre the orbit by 8mm [?] for the SIS18

$$\frac{\Delta R}{R} = \pm 2.4 \cdot 10^{-4} \tag{6.15}$$

From eq. 2.59 and and eq. 2.61, the RF frequency and the magnetic field change at the U^{28+} extraction energy 200MeV/u γ_t= 5.8) are

$$\frac{\Delta f}{f} = \pm 2.4 \cdot 10^{-4} \tag{6.16}$$

$$\frac{\Delta B}{B} = \frac{\Delta f}{f} {\gamma_t}^2 = \pm 8.1 \cdot 10^{-3} \tag{6.17}$$

where the maximum RF frequency de-tune is approximate to 370 Hz at 1.57 MHz for the U^{28+}. Fig. 6.9 shows the rf frequency derivation during the rf ramp. In the simulation, it is assumed that the rf frequency is detuned at 0.2756s with $6.08 \cdot 10^6$Hz/s, see blue rectangle in Fig. 6.9. For the sake of simplicity, 200 Hz is used as the rf frequency detune. SIS18 needs approximate 33us to reach 200 Hz with $6.08 \cdot 10^6$Hz/s.

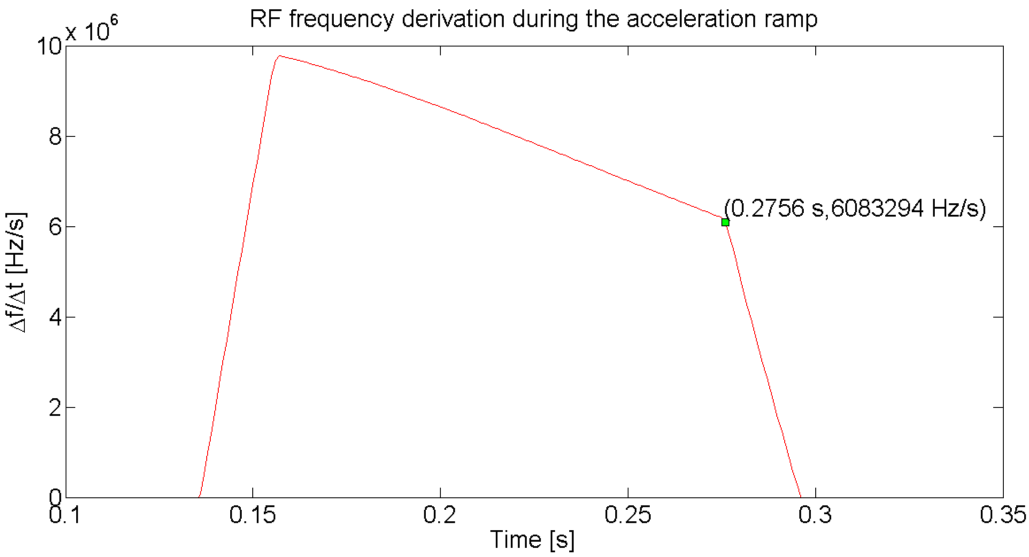

Figure 6.9: RF frequency derivation of the U^{28+} rf ramp

From eq. 2.59 and eq. 2.61, we could get the corresponding radial excursion and the magnetic field change during the detune process. The maximum radial excursion is $-1.27 \cdot 10^{-4}$ at 33us of the rf detune process. The maximum magnetic field change is $4.3 \cdot 10^{-3}$ at 33us of the rf detune process.

6.2 GMT systematic investigation for the B2B transfer system

The B2B transfer system makes use of certain aspects of the GMT system to realize the data collection, merging and redistribution. The main task of the data merging is the calculation of the synchronization window, within which the bunch could be injected into the correct bucket with the bunch to bucket center mismatch smaller than the upper bound. The data collection and redistribution make use of the WR network, so the measurement of the WR network latency is necessary.

6.2.1 Calculation of the synchronization window

According to the phase difference between two synchrotrons, the fine time for the alignment of two Reference RF Signals for both the phase shift and frequency beating methods can be calculated. This time is called "best estimate of alignment" and denoted by t_{best}, see Fig. 6.10. Because of the uncertainty [?] of the phase advance prediction and rf frequency modulation, the fine alignment lies between t_{best} - δt_{best} and t_{best} + δt_{best}, where δt_{best} is the uncertainty of the alignment. [t_{best} - δt_{best}, t_{best} + δt_{best}] is called "probable range of alignment". In Sec. 6.2.1.1 and Sec. 6.2.1.2, the calculation of the best estimation of alignment and the probable range of alignment for the phase shift and frequency beating method will be explained. The probable range of alignment is within the synchronization window. For the correct selection of the same revolution frequency marker at different SCUs, the start of the synchronization window must be properly calculated. In Sec. 6.2.1.3, the calculation of the synchronization window will be explained.

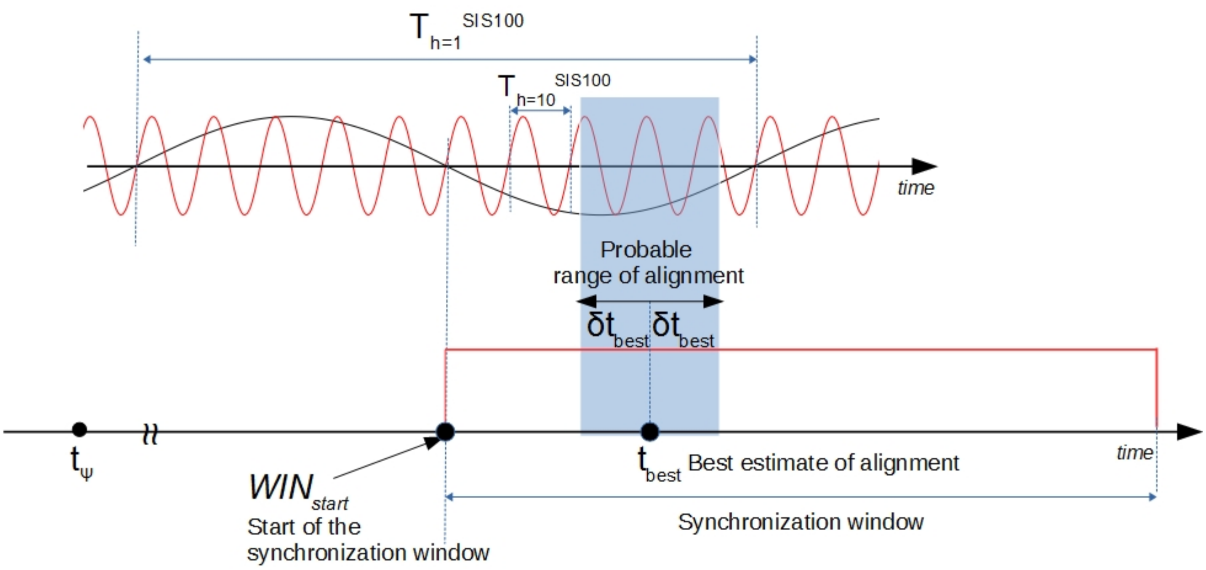

Figure 6.10: The illustration of the best estimate of alignment, the probable range of alignment and the synchronization window

For both the phase shift and frequency beating method, the calculation is based on the predicted phase of the rf signal locally. For example of the U^{28+} B2B transfer from SIS18 to SIS100, the PAP module extrapolates the rf phase $\psi_{h=1}^{SIS100}$ for SIS100 rf h=1 (157kHz) signal and $\psi_{h=1/5}^{SIS18}$ for SIS18 rf h=1/5 (157kHz) signal at t_ψ [?]. The more time is spent for the phase advance prediction, the better the predicted phase will be. Fig. 6.11 illustrates some basic definition of symbols for the calculation. $\phi_{h=2}^{SIS18}$and $\phi_{h=10}^{SIS100}$ are individual rf phase of SIS18 and SIS100 Reference RF Signals

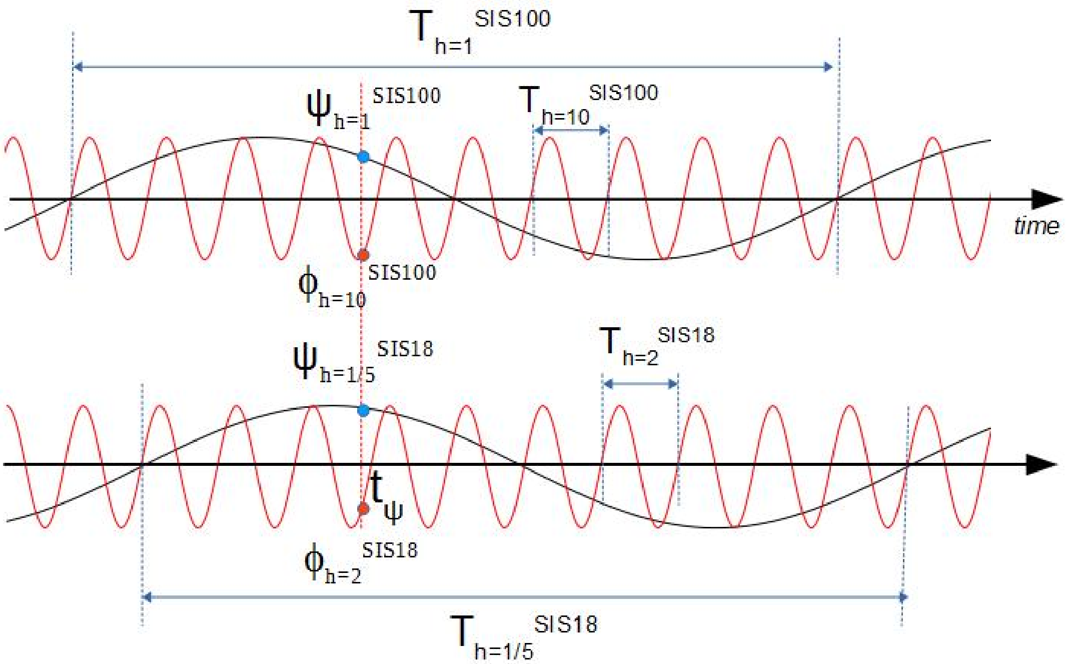

Figure 6.11: The illustration of symbols for the calculation

at t_ψ. The relationship between $\phi_{h=2}^{SIS18}$, $\phi_{h=10}^{SIS100}$ and $\psi_{h=1/5}^{SIS18}$, $\psi_{h=1}^{SIS100}$ are given by eq. 6.18 and eq. 6.19.

$$\phi_{h=2}^{SIS18} = \frac{\frac{\psi_{h=1/5}^{SIS18}}{360^\circ} \cdot T_{h=1/5}^{SIS18} \mod T_{h=2}^{SIS18}}{T_{h=2}^{SIS18}} \cdot 360^\circ \tag{6.18}$$

$$\phi_{h=10}^{SIS100} = \frac{\frac{\psi_{h=1}^{SIS100}}{360^\circ} \cdot T_{h=1}^{SIS100} \mod T_{h=10}^{SIS100}}{T_{h=10}^{SIS100}} \cdot 360^\circ \tag{6.19}$$

substituting $T_{h=2}^{SIS18} \cdot 10 = T_{h=1/5}^{SIS18}$, $T_{h=10}^{SIS100} \cdot 10 = T_{h=1}^{SIS100}$ into eq.6.18 and eq.6.19 yields

$$\phi_{h=2}^{SIS18} = \frac{\frac{\psi_{h=1/5}^{SIS18} \cdot 10}{360^\circ} \cdot T_{h=2}^{SIS18} \mod T_{h=2}^{SIS18}}{T_{h=2}^{SIS18}} \cdot 360^\circ \tag{6.20}$$

$$\phi_{h=10}^{SIS100} = \frac{\frac{\psi_{h=1}^{SIS100} \cdot 10}{360^\circ} \cdot T_{h=10}^{SIS100} \mod T_{h=10}^{SIS100}}{T_{h=10}^{SIS100}} \cdot 360^\circ \tag{6.21}$$

Here we explain the inevitable uncertainty of the phase advance prediction and rf frequency modulation.

- Uncertainty of the predicted phase advance

  If the phase prediction time is 500us, the uncertainty of the predicted phase advance δt_ψ is 100ps [**?**]. We calculate the uncertainty of the predicted phase advance, $\delta\psi_{h=1}^{SIS100}$ and $\delta\psi_{h=1/5}^{SIS18}$, from the time to phase domain.

$$\delta t_\psi = 100ps \tag{6.22}$$

$$\delta\psi_{h=1/5}^{SIS18} = \delta\psi_{h=1}^{SIS100} = \frac{100ps}{1/157kHz} \cdot 360° \approx 0.006° \tag{6.23}$$

Based on the eq. 6.23, eq. 6.20 and eq. 6.21, the uncertainty of the phase at the Reference RF Signal of SIS18 and SIS100, $\delta\phi_{h=10}^{SIS100}$ and $\delta\phi_{h=2}^{SIS18}$, is calculated.

$$\delta\phi_{h=2}^{SIS18} = \sqrt{(\frac{\partial\phi_{h=2}^{SIS18}}{\partial\psi_{h=2}^{SIS18}}\delta\psi_{h=2}^{SIS18})^2} = \sqrt{(10 \cdot \delta\psi_{h=2}^{SIS18})^2} = 0.06° \tag{6.24}$$

$$\delta\phi_{h=10}^{SIS100} = \sqrt{(\frac{\partial\phi_{h=10}^{SIS100}}{\partial\psi_{h=1}^{SIS100}}\delta\psi_{h=10}^{SIS100})^2} = \sqrt{(10 \cdot \delta\psi_{h=10}^{SIS100})^2} = 0.06° \tag{6.25}$$

- Uncertainty of the rf frequency modulation

  For the rf frequency modulation, the uncertainty is 0.2° at 5.4MHz [**?**]. We calculate the uncertainty in time domain, see eq. 6.26.

$$\delta\Delta f_{(t)} = \frac{0.2°}{360°} \cdot \frac{1}{5.4MHz} = 100ps \tag{6.26}$$

6.2.1.1 The best estimate of alignment and the probable range of alignment for the phase shift method

Different relation between $\phi_{h=2}^{SIS18}$ and $\phi_{h=10}^{SIS100}$ requires different phase adjustment for SIS18. Fig. 6.12 illustrates all scenarios of their relation and the required phase adjustment for each scenario. We would like to introduce a phase shift of up to ±180°. The blue and red line represents the phase of SIS100 and SIS18 Reference RF Signal. The clockwise arrow from the SIS18 to SIS100 rf phase represents the negative phase adjustment for SIS18 and the anticlockwise represents the positive phase adjustment. The required phase adjustment of SIS18 is denoted by $\Delta\phi_{shift}$.

- Scenario (a): $\phi_{h=10}^{SIS100} \in [0, 90°)$, see Fig. 6.13 (a).

  - $\phi_{h=10}^{SIS100} < \phi_{h=2}^{SIS18} < \phi_{h=10}^{SIS100} + 180°$, which denotes by the yellow semicircle in Fig. 6.13 (a). The phase adjustment is

$$\Delta\phi_{shift} = -(\phi_{h=2}^{SIS18} - \phi_{h=10}^{SIS100}) \tag{6.27}$$

  - $\phi_{h=2}^{SIS18} < \phi_{h=10}^{SIS100}$ or $\phi_{h=2}^{SIS18} > \phi_{h=10}^{SIS100} + 180°$, which denotes by the white semicircle in Fig. 6.13 (a). The phase adjustment is

$$\Delta\phi_{shift} = 360° - \phi_{h=2}^{SIS18} + \phi_{h=10}^{SIS100} \tag{6.28}$$

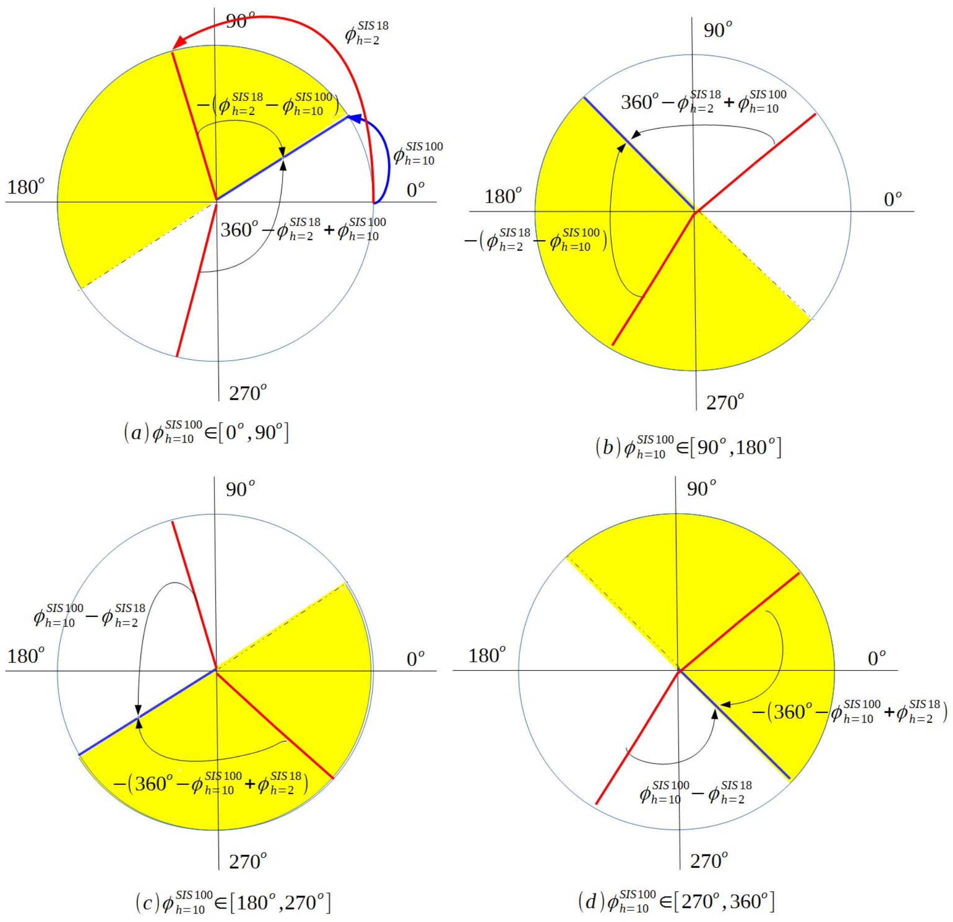

Figure 6.12: Scenarios for the phase shift method

- Scenario (b): $\phi^{SIS100}_{h=10} \in [90, 180°)$, see Fig. 6.13 (b).

  - $\phi^{SIS100}_{h=10} < \phi^{SIS18}_{h=2} < \phi^{SIS100}_{h=10} + 180°$, which denotes by the yellow semicircle in Fig. 6.13 (b). The phase adjustment is

$$\Delta\phi_{shift} = -(\phi^{SIS18}_{h=2} - \phi^{SIS100}_{h=10}) \tag{6.29}$$

  - $\phi^{SIS18}_{h=2} < \phi^{SIS100}_{h=10}$ or $\phi^{SIS18}_{h=2} > \phi^{SIS100}_{h=10} + 180°$, which denotes by the white semicircle in Fig. 6.13 (b). The phase adjustment is

$$\Delta\phi_{shift} = 360° - \phi^{SIS18}_{h=2} + \phi^{SIS100}_{h=10} \tag{6.30}$$

- Scenario (c): $\phi^{SIS100}_{h=10} \in [180, 270°)$, see Fig. 6.13 (c). The phase adjustment is

  - $\phi^{SIS18}_{h=2} > \phi^{SIS100}_{h=10}$ or $\phi^{SIS18}_{h=2} < \phi^{SIS100}_{h=10} + 180° - 360°$, which denotes by the yellow semicircle in Fig. 6.13 (c). The phase adjustment is

$$\Delta\phi_{shift} = -(360° - \phi^{SIS100}_{h=10} + \phi^{SIS18}_{h=2}) \tag{6.31}$$

  - $\phi^{SIS100}_{h=10} - 180° < \phi^{SIS18}_{h=2} < \phi^{SIS100}_{h=10}$, which denotes by the white semicircle in Fig. 6.13 (c). The phase adjustment is

$$\Delta\phi_{shift} = \phi^{SIS100}_{h=10} - \phi^{SIS18}_{h=2} \tag{6.32}$$

- Scenario (d): $\phi_{h=10}^{SIS100} \in [270, 360°)$, see Fig. 6.13 (d).

  - $\phi_{h=10}^{SIS100} - 180° < \phi_{h=2}^{SIS18} < \phi_{h=10}^{SIS100}$, which denotes by the yellow semicircle in Fig. 6.13 (d). The phase adjustment is

$$\Delta\phi_{shift} = \phi_{h=10}^{SIS100} - \phi_{h=2}^{SIS18} \tag{6.33}$$

  - $\phi_{h=2}^{SIS18} > \phi_{h=10}^{SIS100}$ or $\phi_{h=2}^{SIS18} < \phi_{h=10}^{SIS100} + 180° - 360°$, which denotes by the white semicircle in Fig. 6.13 (d).

$$\Delta\phi_{shift} = -(360° - \phi_{h=10}^{SIS100} + \phi_{h=2}^{SIS18}) \tag{6.34}$$

The phase adjustment is achieved by the phase shift method within the upper bound time, $T_{phase\_shift}^{upper\_bound}$. For the U^{28+} B2B transfer from SIS18 to SIS100, we assume that $T_{phase\_shift}^{upper\_bound}$ equals to 7ms, which means that the phase shift $\Delta\phi_{shift}$ is achieved within 7ms. So the best estimate of alignment is expressed by

$$t_{best} = t_\psi + T_{phase\_shift}^{upper\_bound} \tag{6.35}$$

The uncertainty in the phase prediction δt_ψ is 100ps, see eq. 6.22. The phase shift uncertainy $\delta\Delta\phi_{phase}$ is casued by the rf frequency modulation, whose jitter is 100ps, see eq. 6.26. The phase shift uncertainy equals to the uncertainty in the phase shift upper bound time, $\delta T_{phase\_shift}^{upper\_bound} = 100\text{ps}$. Both cause an uncertainty in the best estimate of alignment t_{best}.

$$\begin{aligned}\delta t_{best} &= \sqrt{(\frac{\partial t_{best}}{\partial t_\psi}\delta t_\psi)^2 + (\frac{\partial t_{best}}{\partial T_{phase\_shift}^{upper\_bound}}\delta T_{phase\_shift}^{upper\_bound})^2} \\ &= \sqrt{(\delta t_\psi)^2 + (T_{phase\_shift}^{upper\_bound})^2} = \sqrt{100ps^2 + 100ps^2} \approx 140ps\end{aligned} \tag{6.36}$$

The uncertainty of the alignment for the phase shift method is about 140ps. So the proper range of alignment is [t_{best}-140ps, t_{best}+140ps] for U^{28+} B2B transfer from SIS18 to SIS100.

6.2.1.2 The best estimate of alignment and the probable range of alignment for the frequency beating method

Fig. 6.13 illustrates two scenarios for the frequency beating method. With the frequency beating method, SIS18 can only achieve positive phase adjustment, which is denoted by $\Delta\phi_{adjustment}$. E.q. 6.37 shows the best estimate of alignment for the phase adjustment of $\Delta\phi_{adjustment}$.

$$t_{best} = t_\psi + \frac{\Delta\phi_{adjustment}}{360° \cdot \Delta f} \tag{6.37}$$

where Δf is the beating frequency.

According to the relation between $\phi_{h=2}^{SIS18}$ and $\phi_{h=10}^{SIS100}$, there are two scenarios, see Fig. 6.13.

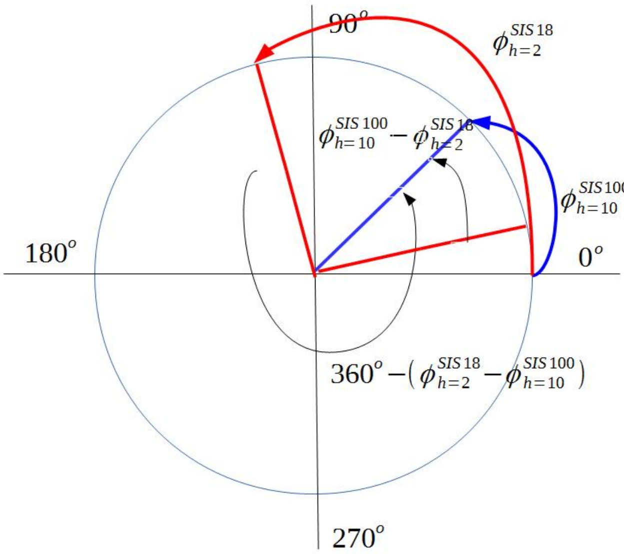

Figure 6.13: Two scenarios for the frequency beating method

- Scenario (a): $\phi_{h=2}^{SIS18} < \phi_{h=10}^{SIS100}$

$$\Delta\phi_{adjustment} = \phi_{h=10}^{SIS100} - \phi_{h=2}^{SIS18} \tag{6.38}$$

Replacing $\Delta\phi_{adjustment}$ in eq. 6.37 with eq. 6.38, we have

$$t_{best} = t_{\psi} + \frac{\phi_{h=10}^{SIS100} - \phi_{h=2}^{SIS18}}{360^{\circ} \cdot \Delta f} \tag{6.39}$$

- Scenario (b): $\phi_{h=2}^{SIS18} \geq \phi_{h=10}^{SIS100}$

$$\Delta\phi_{adjustment} = 360^{\circ} - (\phi_{h=2}^{SIS18} - \phi_{h=10}^{SIS100}) \tag{6.40}$$

Replacing $\Delta\phi_{adjustment}$ in eq. 6.37 with eq. 6.40, we have

$$t_{best} = t_{\psi} + \frac{360^{\circ} - (\phi_{h=2}^{SIS18} - \phi_{h=10}^{SIS100})}{360^{\circ} \cdot \Delta f} \tag{6.41}$$

Based on these two scenarios, we could deduce the formula for the best estimate of alignment.

$$t_{best} = t_{\psi} + \frac{\Delta n \cdot 360^{\circ} - (\phi_{h=2}^{SIS18} - \phi_{h=10}^{SIS100})}{360^{\circ} \cdot \Delta f} \tag{6.42}$$

where $\triangle n$ equals 0 when $\phi_{h=2}^{SIS18} < \phi_{h=10}^{SIS100}$ and equals 1 when $\phi_{h=2}^{SIS18} \geq \phi_{h=10}^{SIS100}$.

The uncertainty of the alignment is the result of the error propagation of uncertainties of the phase prediction and rf frequency detune, see eq. 6.43. Because the rf frequency detune has the long term stability, $\int \delta\Delta f$=0, the uncertainty caused by rf frequency detune is 0. The uncertainty of the phase prediction $\phi_{h=2}^{SIS18}$ and $\phi_{h=10}^{SIS100}$ is 0.06°, see eq. 6.24 and eq. 6.25. Δf is 200Hz. The maximum

$\Delta n \cdot 2\pi - (\phi_{h=2}^{SIS18} - \phi_{h=10}^{SIS100})$ is 2π.

$$
\begin{aligned}
\delta t_{best} &= \sqrt{(\frac{\partial t_{best}}{\partial \phi_{h=2}^{SIS18}} \delta\phi_{h=2}^{SIS18})^2 + (\frac{\partial t_{best}}{\partial \phi_{h=10}^{SIS100}} \delta\phi_{h=10}^{SIS100})^2 + (\frac{\partial t_{best}}{\partial \Delta f} \delta\Delta f)^2} \\
&= \sqrt{(\frac{-1}{2\pi \cdot \Delta f} \delta\phi_{h=2}^{SIS18})^2 + (\frac{1}{2\pi \cdot \Delta f} \delta\phi_{h=10}^{SIS100})^2 + (-\frac{\Delta n \cdot 2\pi - (\phi_{h=2}^{SIS18} - \phi_{h=10}^{SIS100})}{2\pi \cdot \Delta f^2} \delta\Delta f)^2} \\
&\leq \sqrt{(\frac{-1}{2\pi \cdot 200} 0.06°)^2 + (\frac{1}{2\pi \cdot 200} 0.06°)^2 + 0} \\
&\approx 1.178us
\end{aligned}
\tag{6.43}
$$

From eq. 6.43 we could get the uncertainty of the alignment is 1.178us, so the probable range of alignment is $[t_{best}-1.178us, t_{best} + 1.178us]$.

6.2.1.3 Calculation the synchronization window and its accuracy

In the last section, we get the probable range of alignment, within which the two Reference Rf Signals could be aligned with each other. The synchronization window is used to select the revolution frequency marker for the extraction and injection kicker firing, which is closest to the probable range of alignment, See Fig. 6.14. For the selection, the length of the synchronization window must be a least one SIS100 revolution period. The best estimate of the start of the synchronization window is exactly half revolution period before the selected revolution frequency marker. The blue and orange rectangles represent two scenarios of the probable range of alignment. In Fig. 6.14, the 2nd revolution frequency marker is the closest one to the probable range of alignment. The best estimate of the start of the synchronization window aligns with the negative zero crossing point of the revolution marker signal.

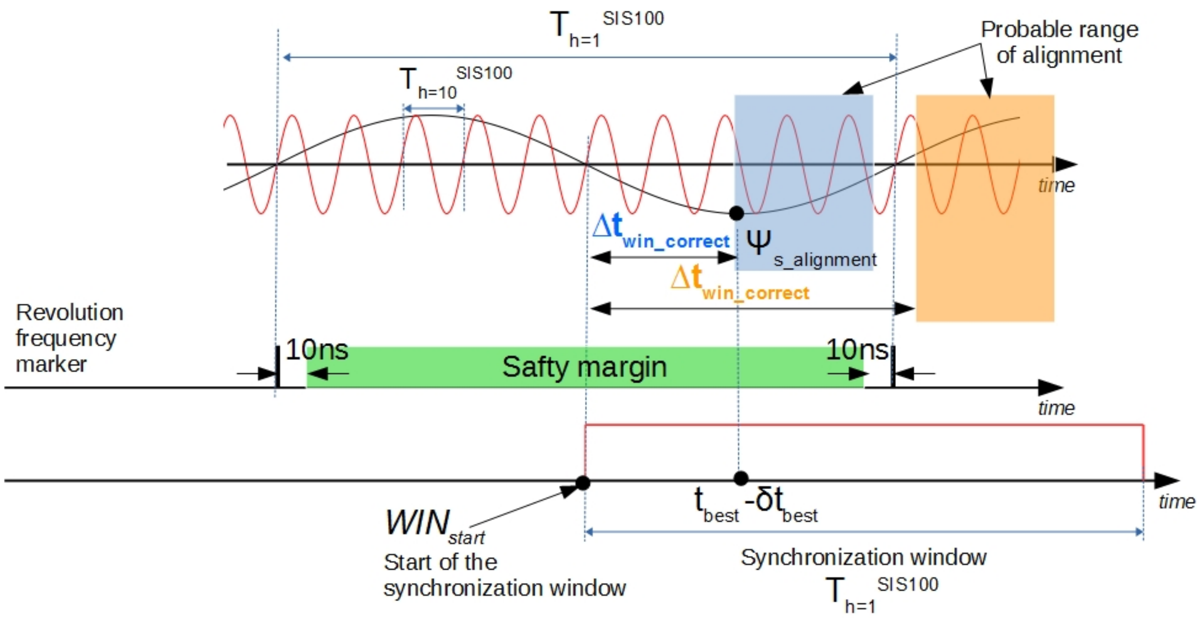

Figure 6.14: The illustration of the synchronization window and its accuracy

For SIS100, the rf phase of the revolution frequency is $\psi_{h=1}^{SIS100}$ at t_ψ. We could calculate the rf phase $\psi_{s\_alignment}$ of the revolution frequency at the start of the probable rang of alignment, t_{best}-δt_{best}.

$$\psi_{s\_alignment} = \frac{(t_{best} - \delta t_{best} - t_{\psi} - \frac{360^\circ - \psi^{SIS100}_{h=1}}{360^\circ} \cdot T^{SIS100}_{h=1}) \mod T^{SIS100}_{h=1}}{T^{SIS100}_{h=1}} \cdot 360^\circ \tag{6.44}$$

For the calculation of the best estimate of the start of the synchronization window, there are two scenarios. $\Delta t_{win\_correct}$ is the time correction for the start of the probable range of alignment to the best estimate of the start of the synchronization window, see Fig. 6.14.

- $\psi_{s\_alignment} \in [0^\circ, 180^\circ)$, the orange rectangle in Fig. 6.14

$$\Delta t_{win\_correct} = \frac{\psi_{s\_alignment}}{360^\circ} \cdot T^{SIS100}_{h=1} + \frac{T^{SIS100}_{h=1}}{2} \tag{6.45}$$

$$WIN_{start} = t_{best} - \delta t_{best} - \Delta t_{win\_correct} \tag{6.46}$$

- $\psi_{s\_alignment} \in [180^\circ, 360^\circ)$, the blue rectangle in Fig. 6.14

$$\Delta t_{win\_correct} = \frac{\psi_{s\_alignment} - 180^\circ}{360^\circ} \cdot T^{SIS100}_{h=1} \tag{6.47}$$

$$WIN_{start} = t_{best} - \delta t_{best} - \Delta t_{win\_correct} \tag{6.48}$$

The actual start of the synchronization window is impossible to be exactly at the best estimate of the start of the synchronization window because of the precision and trueness [**?**]. The precision of the start
of the synchronization window is defined as the closeness of agreement between the actual start of the synchronization window of different SCUs and the trueness of the start
of the synchronization window as the closeness of agreement between the average actual start of the synchronization window of different SCUs and the best estimation start of the synchronization window. The precision comes from the random error, e.g. IO port TTL signal rising osillation. The trueness is the systematic error, e.g. FPGA process time. The accuracy of the start
of the synchronization window is defined as the closeness of agreement between the observed start and the best estimate of the start of the synchronization window, which is the sum of the precision and trueness. The B2B transfer system will be used for many transfers for FAIR. Therefore, we have to find the most stringent accuracy requirement. The shortest revolution period of the target machine is 433 ns, which comes from RIB transfer from CR to HESR. We keep 10ns as a forbidden range, which means that the actual start is not allowed 10 ns before and after the revolution frequency marker. The green region in Fig. 6.14 represents the safty margin for the start of the synchronization window. So the accuracy of the start of the synchronization window must meet the requirement calculated by eq. 6.49.

$$Accuracy = \pm\frac{433 - 10 \cdot 2}{2} \approx \pm 200\,\text{ns} \tag{6.49}$$

6.2.2 Characterization of the WR network for the B2B transfer

Within this dissertation, a network analyzed by Xena is used to characterize the properties of the WR network, which are relevant to B2B transfer. The WR network measurement is achieved by the Xena traffic generator[1], which offers a new class of professional Layer 2-3 Gigabit Ethernet test platform. It is used to measure the frame loss rate[2], frame transfer latency[3] and frame transfer jitter[4] for the WR network. For the measurement, Xena traffic generator sends the traffic streams with a unique stream ID for identifying latency, jitter and packet loss. For the measurements, the following types of traffic are considered [**?**].

- DM Broadcast

  DM forwards broadcast timing frames[5] with 110 bytes ethernet frame length downwards to all FECs. The average bandwidth for the DM broadcast is 100 Mbit/s. The burst[6] speed is 12 packets per 100 µs.

- DM Unicast

  DM sends 10Mbit/s unicast timing frames with 110 bytes ethernet frame length to some specified FECs at the burst speed of 3 packets per 300 µs.

- B2B Unicast

  The source B2B SCU sends the timing frame with 110 bytes ethernet frame length upwards to the DM. For the B2B transfer upper bound time 10 ms of each supercycle, 2 unicast timing frames are send to the DM. The maximum repetition frequency is of the U^{28+} supercycle, 2.82 Hz. For the estimation of the upper bound bandwidth, we use 3Hz/s as the maximum repetition frequency. So the bandwidth is 3 Hz/s $\cdot$ 2 packets/supercycle $\cdot$ 110 byte $\cdot$ 8 bit $\approx$ 5.5 kbit/s.

- B2B Broadcast

  Maximum 10 B2B broadcast timing frames with 110 ethernet frame length are sent within 10 ms. So the bandwidth is 3 Hz/s $\cdot$ 10 packets/supercycle $\cdot$ 110 byte $\cdot$ 8 bit $\approx$ 26.5 kbit/s.

- Management Traffic

  The average bandwidth for the management traffic is 10 Mbit/s. It broadcasts packets with random ethernet frame length from 64 bytes to 1518 bytes.

---

[1] `http://xenanetworks.com/layer-2-3-platform/`

[2] The ratio of the number of the lost frames to the number of the theoretic received frames of a tested port.

[3] The time interval between the time of Xena port receiving frame and the time of another Xena port sending frame.

[4] The absolute value of the difference between the latency of two consecutive received frames belonging to the same stream from one Xena port to another Xena port. `http://www.xenanetworks.com/wp-content/uploads/Measuring_Frame_latency_Variation.pdf`

[5] `https://www-acc.gsi.de/wiki/Timing/TimingSystemEvent`

[6] A group of consecutive frames with shorter interframe gaps than frames arriving before or after the burst of frames.

The requirements for the B2B Broadcast and Unicast traffic are summarized in Tab. ?? [?].

Table 6.4: The B2B transfer requirements for the WR network

	Frame Loss Rate	Upper bound latency of WR network	Upper bound latency per WR switch layer
B2B Broadcast	10^{-12}	500 µs	30 µs
B2B Unicast	10^{-12}	500 µs	30 µs

For the WR network for FAIR, three VLANs with different priorities are applied according to the importance of the traffic.

6.2.2.1 WR network test setup

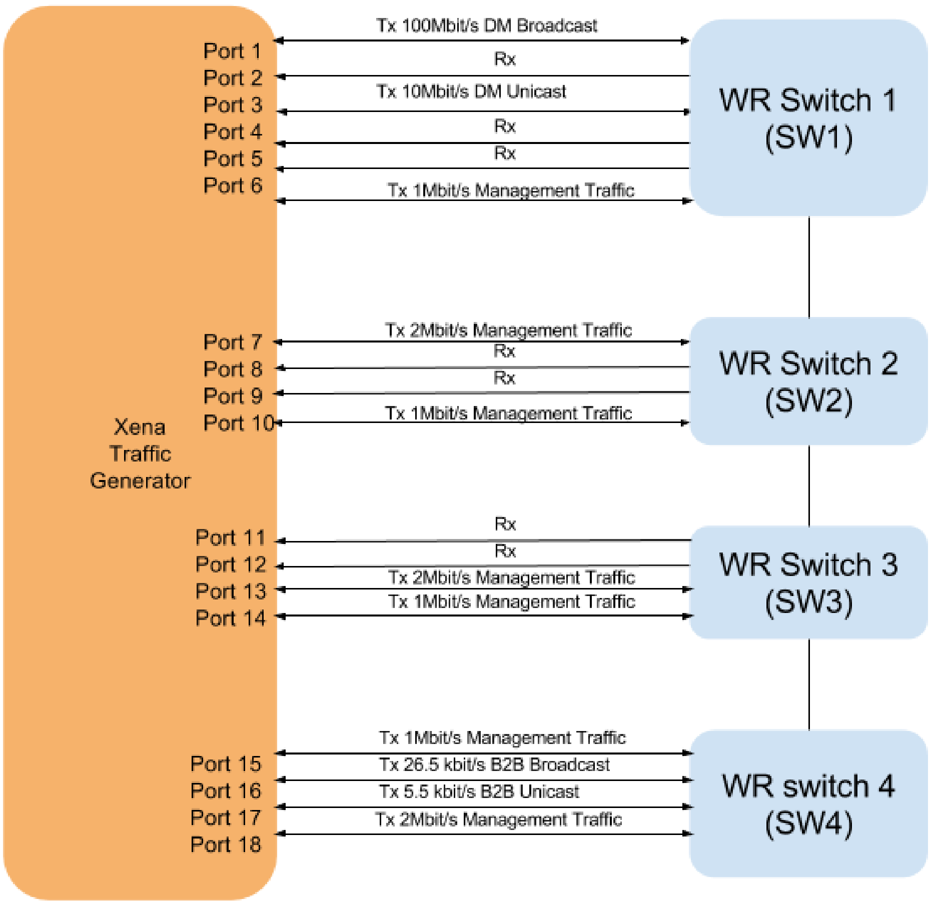

Figure 6.15: The WR network test setup

Based on the mentioned traffic, the measurement setup is built, see Fig. 6.15 [?]. Four WR switches are connected to the port 1 to 18 of the Xena traffic generator. All ports of four WR switches are assigned to three VLANs, VLAN 5, VLAN 6 and

VLAN 7. Tab. 6.5 shows the bandwidth, VLAN, VLAN priority and usage of the traffic of each Xena port in details. The test is running for 14 hours.

Table 6.5: The connection between the traffic generator and WR switches

Switch	Xena Port	Traffic	VLAN	Priority	Usage
WR switch 1	Port 1	100 Mbit/s 110bytes	7	7	DM Broadcast
	Port 2	Rx traffic			
	Port 3	10 Mbit/s 110bytes	7	7	DM Unicast
	Port 4	Rx traffic			
	Port 5	Rx traffic			
	Port 6	1 Mbit/s 64 - 1518 bytes	5	5	Management Broadcast
WR switch 2	Port 7	2 Mbit/s 64 - 1518 bytes	5	5	Management Broadcast
	Port 8	Rx traffic			
	Port 9	Rx traffic			
	Port 10	1 Mbit/s 64 - 1518 bytes	5	5	Management Broadcast
WR switch 3	Port 11	Rx traffic			
	Port 12	Rx traffic			
	Port 13	2 Mbit/s 64 - 1518 bytes	5	5	Management Broadcast
	Port 14	1 Mbit/s 64 - 1518 bytes	5	5	Management Broadcast
WR switch 4	Port 15	1 Mbit/s 64 - 1518 bytes	5	5	Management Broadcast
	Port 16	26.5 kbit/s 110bytes	6	6	B2B Broadcast
	Port 17	5.5 kbit/s 110bytes	7	7	B2B Unicast
	Port 18	2 Mbit/s 64 - 1518 bytes	5	5	Management Broadcast

6.2.2.2 Frame loss rate test result for B2B frames

The frame loss rate of the stream from port 17 to port 1 is measured for the B2B Unicast frames. The frame loss rate of the stream from port 16 to other ports is measured for the B2B Broadcast frame. Fig. 6.16 [**?**] shows the test result for both traffics. For the B2B Broadcast frames, the frame loss rate of each port is 0 %. For the B2B Unicast frames, the frame loss rate of port 1 is 0 %. So there is no B2B frame loss of the test WR network.

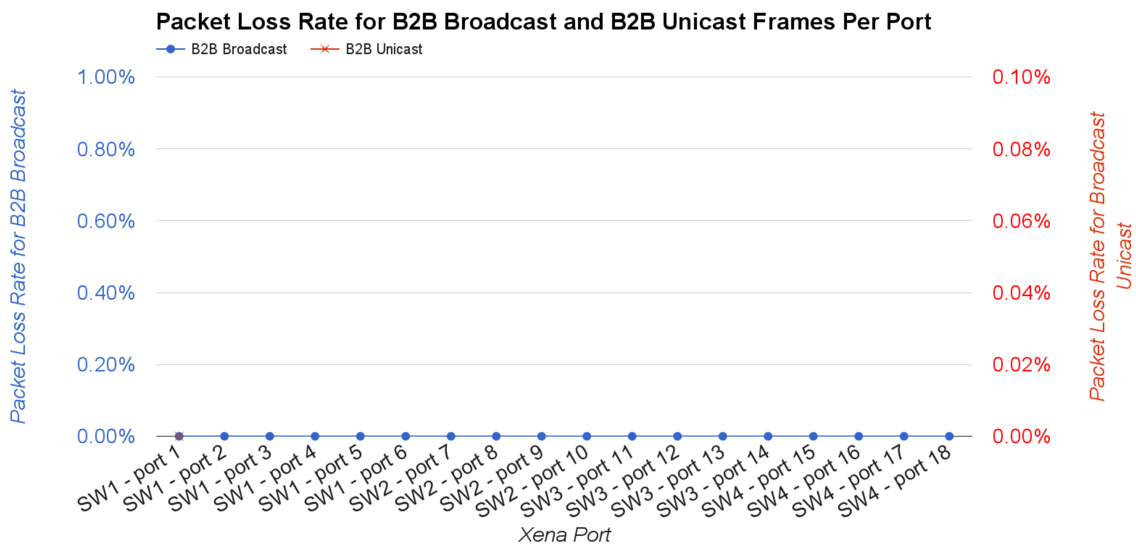

Figure 6.16: The frame loss rate for B2B Broadcast and B2B Unicast frames

6.2.2.3 Latency and jitter test result for B2B frames

The latency and jitter of the stream from port 16 to other ports are measured.

- Latency and jitter for B2B Broadcast frames
  - Average Latency and jitter

    Fig. 6.17 [?] shows the test result for the average latency and jitter for the B2B Broadcast frames. Tab. 6.6 shows the average latency and jitter of different WR switch layers. They meet the requirements of the B2B transfer.

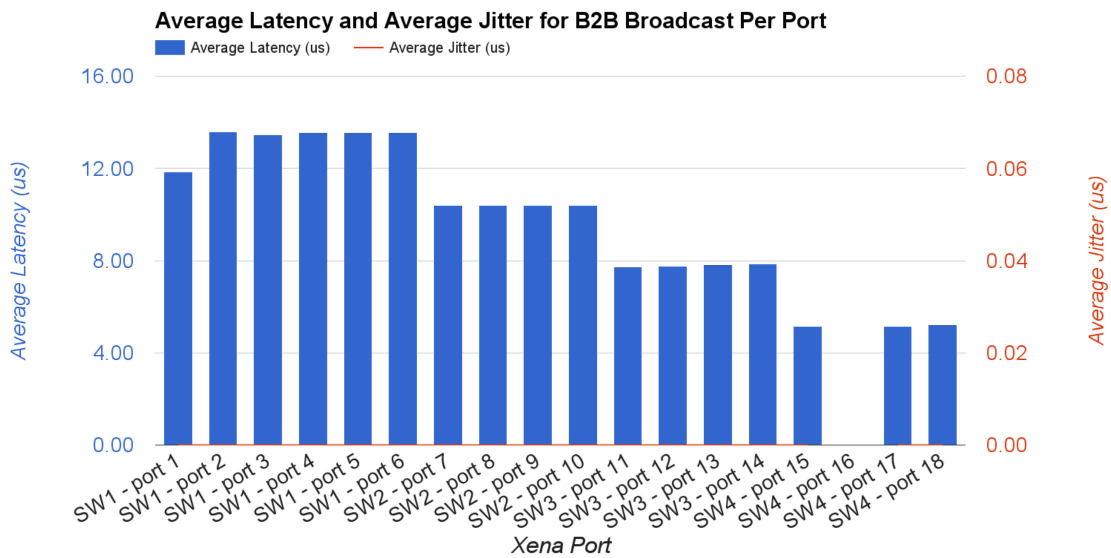

Figure 6.17: The average latency and jitter for B2B Broadcast frames

Table 6.6: The average latency and jitter of the B2B Broadcast frames

	WR switch 4	WR switch 4, 3	WR switch 4, 3, 2	WR switch 4, 3, 2, 1
Avg latency	6 µs	8 µs	11 µs	14 µs
Avg jitter	0 ns	0 ns	0 ns	0 ns

- Maximum Latency and jitter

  Fig. 6.18 [?] shows the test result for the maximum latency and jitter for the B2B Broadcast frames. Tab. 6.7 shows the maximum latency and jitter of different WR switch layers. They meet the requirements of the B2B transfer.

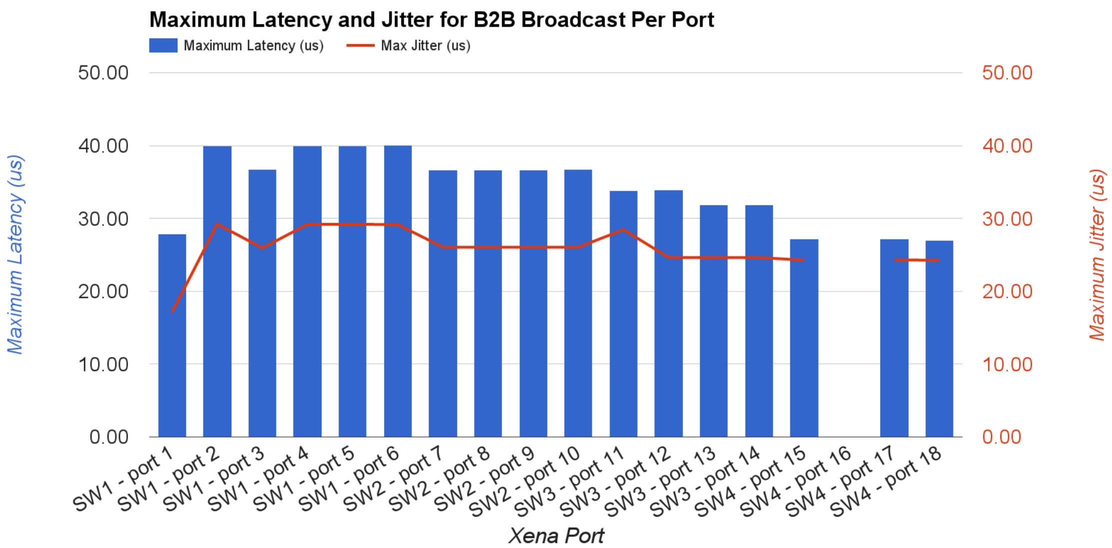

Figure 6.18: The maximum latency and jitter for B2B Broadcast frames

Table 6.7: The maximum latency and jitter of the B2B Broadcast frames

	WR switch 4	WR switch 4, 3	WR switch 4, 3, 2	WR switch 4, 3, 2, 1
Max latency	28 µs	34 µs	37 µs	41 µs
Max jitter	25 µs	25 µs	27 µs	30 µs

- Latency and jitter for B2B Unicast frames

  For the B2B unicast frames, the latency and jitter of the stream from port 16 to port 1 are measured.

- Average Latency and jitter

  For the B2B Unicast frames, 4 WR switch network has approximate 11 µs average latency and 0 µs average jitter.

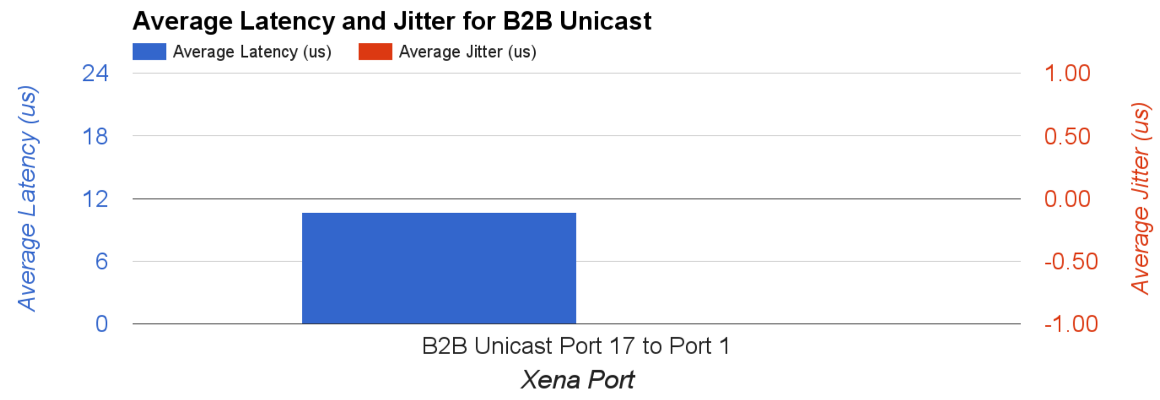

Figure 6.19: The average latency and jitter for B2B Unicast frames

- Maximum Latency and jitter

  For the B2B unicast frames, 4 WR switch network has approximate 23 µs maximum latency and 13 µs maximum jitter.

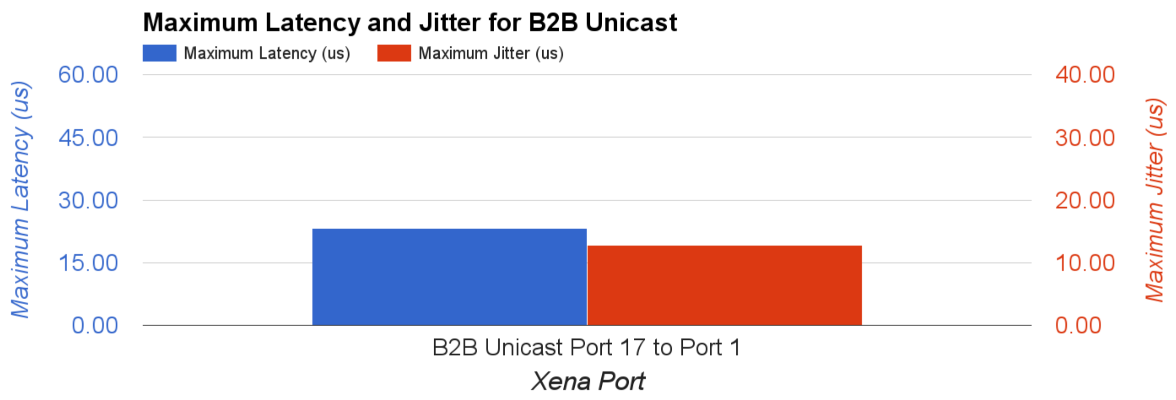

Figure 6.20: The maximum latency and jitter for B2B Unicast frames

More test configuration and results, please see "Testing the WR Network of the FAIR General Machine Timing System".

6.2.2.4 Result and conclusion

Tab. 6.8 shows the result of the test. The frame loss rate and latency meet the requirements of the B2B Broadcast and B2B Unicast traffic.

Table 6.8: The result of the WR network test for the B2B transfer

	Frame Loss Rate	Average Latency	Maximum Latency	Average Jitter	Maximum Jitter
B2B Broadcast	0 %	6 µs/switch	28 µs/switch	0 µs/switch	25 µs/switch
B2B Unicast	0 %	11 µs/4switch 3 µs/switch	23 µs/4switch 6 µs/switch	0 µs/4switch 0 µs/switch	13 µs/4switch 4 µs/switch

For the B2B transfer system, the upper bound latency of the frames in the B2B Broadcast and B2B Unicast traffic is 500 µs, see Tab.6.4. The latency of the WR network is decided by the layers of WR switches and the length of the optical fiber. The latency of the optical fiber is about 204 m/µs [?] and the longest distance in the FAIR campus is around 2 km, so the latency of a 2 km optical fiber is about 10 µs. The layers of WR switches play a more important role in the latency.

- B2B Broadcast

  Here we calculate the layer of the WR switch between the B2B source SCU and B2B target SCU, between B2B source SCU and source trigger SCU and between B2B source SCU and target trigger SCU.

$$\frac{500\,\mu\text{s} - 10\,\mu\text{s}}{28\,\mu\text{s/switch}} \approx 17 \tag{6.50}$$

- B2B Unicast

  Here we calculate the layer of the WR switch between the B2B source SCU and DM.

$$\frac{500\,\mu\text{s} - 10\,\mu\text{s}}{6\,\mu\text{s/switch}} \approx 81 \tag{6.51}$$

6.3 Kicker systematic investigation for the B2B transfer system

The SIS18 extraction kicker consists of 9 kicker units. In the existing topology, 5 kicker units are installed in the 1st crate and the other 4 units are in the 2nd crate. The width of each kicker unit is 0.25m and the distance between two kicker units is 0.09m. The distance between two crates is 19.167m. SIS100 injection kicker consists of 6 kicker units, which are equally located. The width of each kicker unit is 0.22m and the distance between two units is 0.23m. For the B2B transfer, the rise time of SIS18 extraction kicker and SIS100 injection kicker unit are 90ns and 1/20 of the revolution period. The rise time of these kickers must fit within the bunch gap, 25% of rf reference period [? ?]. The bunch gap is denoted by G. All the analysis in this section dose not consider the jitter of the kicker trigger signal. Here we are discussing about the following possibilities.

- For SIS18, whether the kicker units in the 2nd crate could be fired a fixed delay after the firing of the kicker units in the 1st crate for ion beams over the whole range of stable isotopes.
- For SIS100, whether the kicker units could be fired instantaneously.

6.3.1 SIS18 extraction kicker units

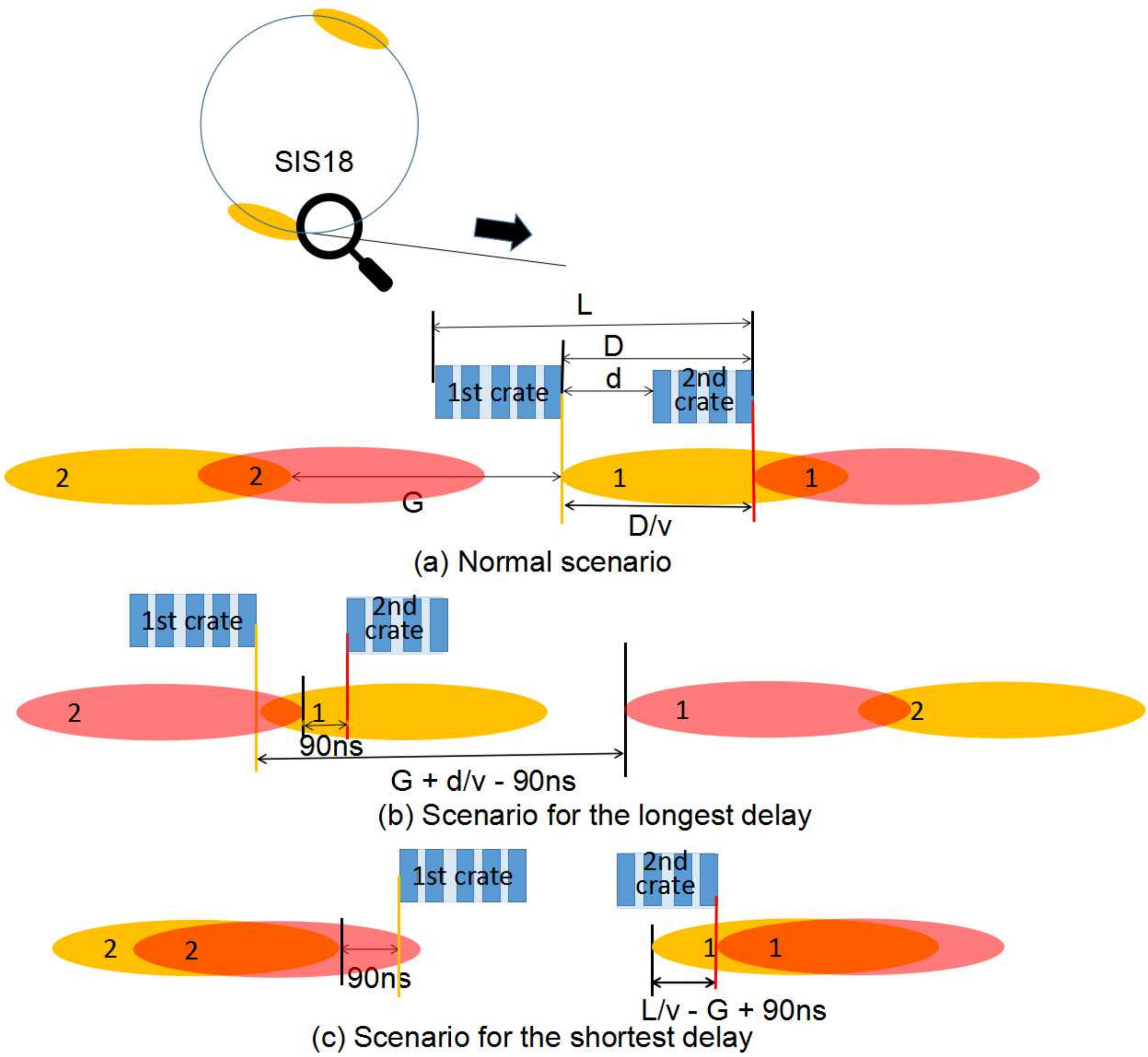

Figure 6.21: Three scenarios for the delay of SIS18 extraction kicker

Here we take three ion beams, H^{+}, U^{28} and U^{73+}, to check the possibility, because the boundary ion species have the most stringent requirements. Fig. 6.21 shows three scenarios of the firing delay between two crates. Beam is firstly kicked by kicker units in the 1st crate and than kicked by the units in the 2nd crate to the transfer line. The yellow and red ellipse represents the position of the bunches, when the kicker units in the 1st and 2nd crate are fired. The number in the ellipse is used to tell different bunches. The head of the bunch is at the right side. The bunch 2 is firstly kicked. Here we assume that the kicker units in the same crate are triggered instantaneous. d denotes the distance between two crates. L denotes the distance from the leftmost to the rightmost kicker unit. D denotes the sum distance of d and the 2nd crate. d equals to 19.167 meter. L equals to 22.047m = d + 9·0.25m + 7· 0.09m. D equals to 20.437m = d + 4·0.25m + 3· 0.09m.

Fig. 6.21 (a) is the easiest scenario. The kicker units in the 1st crate are fired when the tail of the bunch 1 passes by the 1st crate completely. The kicker units in the 2nd crate are fired when the tail of the bunch 1 passes by the 2nd crate completely. The delay for the firing two crates in this scenario is D/βc.

Fig. 6.21 (b) shows the scenario of the maximum delay between the firing of two crates. The kicker units in the 1st crate are fired when the tail of the bunch 1 passes by the 1st crate completely. The kicker units in the 2nd crate are fired 90ns before the head of the bunch 2 passes by it. The delay equals to G+d/βc-90ns.

Fig. 6.21 (c) shows the scenario of the minimum delay. The kicker units in the 1st crate are fired 90ns before the head of the bunch 2 passes by it. The kicker units in the 2nd crate are fired when the bunch 1 passes by the 2nd crate. The delay is L/βc-G+90ns.

Tab. 6.9 shows delay for three scenarios and related parameters. The fixed delay is determined primarily by the boundary delay range from H^+, U^{28} and U^{73+} beams, the delay range for other heavy ion species beams must be contained in these boundary range. According to the result, a fixed delay is available for firing kicker units in two crate for different beams. e.g. 80ns.

Table 6.9: The delay for firing two crates of SIS18 extraction kicker

Beam	β	time L/βc	bunch gap G	minimum delay L/βc-G+90ns	delay D/βc	maximum delay G+d/βc-90ns
H^+	0.982	75ns	184ns	0ns	69ns	163ns
U^{28+}	0.568	130ns	159ns	61ns	120ns	189ns
U^{73+}	0.872	84ns	104ns	70ns	78ns	92ns

6.3.2 SIS100 injection kicker units

Two bunches from SIS18 will be continuously injected into two RF buckets after the other in SIS100. See Fig. 6.10. The yellow ellipse represents the circulating bunch in SIS100 and the red one represents the bunch to be injected. The head of the bunch is at the left side. The preparation of the SIS100 injection kicker must be done during the bunch gap and it must be established for at least one SIS18 revolution period. For the instantaneous firing, all kicker units are fired only if the tail of the circulating bunch passes the leftmost kicker unit. The kicker pass time is the time needed for the tail of a bunch to pass from the rightmost unit to the leftmost kicker unit. The rise time of the kicker unit is 1/20 of the revolution period [**?**]. Therefor the preparation time is the sum of the kicker pass time and rise time. The distance from the rightmost to the leftmost kicker unit is 3.79m, 6·0.22m + 5·0.23m. If the preparation time is shorter than bunch gap, all kicker units could be fired instantaneous. Tab. 6.10 shows the preparation time for $H^+, U^{28} and U^{73+}$ beams and their bunch gap. The preparation time is much shorter than the bunch gap. So the kicker units could be fired instantaneous.

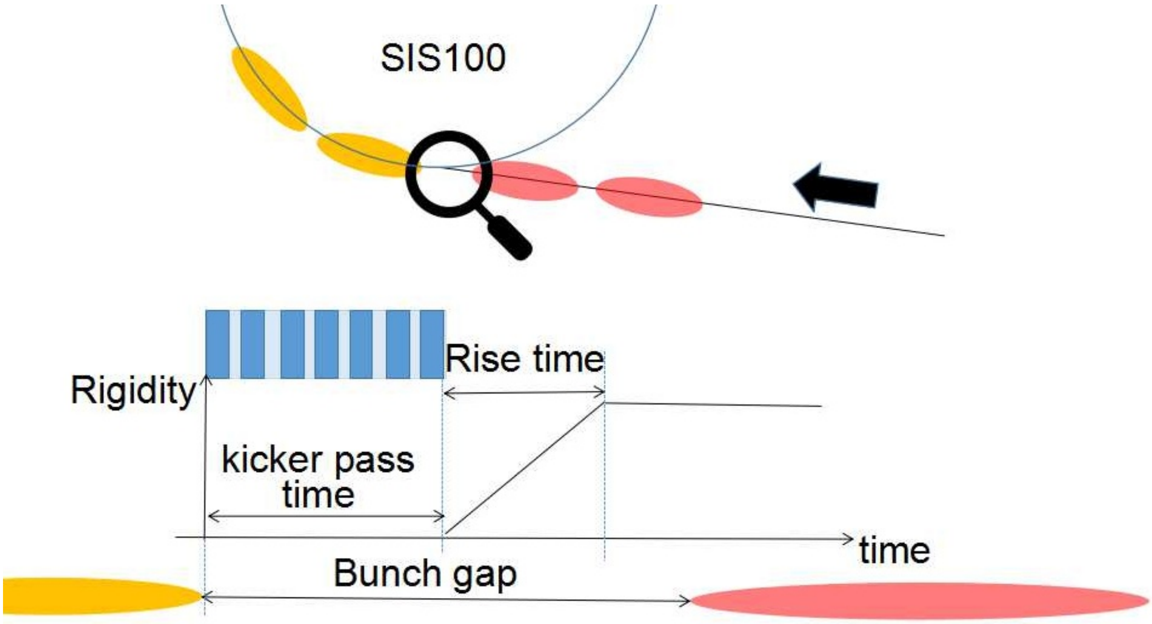

Figure 6.22: SIS100 injection kicker

Table 6.10: The delay for firing SIS00 injection kicker

Beam	β	kicker pass time L/βc	Rise time 1/20$\cdot T_{rev}^{SIS100}$	Preparation time L/βc+1/20$\cdot T_{rev}^{SIS100}$	bunch gap 2.25$\cdot T_{rev}^{SIS100}$
H^+	0.982	3ns	184ns	187ns	828ns
U^{28+}	0.568	22ns	318ns	333ns	1431ns
U^{73+}	0.872	15ns	207ns	222ns	932ns

6.4 Test setup for the data collection, merging and redistribution of the B2B transfer system

In this section, the test setup for the B2B transfer system is described, focusing only on the timing aspects.

6.4.1 Test functional requirement

The test setup achieves the following functional requirement.

- After receiving CMD_B2B_START, both the B2B source and target SCUs collect predicted phase equivalent data locally. The equivalence is a timestamp for the zero crossing point of the simulated Reference RF Signal of SIS18 and SIS100.

- The B2B target SCU transfers the frame containing the timestamp to the B2B source SCU.

- After receiving the data, the B2B source SCU calculates the synchronization window.

- The B2B source SCU sends the frame containing the beginning of the synchronization window to the WR network.

- After receving the frame, the trigger SCU produces TTL output indicating the start of the synchronization window.

6.4.2 Test setup

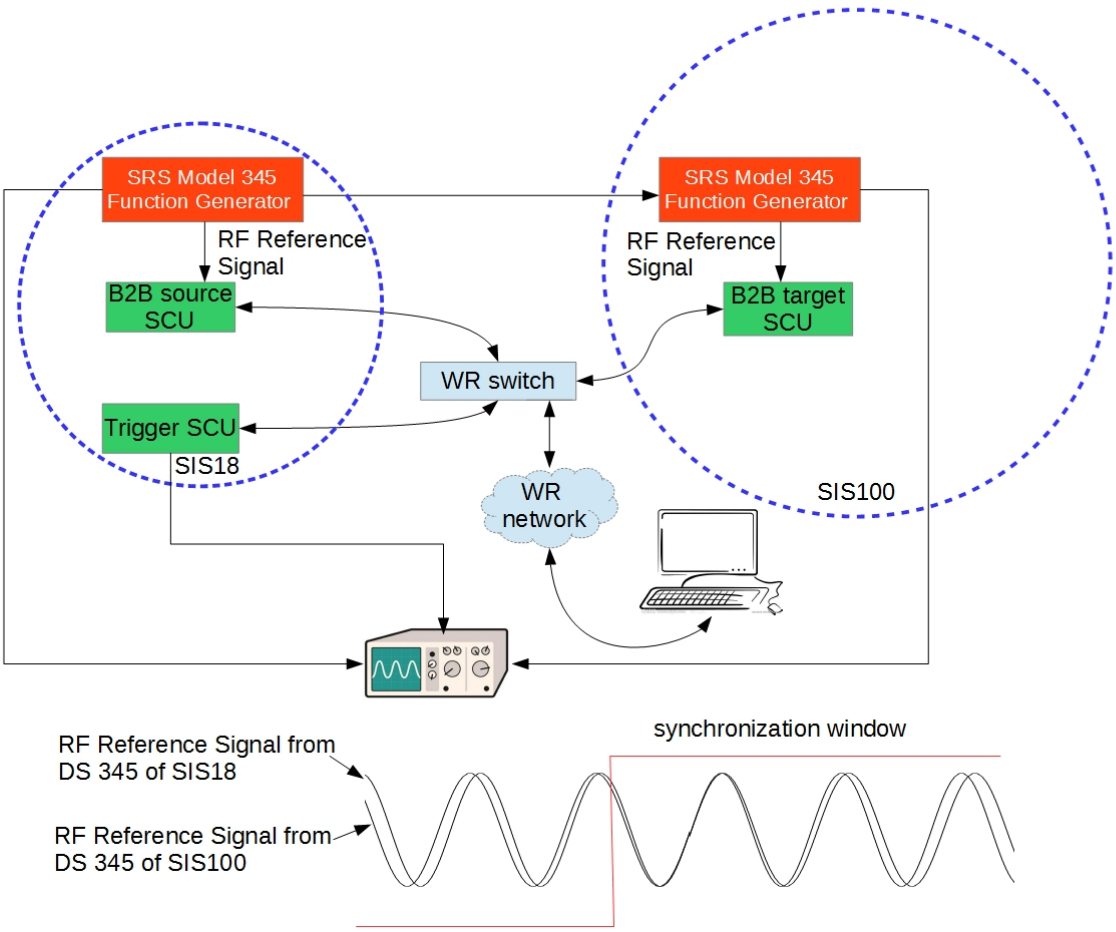

Figure 6.23: Schematic of the test setup

Fig. 6.23 shows the schematic of the test setup. In this test setup, two MODEL DS345 Synthesized Function Generators[7] are used, which are with the frequency accuracy of ±5 ppm of the selected frequency to simulate Reference RF Signals of SIS18 and SIS100. DS345 of SIS18 uses an internal 10 MHz clock as an external reference clock for DS345 of SIS100. The B2B source SCU, B2B target SCU and trigger SCU are connected to the same WR switch, which connects to the timing

[7]http://www.thinksrs.com/downloads/PDFs/Manuals/DS345m.pdf

network. A PC[8] is used as a DM to produce the B2B start timing frame. Besides, it monitors the status of the B2B transfer programs in all SCUs. The oscilloscope is used to monitor the alignment of the two simulated Reference RF Signals within the synchronization window provided by the trigger SCU.

Fig. 6.24 shows the front and back view of the test setup. DS345 of SIS18 produces the sine wave of 1.572 200 MHz frequency for the oscilloscope and DS345 of SIS100 produces the sine wave of 1.572 000 MHz for the oscilloscope, which are achieved by the LEMO cables, see green line in Fig. 6.24. DS345 produces the TTL signal for the B2B source SCU, whose rising edge is synchronized to the positive zero crossing of the sine wave of 1.572 200 MHz frequency and DS345 of SIS100 produces the TTL signal for the B2B target SCU, whose rising edge is synchronized to the sine wave of 1.572 000 MHz, which are achieved by the LEMO cables, see red line in Fig. 6.24. So the beating frequency is 200 Hz and the synchronization period is 5 ms. The B2B source, target and trigger SCUs are connected to the WR switch, which are achieved by the optical fiber, see yellow line. The WR switch is connected to the PC and the WR network. The output of the synchronization window from the B2B trigger SCU is connected to the oscilloscope, which is achieved by the LEMO cable, see green line.

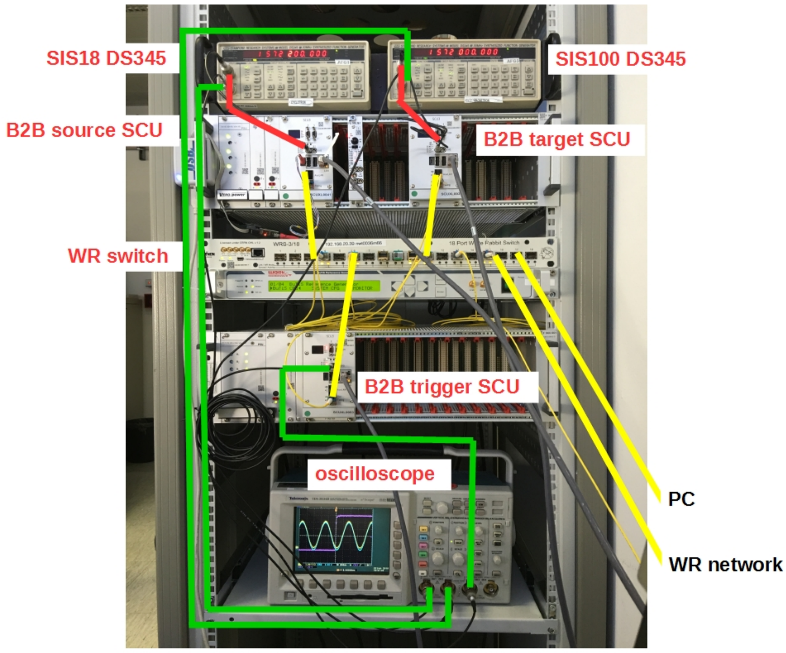

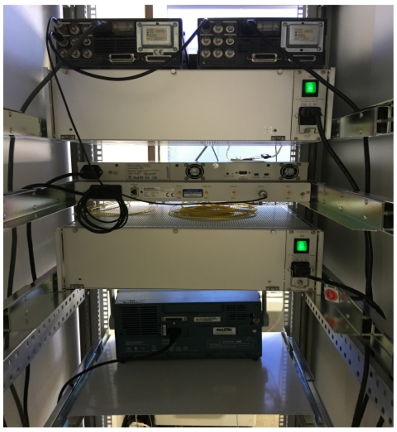

Figure 6.24: The front and back view of the test setup

Compared with the final scenario, there are some difference of the test setup.

- The SIS18 and SIS100 DS345 will be replaced by the PAP modules, which are installed in the B2B source and target SCUs as SCU slaves.
- All devices are installed in different racks. The SIS18 source SCU and B2B trigger SCU of the extraction kicker are installed in SIS18 and the SIS18 target SCU and B2B trigger SCU of the injection kicker are installed in SIS100. The connection is done via the WR network.

[8]A Linux personal computer is installed with the standard TR tools and library. `https://www-acc.gsi.de/wiki/Timing/TimingSystemNodesCurrentRelease`

- The B2B source SCU has several other SCU slaves, e.g. Phase Shift Module (PSM) for the phase shift.

- The B2B trigger SCU considers not only the synchronization window, but also the kicker delay compensation from the SM. Besides, it has several SCU slaves, which coordinate the correct B2B extraction and injeciton kicker with other systems, e.g. MPS.

6.4.3 The firmware of the B2B transfer system

The B2B source, B2B target and trigger SCUs have different firmware running on their soft CPU, LM32[9]. The firmware are activated by the B2B start timing frame, *CMD_START_B2B*, which indicates the source and target synchrotrons of the B2B transfer.

- Firmware for the B2B source SCU

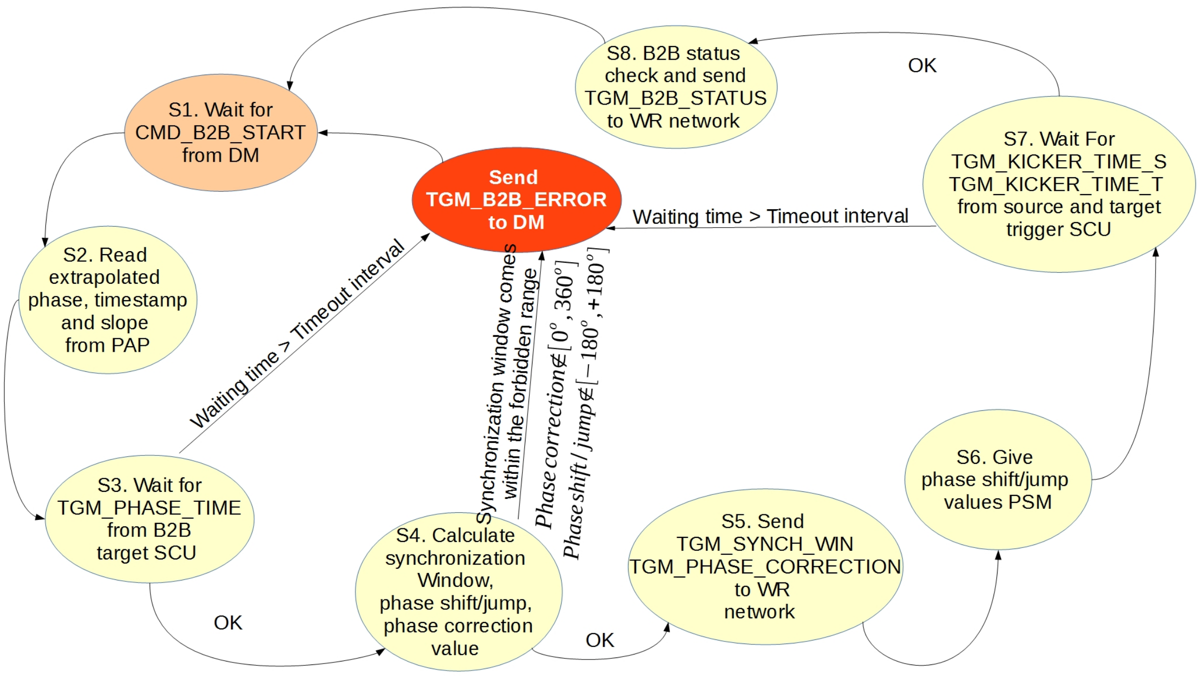

Figure 6.25: Flow chart of the firmware for B2B source SCU.
Flow chart of the firmware for B2B source SCU. “Step“ is represented as “S“ in the figure.

The firmware for the B2B source SCU is the core program of the B2B transfer system. See Fig. 6.25.

- Step 1. The program waits for the CMD_START_B2B timing frame.
- Step 2. When it receives the timing frame CMD_START_B2B, it reads the extrapolated phase, the corresponding timestamp and the phase advance slope from the PAP module.

[9] LatticeMico32 is a 32-bit microprocessor soft core from Lattice Semiconductor optimized for field-programmable gate arrays (FPGAs).

- Step 3. It waits for the TGM_PHASE_TIME timing frame from the B2B target SCU, which contains the extrapolated phase, the corresponding timestamp and the slope of the phase advance.

- Step 4. When it receives the timing frame TGM_PHASE_TIME within a specified timeout interval, it calculates the synchronization window, the phase shift/jump value and the phase correction value. Or it sends a timing frame TGM_B2B_ERROR to the WR network and goes back to the step 1, which indicates the timeout error of the frame. Besides, it checks whether the phase correction is in the range of $0°$ to $360°$, the required phase shift in the range of $-180°$ to $180°$ and the start of the synchronization window not in the forbidden range. If at least one of them is not correct, it sends a timing frame TGM_B2B_ERROR to the WR network and goes back to the step 1, which indicates the calculation error.

- Step 5. It sends the timing frame TGM_SYNCH_WIN and TGM_PHASE _CORRECTION to the WR network. TGM_SYNCH_WIN indicates the start of the synchronization window and TGM_PHASE_CORRECTION is used for the trigger SCUs for the reproduction of the bucket label signal.

- Step 6. It gives the phase correction and phase shift/jump values to corresponding modules.

- Step 7. It waits for the timing frame TGM_KICKER_TIME_S from the source trigger SCU and TGM_KICKER_TIME_T from the target trigger SCU, which contains the extraction/injection kicker trigger and firing timestamp. When it does not receive the timing frames within a specified timeout interval, it sends a timing frame TGM_B2B_ERROR to the WR network and goes back to the step 1, which indicates the timeout error of the frame.

- Step 8. When it receives the timing frames mentioned in the step 7 within a specified timeout interval, it checks the B2B transfer status and sends TGM_B2B_STATUS to the WR network and goes to the step 1. The B2B transfer is successful, if all of the following checks are correct. Or the B2B transfer is failure.

  * Trigger time $<$ firing time of the extraction kicker of the source synchrotron
  * Trigger time $<$ firing time of the injection kicker of the target synchrotron
  * Firing time of the extraction kicker $<$ firing time of the injection kicker

• Firmware for the B2B target SCU

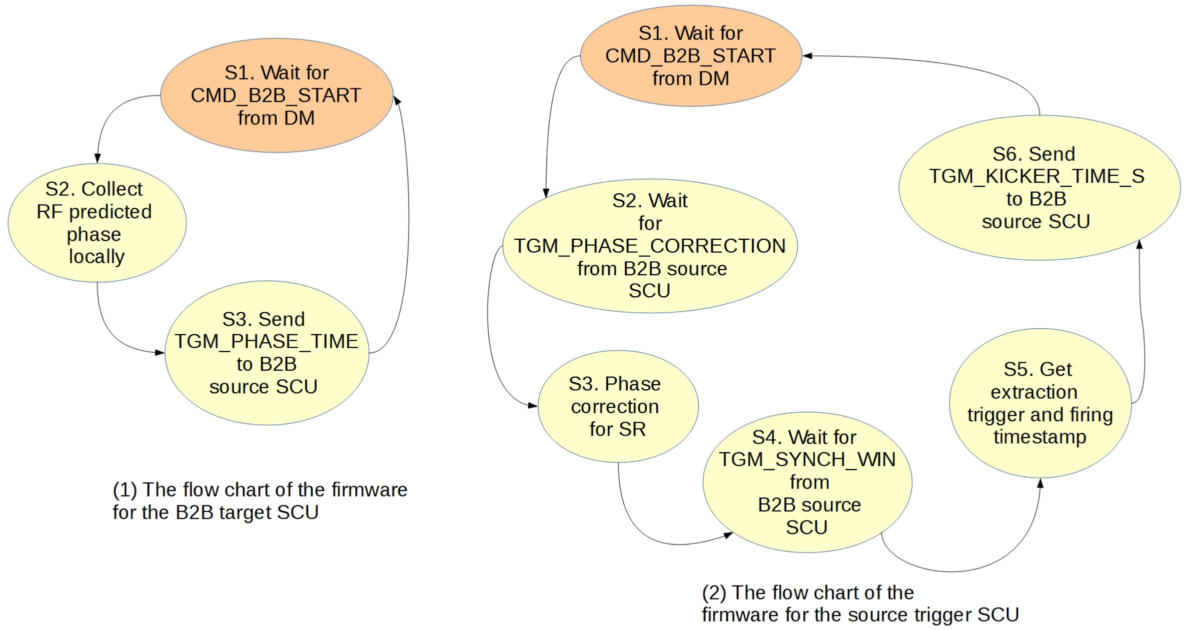

Figure 6.26: Flow chart of the firmware for B2B target SCU.
Flow chart of the firmware for B2B target SCU. “Step“ is represented as “S“ in the figure.

Fig. 6.26 (a) shows the flow chart of the program of the B2B target SCU.

- Step 1. The program waits for the CMD_START_B2B timing frame.
- Step 2. When it receives the timing frame CMD_START_B2B, it collects the predicted phase.
- Step 3. It sends the TGM_PHASE_TIME timing frame to the B2B source SCU and goes back to the step 1.

- Firmware for the trigger SCU

  Fig. 6.26 (b) shows the flow chart of the program of the source trigger SCU. For the target trigger SCU, the flow chat is same only with the different name of the timing frame TGM_KICKER_TIME_T.

  - Step 1. The program waits for the CMD_START_B2B timing frame.
  - Step 2. The program waits for the TGM_PHASE_CORRECTION timing frame.
  - Step 3. The program gives the phase correction value to the corresponding module for the bucket label signal reproduction.
  - Step 4. When it receives the timing frame CMD_START_B2B, it waits for the timing frame TGM_SYNCH_WIN to indicate the synchronization window for the kicker trigger.
  - Step 5. After the beam extraction, it collects the trigger and firing timestamp.
  - Step 6. It sends the TGM_KICKER_TIME_S timing frame to the B2B source SCU and goes back to the step 1.

6.4.4 The time constraints of the B2B transfer system

For the B2B transfer system, the time constraints are very important and strict. Fig. 6.27 shows the time constraint of the system. The CMD_START_B2B is executed at t_{B2B}. The RF phase prediction needs 500 µs, so the B2B source and target SCUs collect the phase data at t_{B2B} + 500 µs and need about 450 ns for the data collection. The B2B source SCU receives the timing frame TGM_PHASE_TIME at around t_{B2B} + 500 µs + 450 ns + 500 µs ≈ t_{B2B} + 1 ms. The second 500 µs is the upper bound latency of the WR network. After that, the B2B source SCU needs about 100 µs for the calculation, the sending of the timing frame TGM_SYNCH_WIN and TGM_PHASE_CORRECTION and data transferring to the corresponding module. TGM_SYNCH_WIN is sent at around t_{B2B} + 1 ms + 100 µs ≈ t_{B2B} + 1.1 ms. The trigger SCU receives TGM_PHASE_CORRECTION and TGM_SYNCH_WIN at around t_{B2B} + 1.1 ms + 500 µs ≈ t_{B2B} + 1.6 ms. The 500 µs is the latency of the WR network. The start of the synchronization window must be later than t_{B2B} + 1.1 ms + 2·500 µs ≈ t_{B2B} + 2.1 ms, because the TGM_SYNCH_WIN must be transferred back to the DM and the DM transfers it further to the beam instrumentation devices via WR network. The upward to DM transfer needs maximum 500 µs and the transfer from the DM to BI needs another 500 µs. The upper bound B2B transfer time is 10 ms, which is decided by the duration of the stable beam. There is no hard real time for the collection of the trigger and firing timestamps and timing frame TGM_KICKER_TIME_S sending, we give 1 ms for the source trigger SCU to do this task and the source trigger SCU sends TGM_KICKER_TIME_S at around t_{B2B} + 10 ms + 1 ms ≈ t_{B2B} + 11 ms. The same time constraints is also for the target trigger SCU. The B2B source SCU receives TGM_KICKER_TIME_S and TGM_KICKER_TIME_T at around t_{B2B} + 11 ms + 500 µs ≈ t_{B2B} + 11.5 ms. The 500 µs is the latency of the WR network. The B2B source SCU sends TGM_B2B_STATUS at around t_{B2B} + 11.5 ms + 100 µs ≈ t_{B2B} + 11.6 ms. The BI devices receives the timing frame TGM_B2B_STATUS at around t_{B2B} + 11.6 ms + 2·500 µs ≈ t_{B2B} + 12.6 ms.

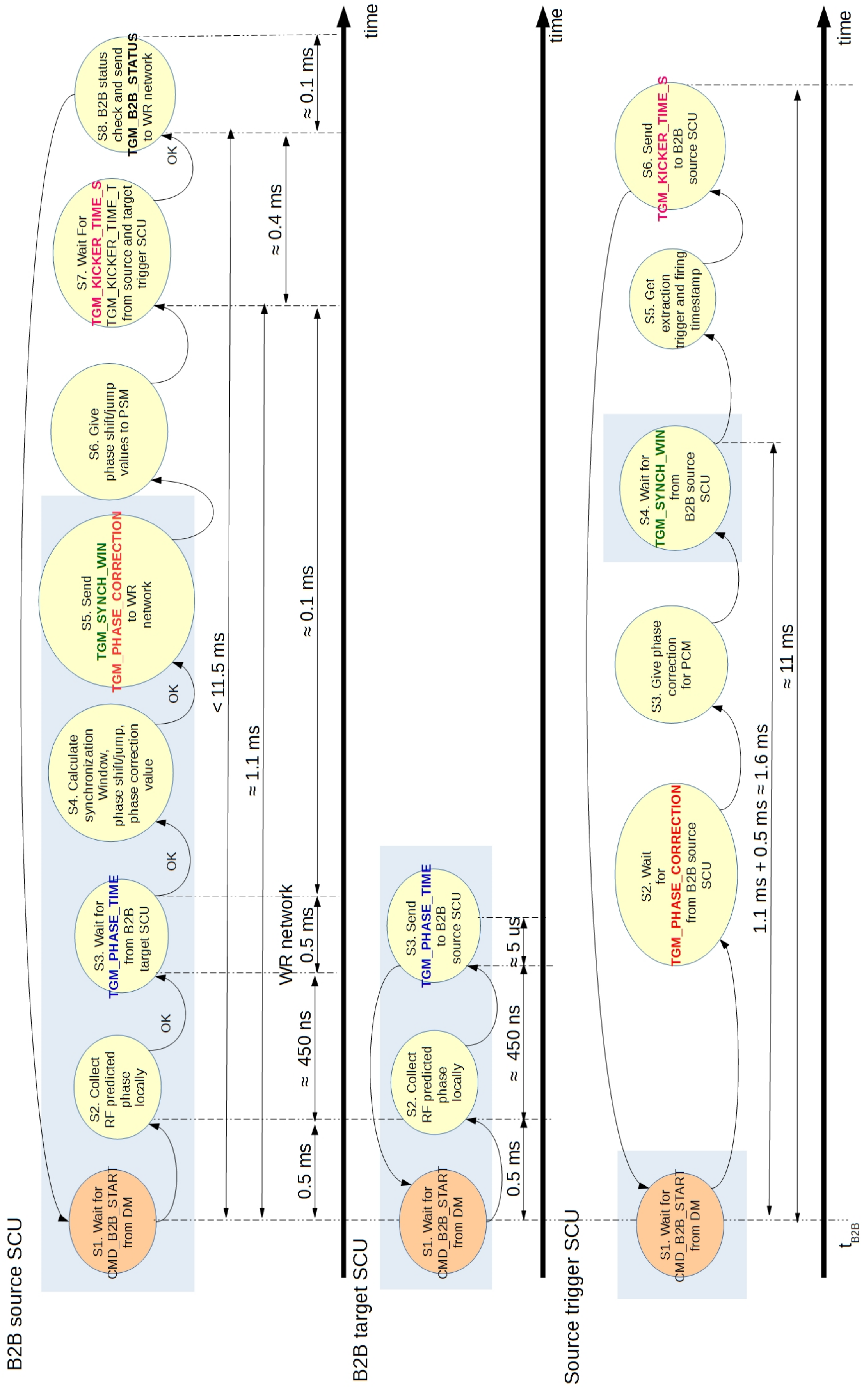

Figure 6.27: The time constraints of the B2B transfer system. The sent and received timing frame pairs have the same color. The test setup realizes the steps in the blue rectangle. (not drawn to accurate timescale)

6.4.5 Test result

Because some modules of the B2B transfer system are still under the development, the test setup realizes parts of the whole function, mainly concentrated on the data collection from two simulated Reference RF signals, the calculation of the synchronization window and the distribution of the start of the synchronization window. The steps with the blue rectangle in Fig. 6.27 are realized in this test setup. The test result of the B2B programs on B2B source, B2B target and trigger SCUs are shown as follows.

```

U28+ B2B transfer from SIS18 to SIS100 => Source B2B SCU
==================================================
SIS18: Frequency of the Reference RF Signal = 1.572200MHz
SIS100: Frequency of the Reference RF Signal = 1.572000MHz
SIS18: Period of the Reference RF Signal = 636051(ps)
SIS100: Period of the Reference RF Signal = 636132(ps)

>>>>>>>>>>>>>>>>>>>>>>>>> Receive CMD_START_B2B from WR network
Timestamp of the Reference RF Signal from SIS18 (accuracy to 1ns)
GMT: Thu, Jan 8, 1970, 21:07:27.445405856

>>>>>>>>>>>>>>>>>>>>>>>>> Receive TGM_PHASE_TIME from WR network
Timestamp of the Reference RF Signal from SIS100 (accuracy to 1ns)
GMT: Thu, Jan 8, 1970, 21:07:27.445364560

Beating time: 5 (ms)
Synchronization time: 4.622818 (ms)
The number of the SIS18 revolution for the synchronization: 3634
Start of the synchronization window: GMT: Thu, Jan 8, 1970, 21:07:27.450028674

<<<<<<<<<<<<<<<<<<<<<<<<< Send TGM_SYNCH_WIN to WR network
```

```

U28+ B2B transfer from SIS18 to SIS100 => Target B2B SCU
==================================================
>>>>>>>>>>>>>>>>>>>>>>>>> Receive CMD_START_B2B from WR network
Timestamp of the Reference RF Signal from SIS100 (accuracy to 1ns)
GMT: Thu, Jan 8, 1970, 21:07:27.445364560

<<<<<<<<<<<<<<<<<<<<<<<<< Send TGM_PHASE_TIME to WR network
```

```

U28+ B2B transfer from SIS18 to SIS100 => Trigger SCU
==================================================
Waiting for timing frames ...
```

```
5 >>>>>>>>>>>>>>>>>>>>>>>>>>> Receive TGM_SYNCH_WIN from
        WR network
6 Event execution timestamp: GMT 1970-01-08 21:07:27.450028674
```

After both B2B source and target programs receive the CMD_START_B2B frame, they trigger another unit connected to the System-on-Chip[10] (SoC) bus to get the timestamp of the next zero crossing point of the DS345 sine waves, which is simulated as an equivalent to the predicted phase. All timestamp are shown in the format of Greenwich Mean Time (GMT). The timestamp got by the B2B source SCU is Thu, Jan 8, 1970, 21:07:27 0.445405856 second and the timestamp got by the B2B target SCU is Thu, Jan 8, 1970, 21:07:27 0.445364560 second, see Line 10 and 14 of the test result of the B2B source SCU. The time difference between two timestamps is 41.296 µs. The frequency difference between SIS18 and SIS100 Reference RF Signals is 200 Hz. It means that there are 200 more periods of the SIS18 Reference RF Signal within one second compared with the SIS100 Reference RF Signal. Every 5 ms (1/200 Hz) SIS18 Reference RF Signal has one period more than that of SIS100. The time is calculated by eq. 6.52, indicating the alignment of the zero crossing of two DS345 sine waves of SIS18 and SIS100. The time is named as "synchronization time", denoted by Δt.

$$\frac{T_{h=2}^{SIS18}}{1/(f_{h=2}^{SIS18} - f_{h=10}^{SIS100})} = \frac{41.296us \mod T_{h=10}^{SIS100}}{\Delta t} \tag{6.52}$$

$$\Delta t = 4.622\,818\,\mathrm{ms} \tag{6.53}$$

The number of the SIS18 Reference RF Signal periods for the synchronization is calculated as

$$\frac{\Delta t}{T_{h=2}^{SIS18}} = 7268 \tag{6.54}$$

we could get that the beating time Δt is 4.622 818 ms and the number of the SIS18 Reference RF Signal periods for the synchronization is 7268 for the test.

[10] A system-on-chip is an integrated circuit that integrates all components of a computer or other electronic system into a single chip.

Chapter 7

Conclusion and outlook

For many large scale accelerator facilities, it is inevitable to transfer bunched beam from one ring accelerator to another to gain higher energy or to accumulate beam for some research experiments. Without the proper transfer, the beam will be subject to various disturbances and even beam loss, e.g. dipole oscillation caused by the injection energy or phase error, quadrupole oscillation caused by the cavity voltage error. Hence, the proper bunch-to-bucket transfer between two accelerators is of great importance.

Facility for Antiproton and Ion Research (FAIR) aims at providing high-energy beam with high intensities. SIS100/300 of FAIR is under construction at GSI Helmholtz Centre for Heavy Ion Research GmbH at current stage. The B2B transfer has never been practiced between the existing machines, e.g. SIS18, ESR and CRYRING. The new developed Bunch-to-Bucket transfer system for FAIR in the dissertation is designed for all complex B2B transfer between FAIR accelerators. It is capable to transfer different species beam from one machine cycle to another. It is capable to parallel transfer beam through FAIR accelerators. It is also able to transfer the beam between two synchrotrons via FRS or Super FRS. It focuses first of all on the transfer from SIS18 to SIS100, but it will be firstly tested for the transfer from SIS18 to ESR and further to CRYRING.

The B2B transfer system for FAIR is introduced in the dissertation at hand from the functional point of view. The basic principles for B2B transfer are realized based on the existing FAIR technical basis (e.g. LLRF and FAIR control systems) and unique FAIR demands (e.g. Machine Protection System, MPS). The phase difference between two RF systems of two ring accelerators is obtained with the help of a shared reference signal at two ring accelerators. The source synchrotron works as the "B2B transfer master" for the rf phase collection, data (e.g. synchronization window, phase correction, phase shift and so on) calculation, synchronization window redistribution and B2B status check. In addition, the dissertation presents how FAIR accelerators apply the B2B transfer system and how precise the bunch-to-bucket transfer is achieved with the system. The rules for the application of the system is explained, which is determined by the relation between the circumference ratio/energy ratio and the cavity harmonic number of two synchrotron.

In addition, the beam dynamic of the U^{28+} B2B transfer from SIS18 to SIS100 is simulated for two synchronization methods, the phase shift and frequency beating method. The dissertation explains the timing constraints of the system, the calculation of the synchronization window and presents the usage of the WR network for the B2B transfer system. Further, the SIS18 extraction and SIS100 injection kickers are analyzed for the different triggering possibilities.

The dissertation presents a test setup for the system, achieving the phase collection of two synchrotrons locally, phase transfer from the target to source synchrotron, synchronization window calculation at the source synchrotron, synchronization window redistribution to the WR network, synchronization window reproduced at the source/target synchrotron.

Although the B2B transfer system for FAIR is flexible and with high compatibility, there still exists several improvement.

In order to reduce the synchronization time, the synchronization process could be started during the acceleration. The phase difference between two Reference RF Signals of the source and target synchrotrons at the flattop could be predicted by comparison the phases of these two signals at any time during the acceleration. Once the phase difference at the flattop is predicted, the synchronization process can be carried out.

- Phase shift method

  First, the radial loop must be turned off. At some time during the acceleration, the phases difference between the source and target synchrotrons are obtained with the help of the Synchronization Reference Signal, and the phase difference at the flattop is picked up from the look-up table. Then, a rf frequency modulation is superposed on the initial frequency pattern. The integration of the rf frequency modulation equals to the required phase difference. With this new frequency pattern, the phase difference at the flattop will be the required phase difference when the cavity rf frequency of the source and target synchrotrons reach the flattop.

- Frequency beating method

  The radial loop keeps on. At some time during the acceleration, the phases difference between the source and target synchrotrons are obtained. Then, a frequency detune is superposed on the initial frequency pattern. With this new frequency pattern, the synchronization window will be calculated.